Elementary processes

Interactions of electron with atoms, molecules, ions ….

Ionization

Collisions of electrons with atoms

Classical or quantum approach?

Electron:

1eV → $v = 5.9\times10^{7}\,cm\ s^{-1}$

$\tau \sim a_0/v \sim 10^{-8}/\ 5.9\times10^{7} = 2\times10^{-16}s$

$\lambda \sim 2A = 2\times10^{-8}cm$ de Broglie

Ar+:

1eV → $v = 2\times10^{5}\,cm\ s^{-1}$

$\tau \sim a_0/v \sim 10^{-8}/\ 2\times10^{5} \sim 6\times10^{-14}s$

$\lambda \sim 9\times10^{-11}cm$ de Broglie

Illustration of a variety of applications wherein cross-section data involving atomic & molecular physical processes are important.

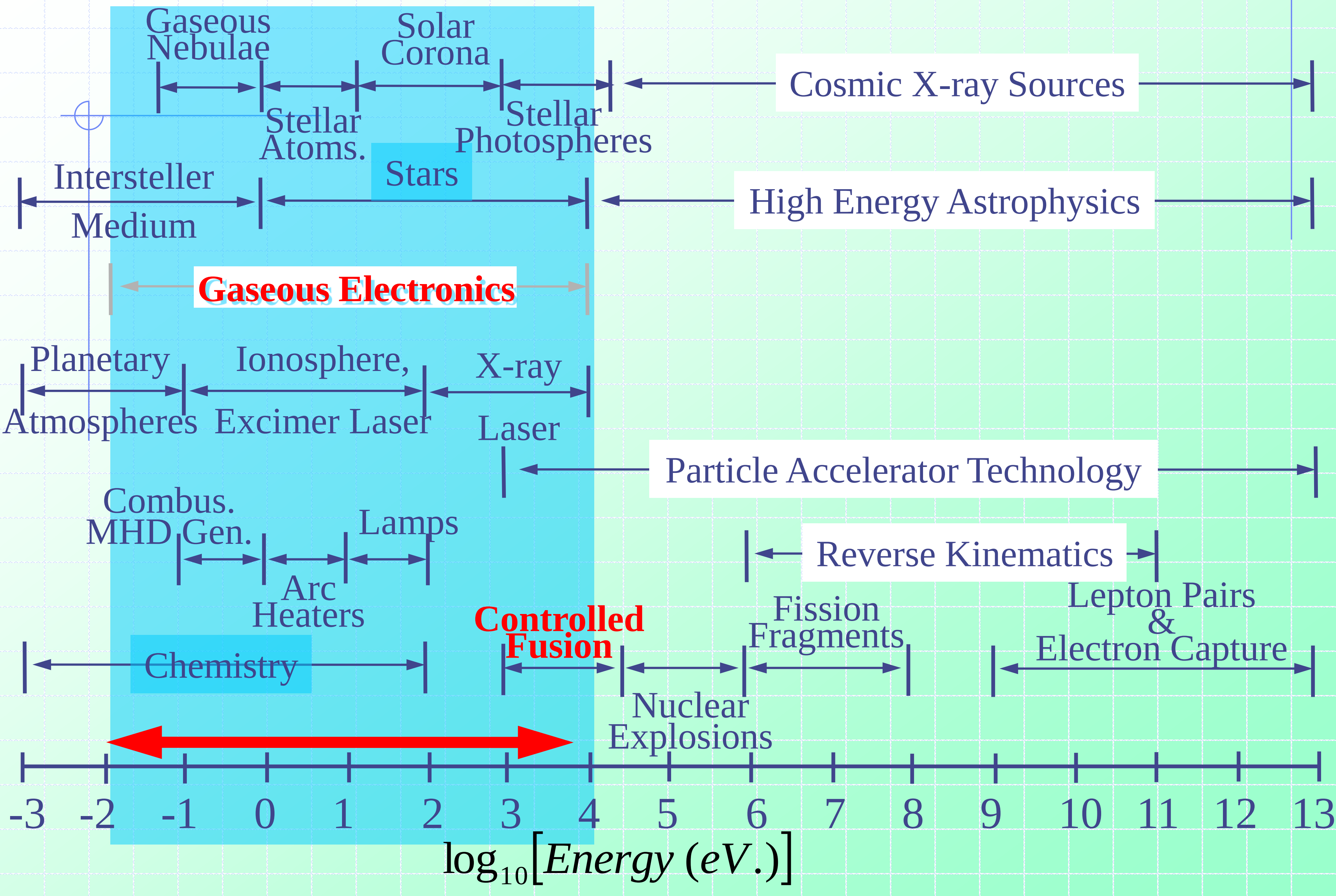

Single collision

$$e + Ar \Rightarrow Ar^{+} + 2e$$

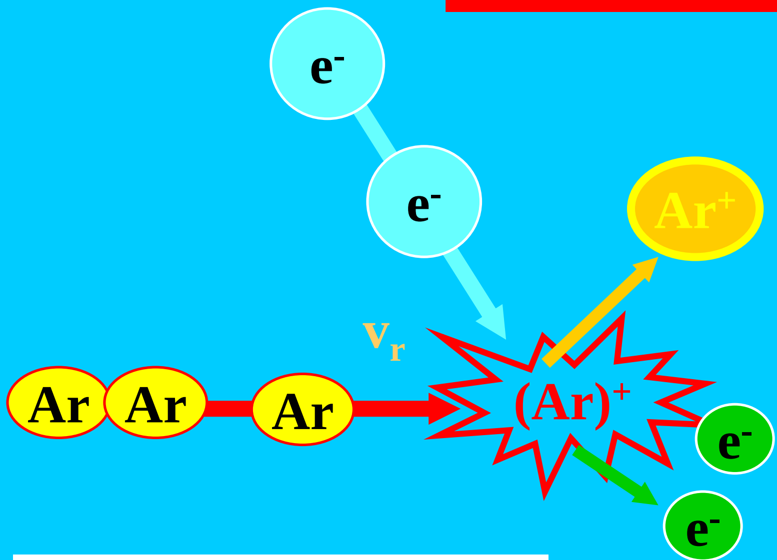

reaction cross section

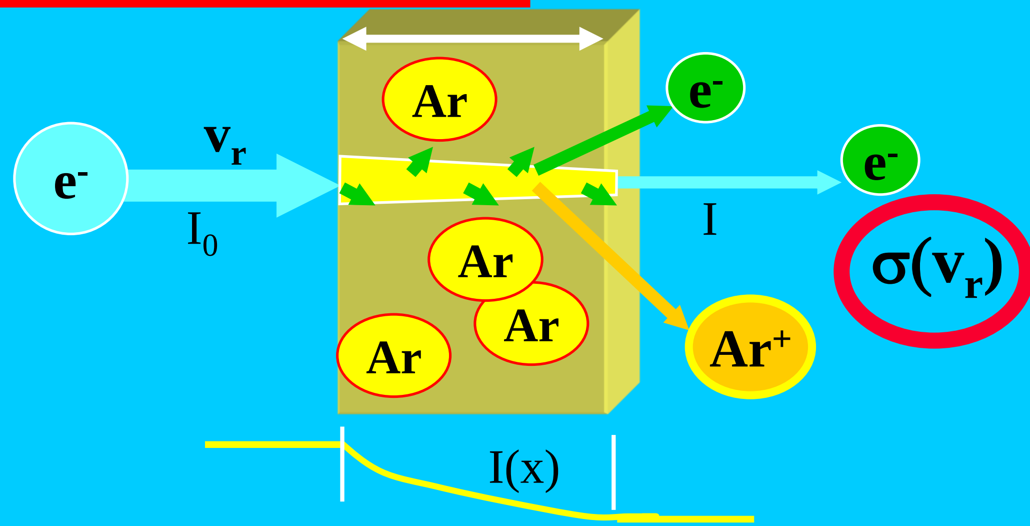

$I=I_0 \exp(-\sigma n_{Ar} x)$

Proportionality factor

$$\frac{dI}{dx} \sim -IN \qquad \frac{dI}{dx} = -\sigma I N$$

$$\frac{dI}{Idx} = \frac{d\ln(I)}{dx} = -\sigma N$$

$$I(x) = I_0 \exp(-\sigma N x)$$

Single collision

$$e + Ar \Rightarrow Ar^{+} + 2e$$

X

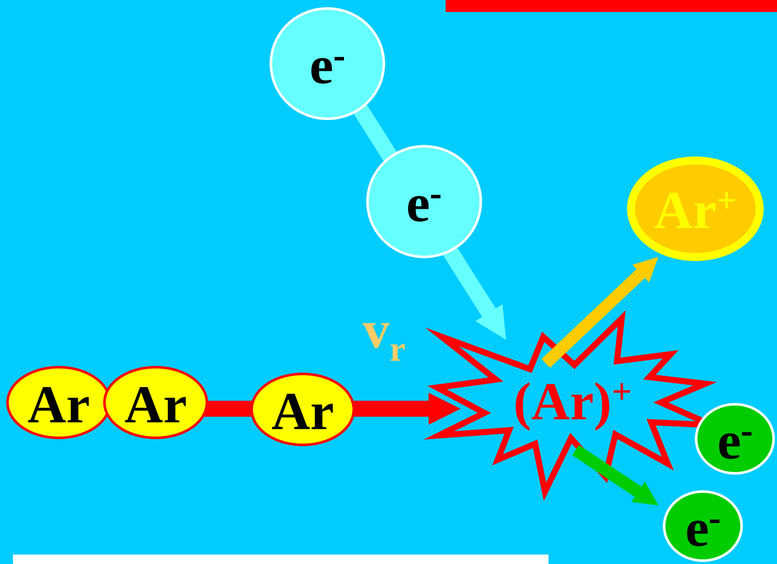

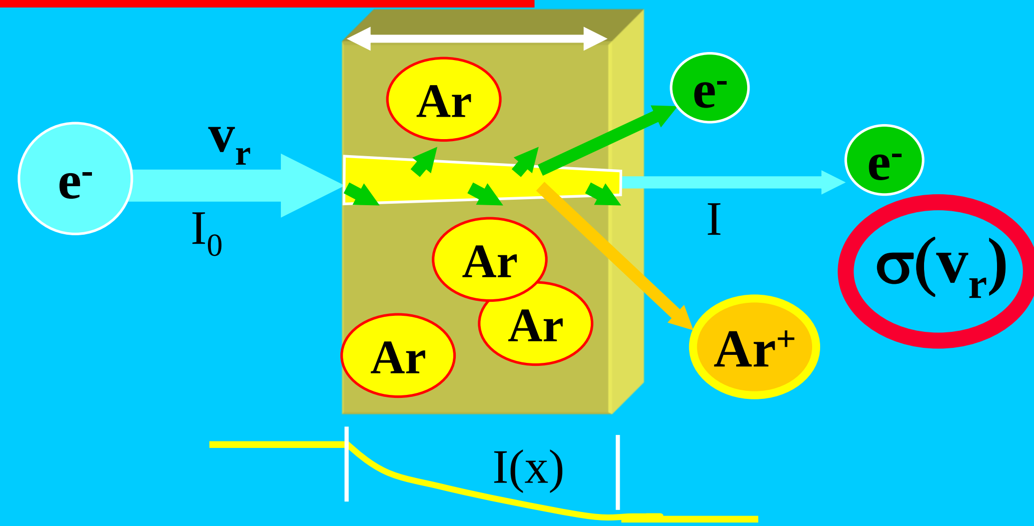

reaction cross section

$I=I_0 \exp(-\sigma n_{Ar} x)$

$$\nu_{coll} = -nV_{rel} = -n\,vS = -n\,v\pi\delta^2 = -nv\sigma$$

$$\frac{dI}{dt} = -\frac{I}{\tau_{coll}} = -I\nu_{coll}$$

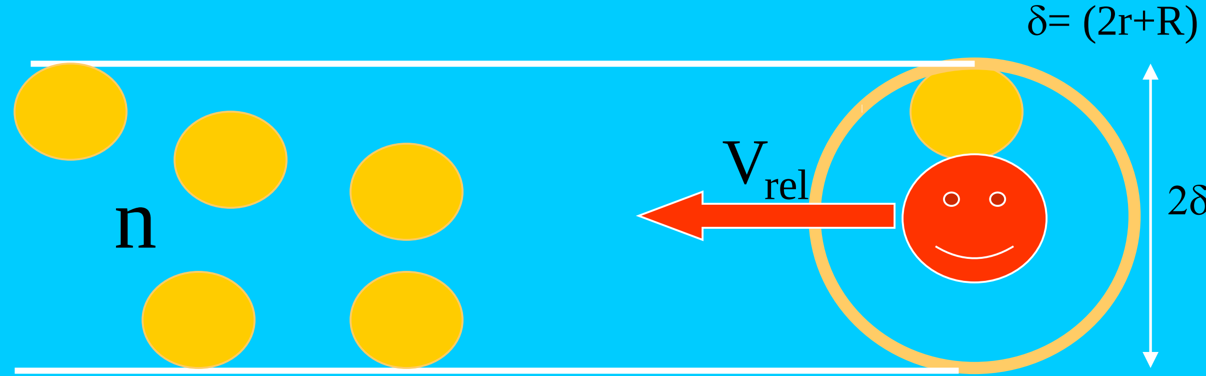

$$I(t) = I_0 \exp(-\nu_{coll} t) = I_0 \exp(-\sigma n\, v_{rel} t)$$

$I=I_0 \exp(-\sigma n_{Ar} x)$

At low energies

Threshold Photoelectron Source for Ultra-Low-Energy Electron Collision Experiments

low energies - 2010

We have developed a new experimental technique for measuring the total cross section of ultra-low energy electron collisions with atoms and molecules utilizing synchrotron radiation. The present technique employs a combination of the penetrating field technique and the threshold photoionization of rare gas atoms using synchrotron radiation as an electron source in order to produce a high resolution electron beam at very low energy. The total cross sections for electron scattering from Kr in the energy range from 14 meV to 20 eV are obtained with the new technique. In addition, resonant structures in the total cross sections due to Kr^- $(4p^5 5s^2\ ^2P_{3/2})$ and Kr^- $(4p^5 5s^2\ ^2P_{1/2})$ Feshbach resonances are also observed for the first time.

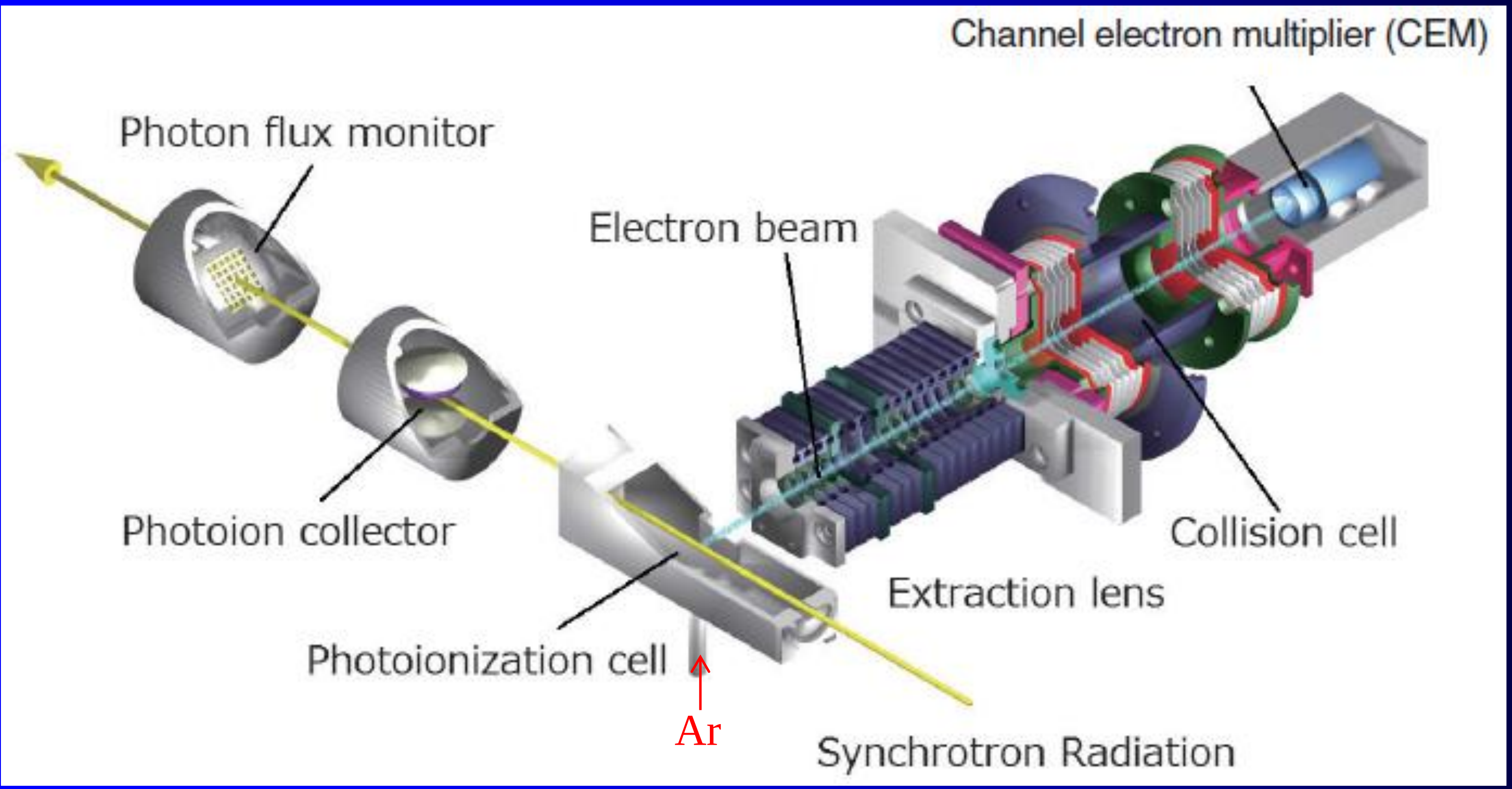

Figure 1
Schematic view of the experimental set-up. The system consists of an electron scattering apparatus with a photoion cell, a photoion collector, and photon flux monitor of the monochromatized SR.

Cold Collision Experiments

- *photoelectron source induced by SR -*

$$Ar + h\nu \rightarrow Ar^{+} + e$$

$$\Delta E \leq 10\ \mathrm{meV}$$

$$E_0 \leq 30\mathrm{meV}$$

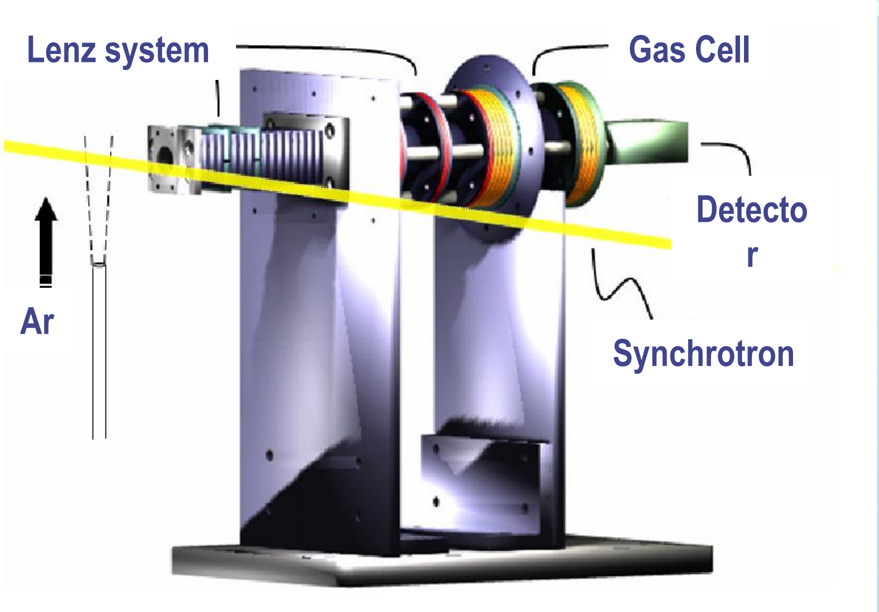

Schematic view of experimental setup

Research site: Photon Factory at KEK

Total cross section of Xe in low energy region (preliminary data)

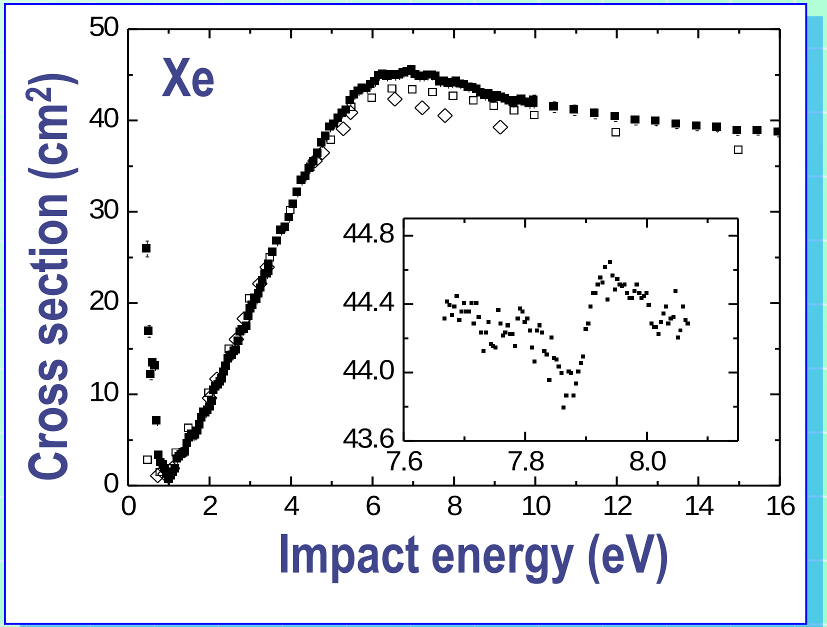

Xe, Kr, O_2

Threshold Photoelectron Source for Ultra-Low-Energy Electron Collision Experiments

We have developed a new experimental technique for measuring the total cross section of ultra-low energy electron collisions with atoms and molecules utilizing synchrotron radiation. The present technique employs a combination of the penetrating field technique and the threshold photoionization of rare gas atoms using synchrotron radiation as an electron source in order to produce a high resolution electron beam at very low energy. The total cross sections for electron scattering from Kr in the energy range from 14 meV to 20 eV are obtained with the new technique. In addition, resonant structures in the total cross sections due to Kr^- ($4p^55s^2\ ^2P_{3/2}$) and Kr^- ($4p^55s^2\ ^2P_{1/2}$) Feshbach resonances are also observed for the first time.

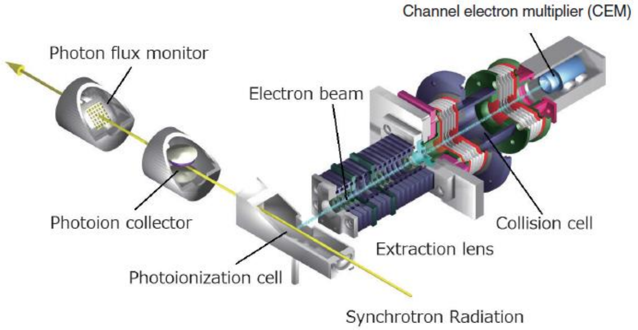

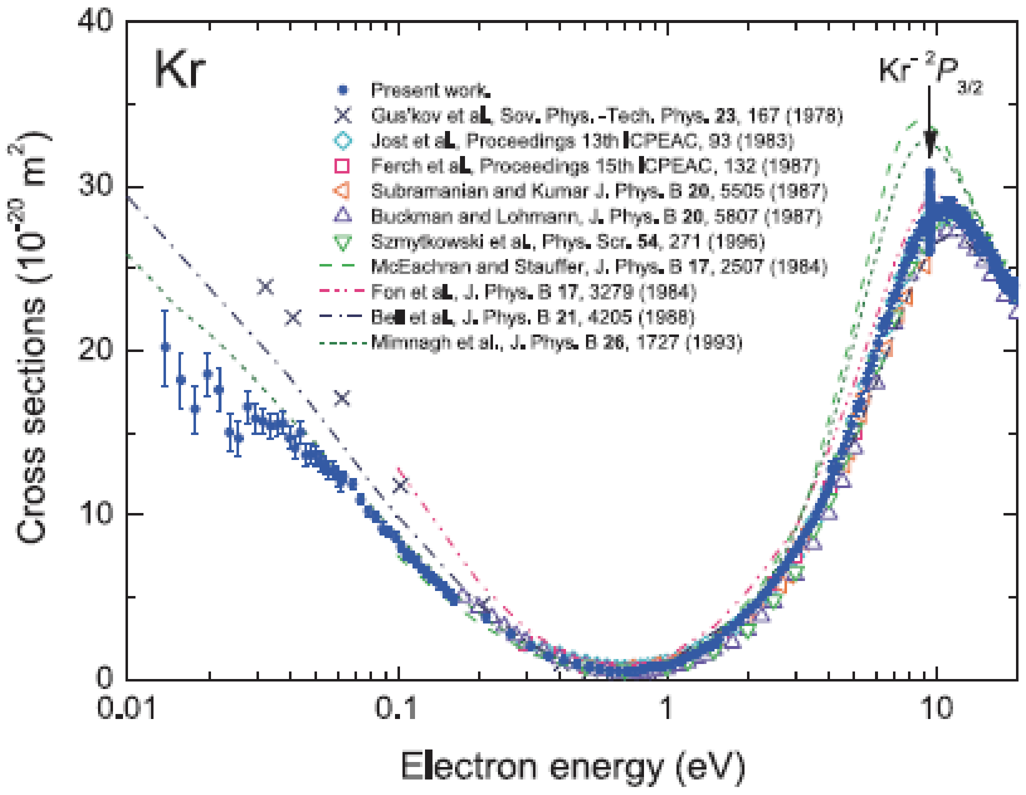

Figure 2

Total cross sections for electron scattering from krypton. The vertical arrow at around 10 eV shows the position of the structure due to Kr^- ($4p^55s^2\ ^2P_{3/2}$) Feshbach resonance.

Details of Ramsauer effect

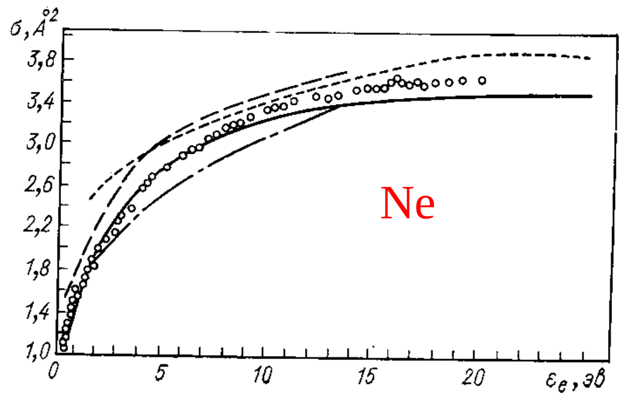

Рис. 5.8. Полное сечение рассеяния электрона на атоме неона.

Эксперимент (метод Рамзауэра): ○ — [101]; ——— — [29]; ········· — [92]; — · — — [95]. Теория: — — — [109].

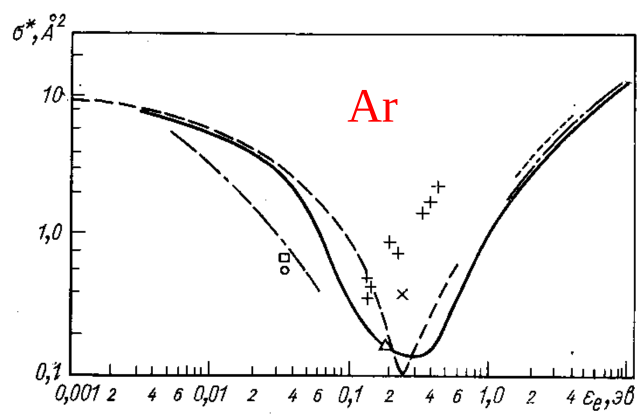

Рис. 5.9. Диффузионное сечение столкновения электрона с атомом аргона.

Эксперимент (подвижность электронов при малых полях и температурах): ········· — [21]; ——— — [47]; × — [60]; ○ — [91]; □ — [112]; △ — [44]; — · — — [16]; — — · — — [108]; + — [43]. Теория: — — — [87].

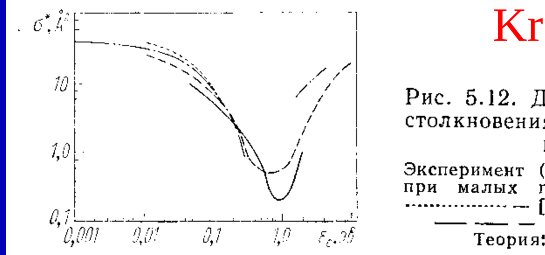

Рис. 5.12. Диффузионное сечение столкновения электрона с атомом криптона.

Эксперимент (подвижность электронов при малых полях и температурах): ········· — [34]; — · · — — [21]; — — — [47]; ——— — [63]. Теория: — · — — [87].

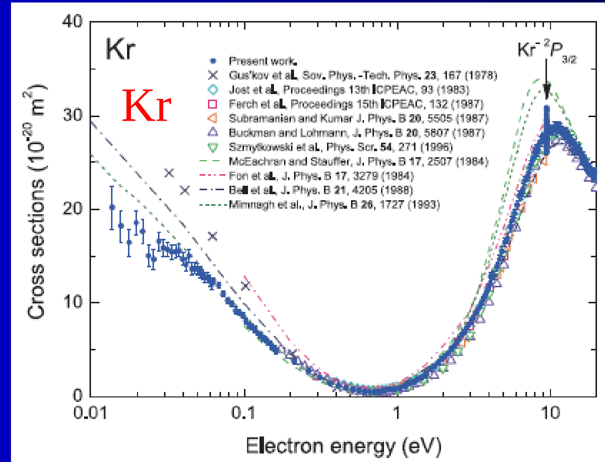

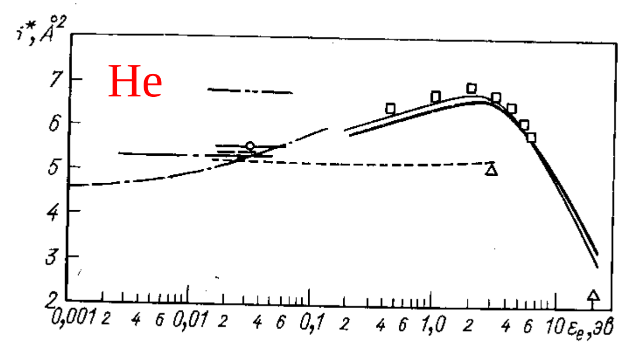

Рис. 5.3. Диффузионное сечение столкновения электрона с атомом гелия.

Эксперимент (подвижность электронов при малых полях и температурах): □ — [39]; △ — [73]; — · — — [88]; — — — — [91]; ············ — [58]; — ····· — — [13]; —○— — [62]. Теория: ——— — [75]; ——— — [32]; — — · — — — расчет по формуле (5.37).

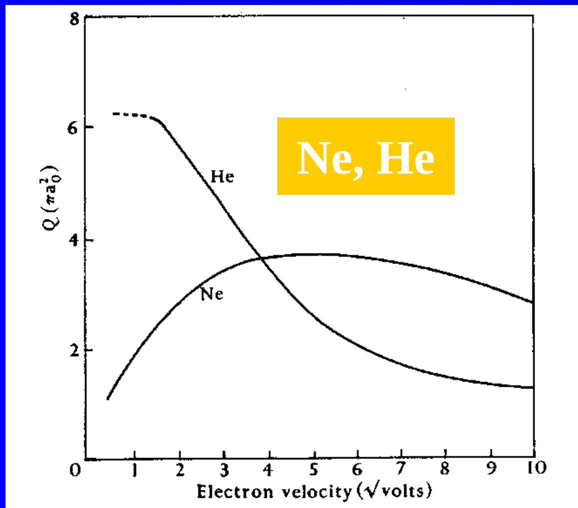

FIG. 1.10. Observed total collision cross-sections of He and Ne.

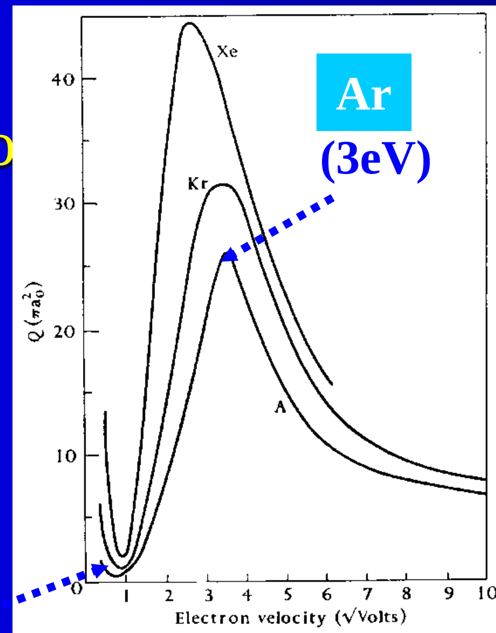

FIG. 1.9. Observed total collision cross-sections of A, Kr, and Xe.

(0,3eV)

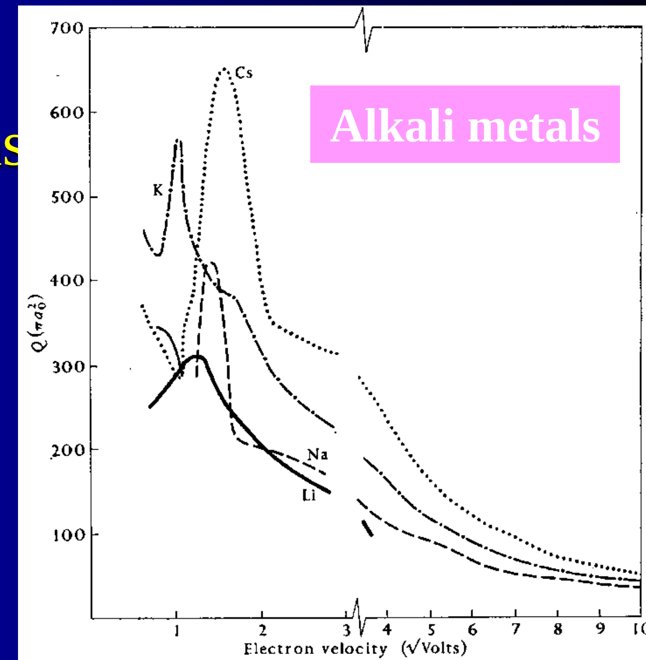

FIG. 1.16. Observed total collision cross-sections of Li, Na, K, and Cs.

$\sigma(v)$

$e^-(v)$

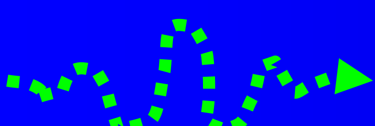

Ar

(3eV)

Ne

Ar

(0.3eV)

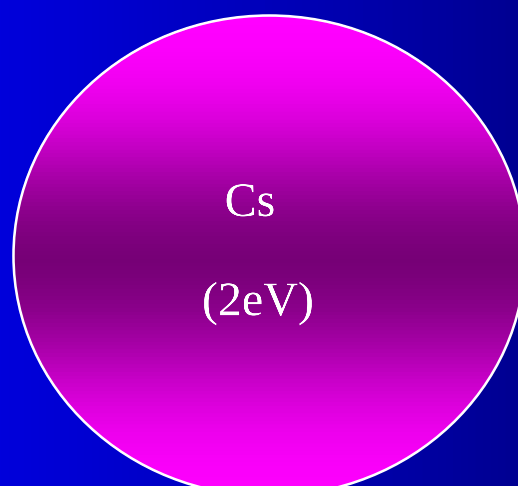

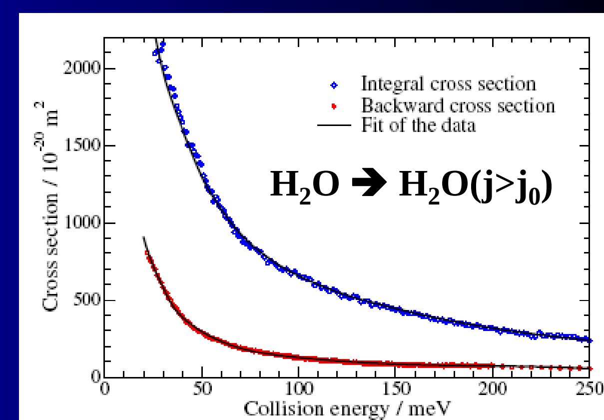

$H_2O\ (j_0) + e(\varepsilon) \rightarrow H_2O(j>j_0) + e(\varepsilon)$

Frequencies of elastic collisions

$\delta I = -NQI_p\,\delta x$

$I_P = I_0 \exp(-QNx)$

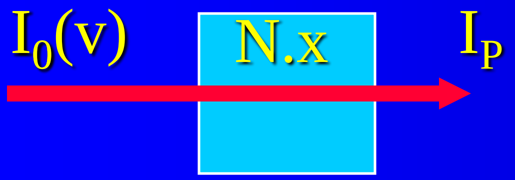

Q(v)

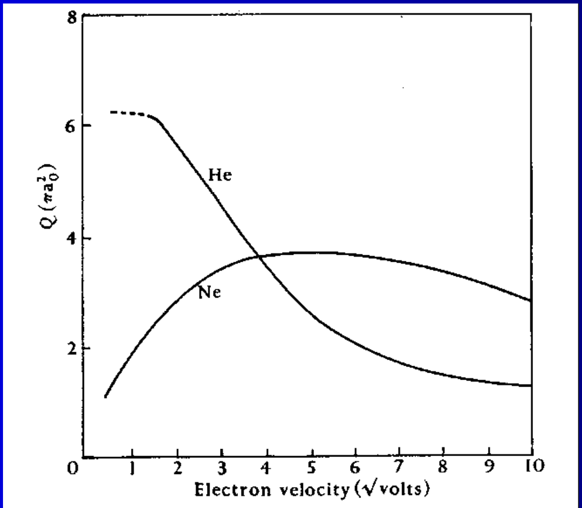

FIG. 1.10. Observed total collision cross-sections of He and Ne.

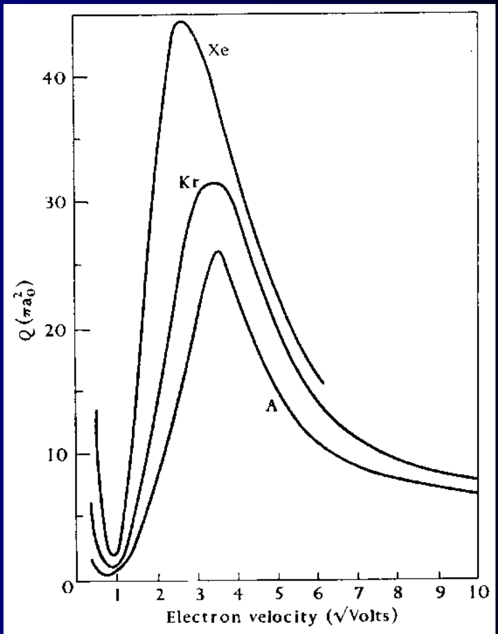

FIG. 1.9. Observed total collision cross-sections of A, Kr, and Xe.

$a_0 = 0.53 \times 10^{-8}$cm~0.5A

Radius of the first Bohr orbit of H atom

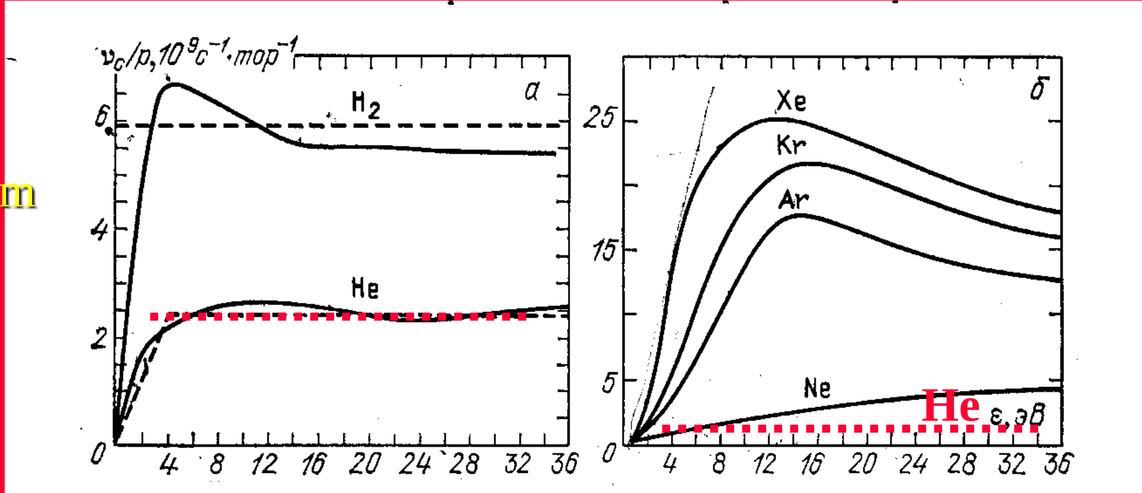

Рис. 2.5. Частоты упругих столкновений электронов, $p=1$ тор: *а* — в H_2 и He; *б* — в инертных газах; штриховые линии — удобная аппроксимация при расчетах [24]

$\nu \sim nv\sigma$

Collision Frequencies

Very low energies

Very low collision energies

TOPICAL REVIEW

Electron–molecule collisions at very low electron energies

F B Dunning

Department of Physics and the Rice Quantum Institute, Rice University, PO Box 1892, Houston, TX 77251, USA

J. Phys. B: At. Mol. Opt. Phys. 28 (1995) 1645–1672. Printed in the UK

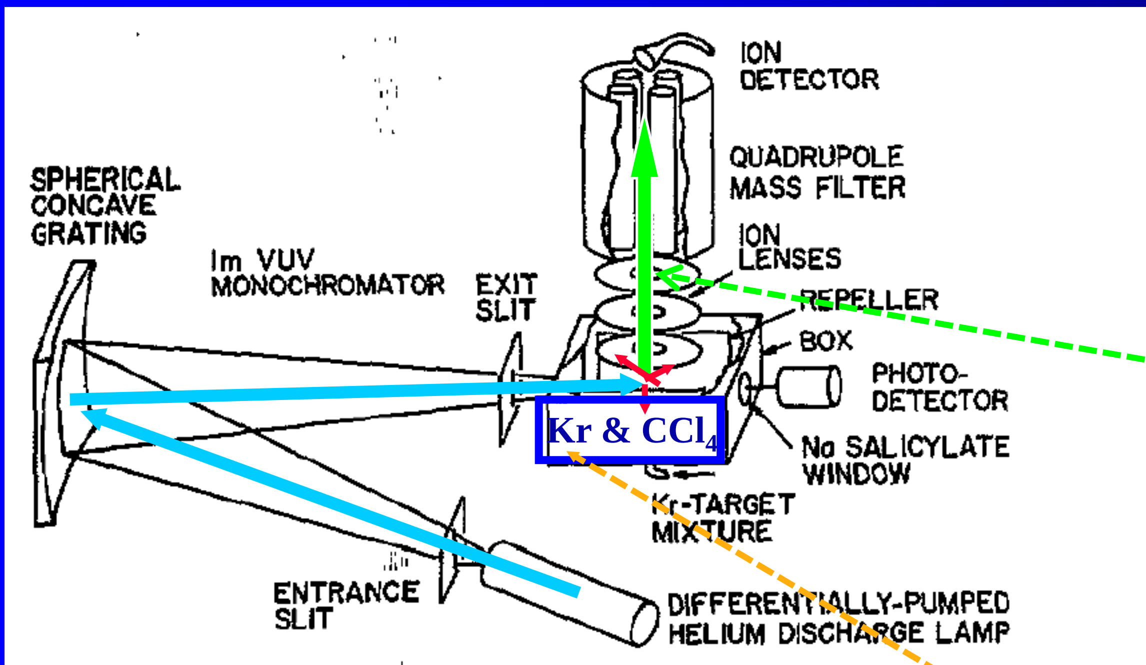

Figure 1. Schematic diagram of the VUV photoionization apparatus used for attachment studies (Chutjian and Alajajian 1985a, b).

$$e^- + CCl_4 \rightarrow CCl_4^{-*} \rightarrow CCl_3 + Cl^-$$

$$Kr(^1S_0) + \hbar\omega \rightarrow Kr^+(^2P_{1/2}) + e^-(\varepsilon)$$

Electron attachment at very low electron energies

10^5 Å

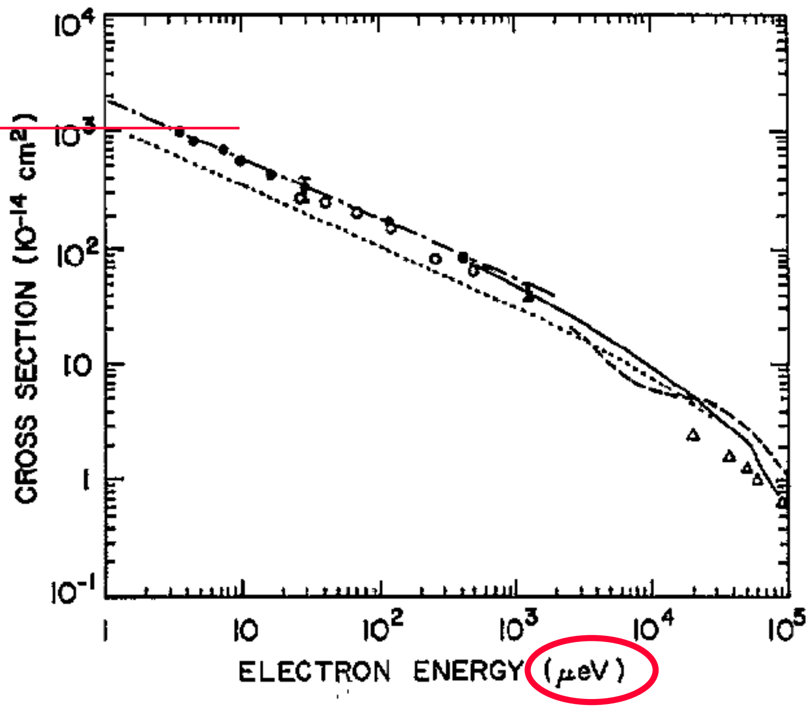

Figure 3. Cross sections for electron attachment to CCl_4. ●, $\bar{\sigma}_e$-K(*n*p); —·—, $\sigma_e(\nu)$-K(*n*p) (Frey *et al* 1994b); ○, $\bar{\sigma}_e$-K(*n*p) (Ling *et al* 1992); ——, free electrons (Hotop 1994); – – –, free electrons (Orient *et al* 1989); △, free electrons (Christodoulides and Christophorou (1971); -----, theory (Klots 1976).

10^5 Å

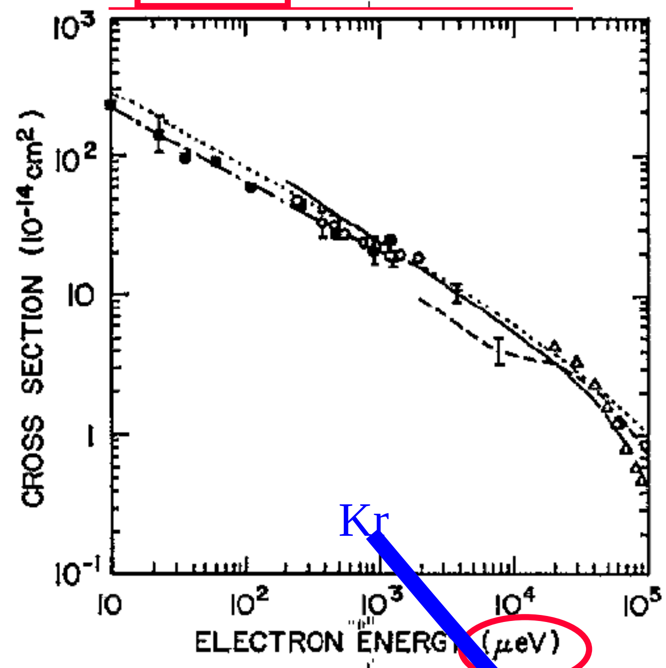

Figure 2. Cross section for electron attachment to SF_6. ■, $\bar{\sigma}_e$-K(*n*p); —·—, $\sigma_e(\nu)$-K(*n*p) (Ling *et al* 1992). ○, $\bar{\sigma}_e$-Rb(*n*s) (Zollars *et al* 1985); ——, free electrons (Klar *et al* 1992a, b); – – –, free electrons (Chutjian and Alajajian 1985); △, free electrons (Pai *et al* 1979, Chutjian and Alajajian 1985a); -----, theory (Klots 1976).

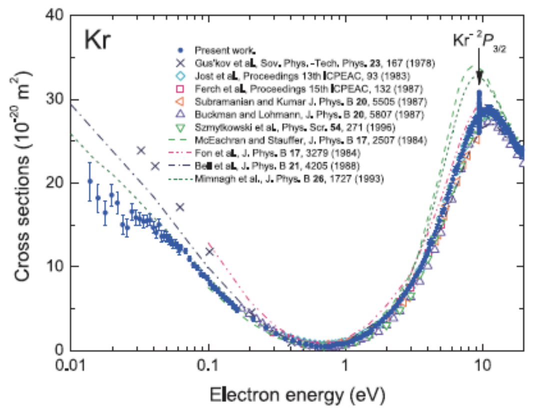

Kvantová mechanika
Jednorozměrný rozptyl

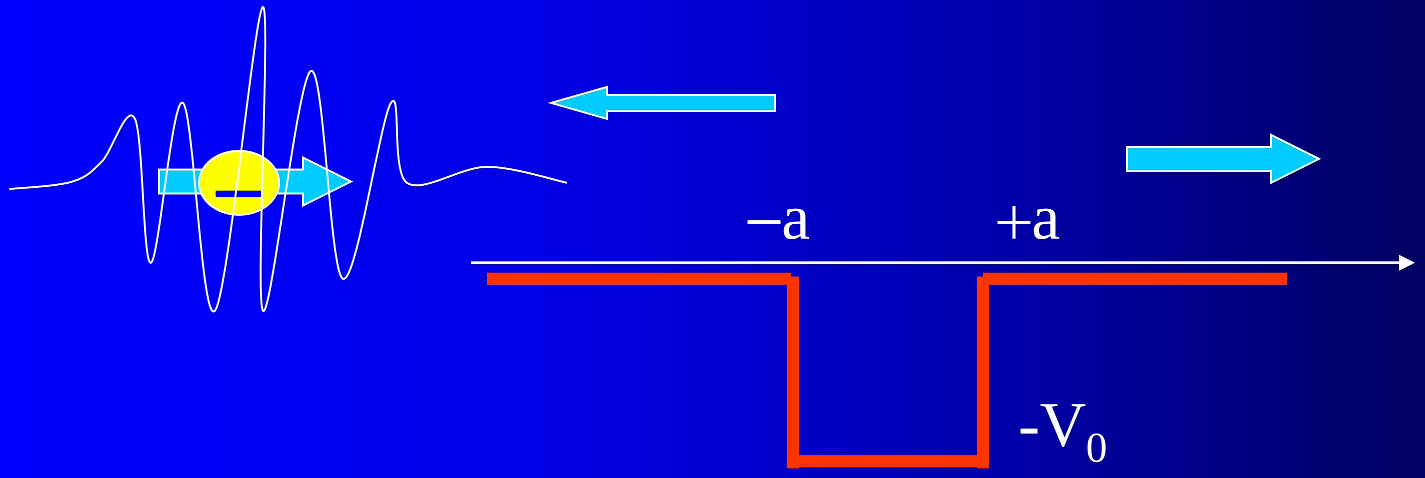

Kvantová mechanika I
J. Klíma B. Velický
MFF 1992

Jednorozměrný rozptyl

Vlnová funkce má tvar superposice Brogoliových vln

$$k = \sqrt{2mE / h^2}$$

$$\psi_k(x,t) = (Ae^{ikx} + Be^{-ikx})e^{iE_k t/h} \qquad x \le -a$$

$$k = \sqrt{2mE / h^2}$$

$$\psi_k(x,t) = (Fe^{ikx} + \cancel{G}e^{-ikx})e^{iE_k t/h} \qquad x > a$$

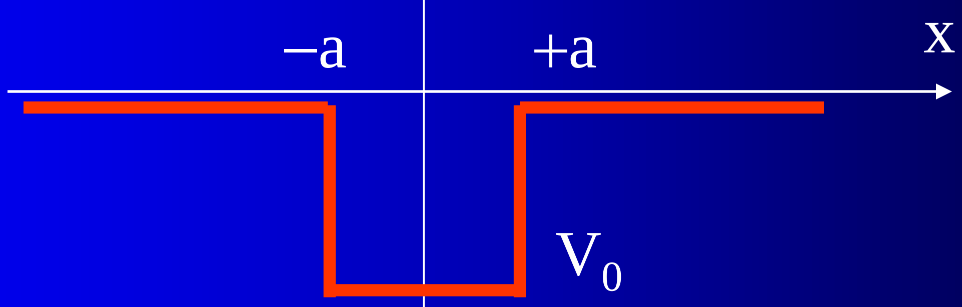

$$\psi_k(x,t) = (Ce^{ik'x} + De^{-ik'x})e^{iE_k t/h} \qquad |x| \le a$$

$$k' = \sqrt{2m(E + V_0) / h^2}$$

a) dopadající částice → A

b) odražená částice → B

c) procházející částice → F≠0, G=0

Jednorozměrný rozptyl

$$\psi_k(x,t) = (Fe^{ikx})e^{iE_k t/h} \qquad x > a$$

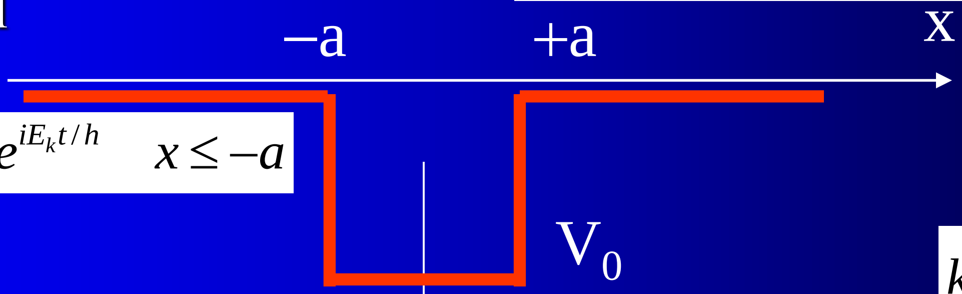

$$\psi_k(x,t) = (Ae^{ikx} + Be^{-ikx})e^{iE_k t/h} \qquad x \le -a$$

$$k = \sqrt{2mE/h^2}$$

$$k' = \sqrt{2m(E+V_0)/h^2}$$

$$\psi_k(x,t) = (Ce^{ik'x} + De^{-ik'x})e^{iE_k t/h} \qquad |x| \le a$$

Parametry jsou E, V_0, a

Hladkost řešení v bodech ±a
Určí konstanty B, C, D, G,
Hodnota A je vstupní parametr

Tok dopadajících částic

$$j_{in} = \frac{hk}{m}|A|^2$$

$$C = \frac{F}{2}(1 + k/k')e^{i(k-k')a}$$

$$D = \frac{F}{2}(1 - k/k')e^{i(k+k')a}$$

Tok odražených částic

$$j_{rf} = \frac{hk}{m}|B|^2$$

Tok prošlých částic

$$j_{tr} = \frac{hk}{m}|F|^2$$

$$A = function(F)$$

Jednorozměrný rozptyl

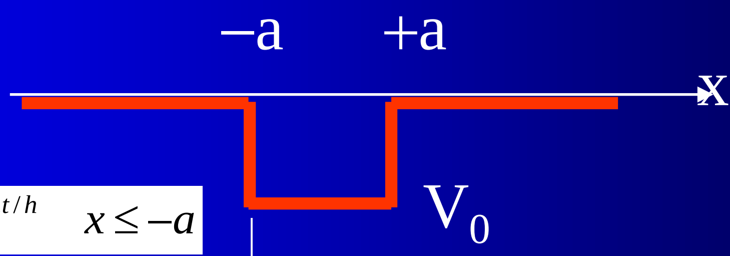

$$k = \sqrt{2mE / h^2}$$

$$k' = \sqrt{2m(E+V_0)/h^2}$$

$$\psi_k(x,t) = (Ae^{ikx} + Be^{-ikx})e^{iE_k t/h} \qquad x \le -a$$

$$\psi_k(x,t) = (Ce^{ik'x} + De^{-ik'x})e^{iE_k t/h} \qquad |x| \le a$$

$$\psi_k(x,t) = (Fe^{ikx})e^{iE_k t/h} \qquad x > a$$

Parametry jsou E, V_0 , a

$$j_{in} = \frac{hk}{m}|A|^2$$

$$j_{rf} = \frac{hk}{m}|B|^2$$

$$j_{tr} = \frac{hk}{m}|F|^2$$

Hladkost řešení v bodech ±a
Urči konstanty B, C, D, F,
Hodnota A je vstupní parametr

$$A = \ function(F)$$

$$\varepsilon = \frac{k'}{k} + \frac{k}{k'}$$

$$A = e^{2ika}(\cos(2k'a) - i(\varepsilon/2)\sin(2k'a))F$$

Koeficient průchodu T, koeficient odrazu R

$$\frac{1}{T} = \left|A/F\right|^2 = 1 + \frac{V_0^2}{4E(E+V)}\sin^2(2k'a)$$

Jednorozměrný rozptyl

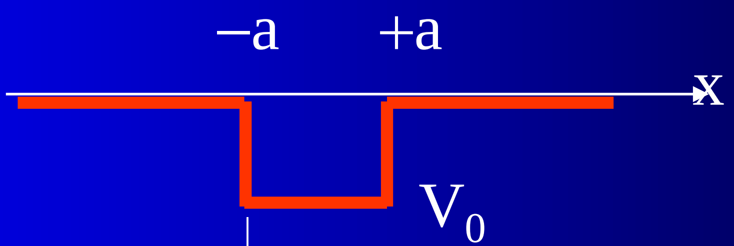

$$k = \sqrt{2mE/h^2}$$

$$k' = \sqrt{2m(E+V_0)/h^2}$$

Parametry jsou E, V_0, a

Koeficient průchodu T, koeficient odrazu R

Pro velké E se T→1,

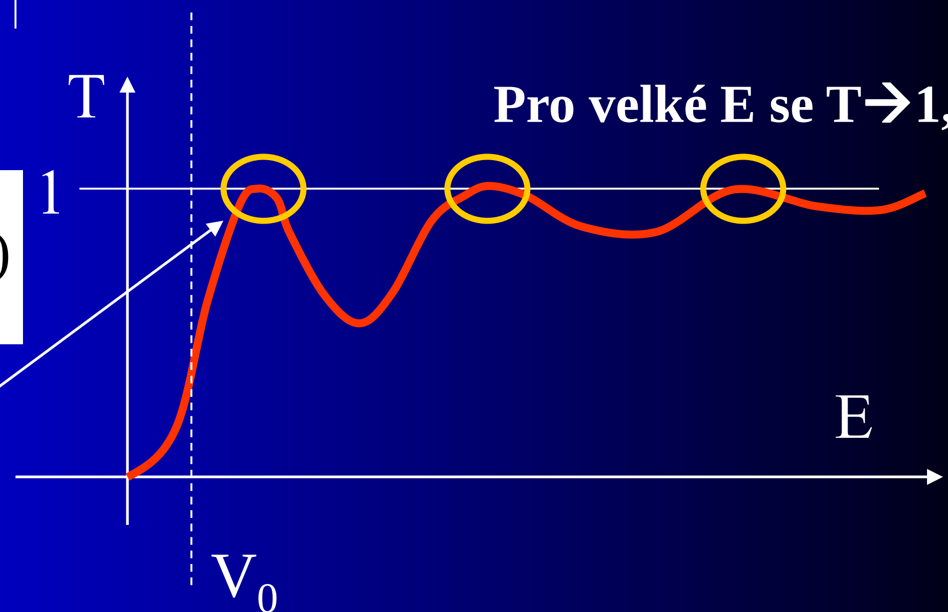

$$\frac{1}{T} = \left|\frac{A}{F}\right|^2 = 1 + \frac{V_0^2}{4E(E+V_0)}\sin^2(2k'a)$$

T=1 $$2k_n'a = n\pi$$

Efekt Ramsauera - Kr

Parametry jsou E, V_0 , a

Pro velké E se T→1,

$$\frac{1}{T} = \left|{A}/{F}\right|^2 = 1 + \frac{V_0^2}{4E(E+V_0)}\sin^2(2k'a)$$

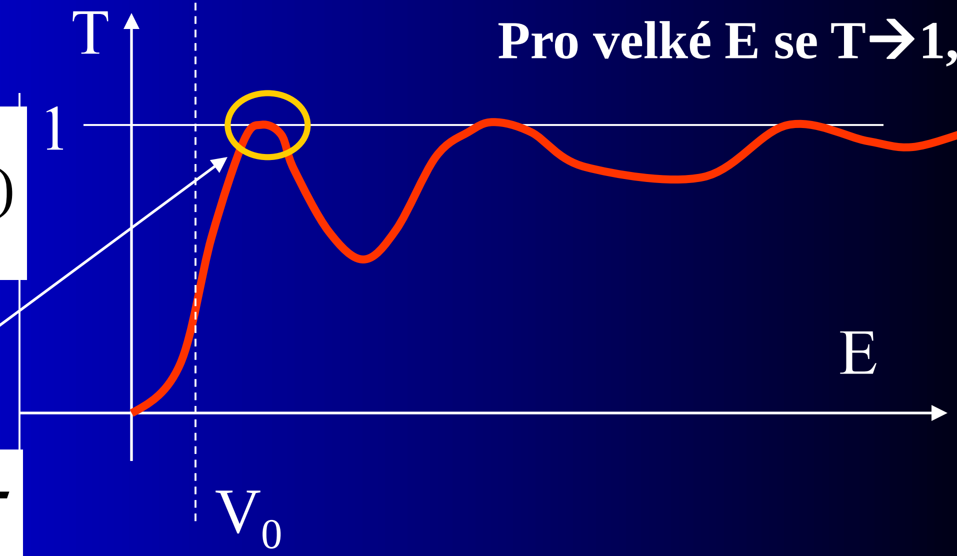

T=1 pro

$$2k_n'a = n\pi$$

$$k' = \sqrt{2m(E+V_0)/h^2}$$

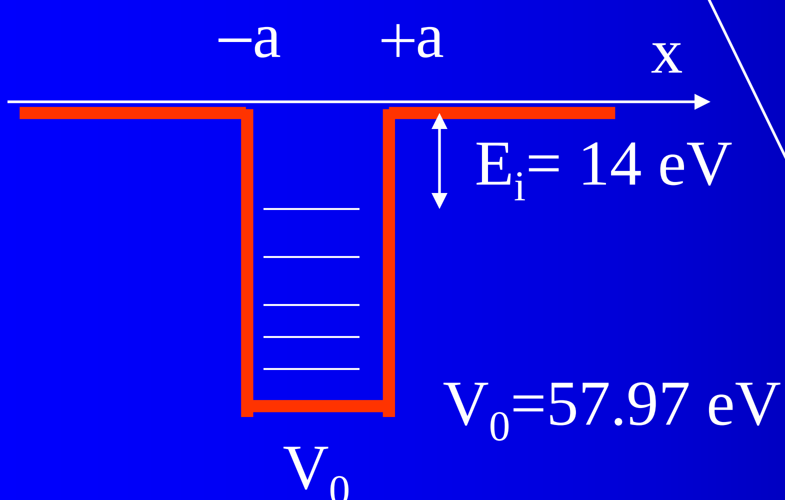

Kr; a=2Å

E_i= 14 eV → V_0=57.97 eV

E=0.013 V_0=0.75 eV

Jednorozměrný rozptyl

Parametry jsou **E, V_0 , a** **T+R=1** **Pro velké E se T→1,**

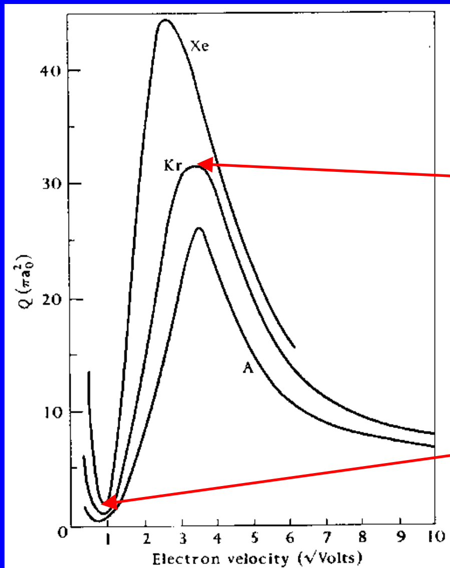

FIG. 1.9. Observed total collision cross-sections of A, Kr, and Xe.

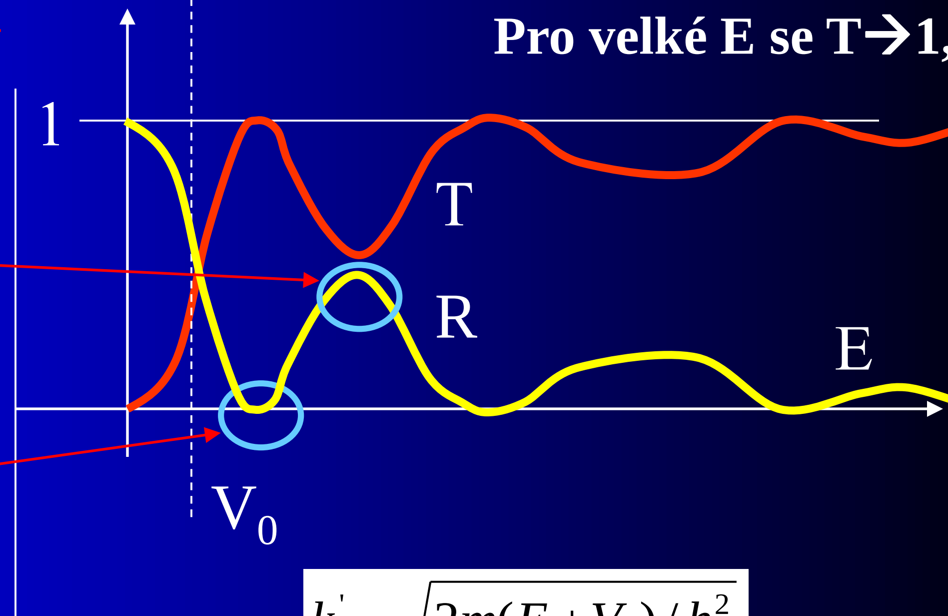

$$2k_n' n = n\pi$$

$$k' = \sqrt{2m(E+V_0)/h^2}$$

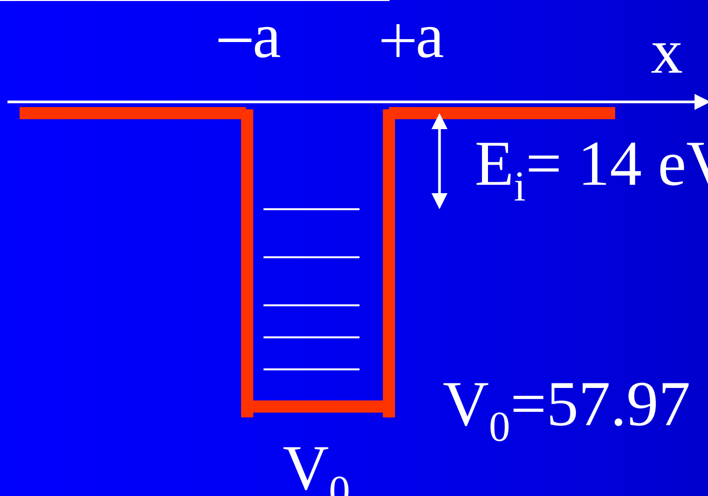

E_i= 14 eV

V_0=57.97 eV

Kr; a=2Å

E_i= 14 eV → V_0=57.97 eV

E=0.013 V_0=0.75 eV

Excitation energies

Energy levels H

- Rotational states
- Vibrational states
- Electronic states
- Ionisation

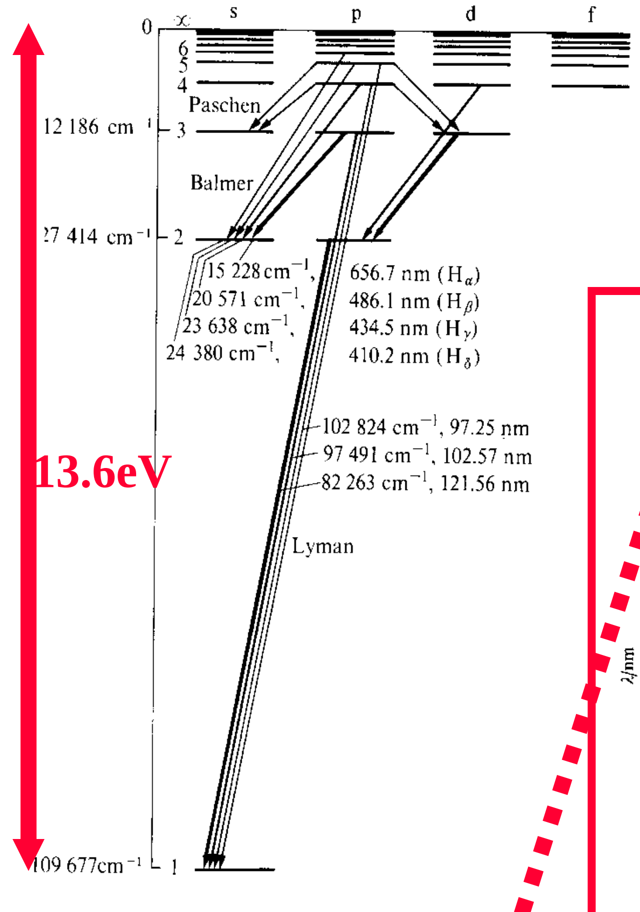

Fig. 15.12. A *Grotrian diagram* which summarizes the appearance and analysis of the spectrum of atomic hydrogen. The thicker the line, the more intense the transition.

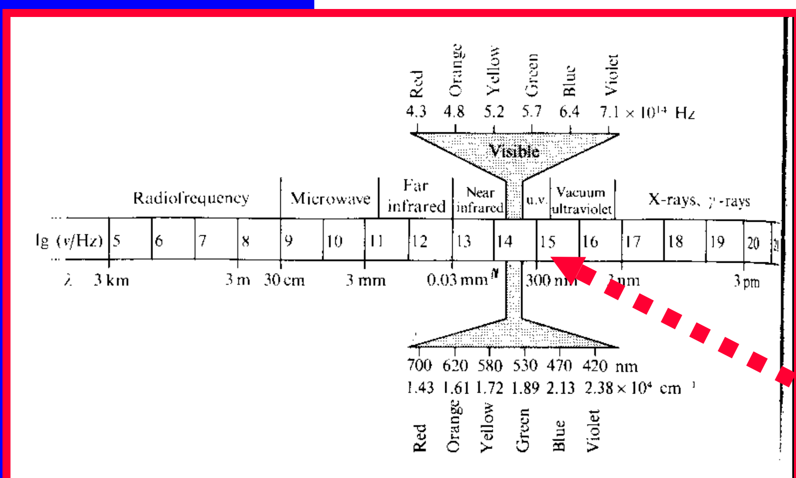

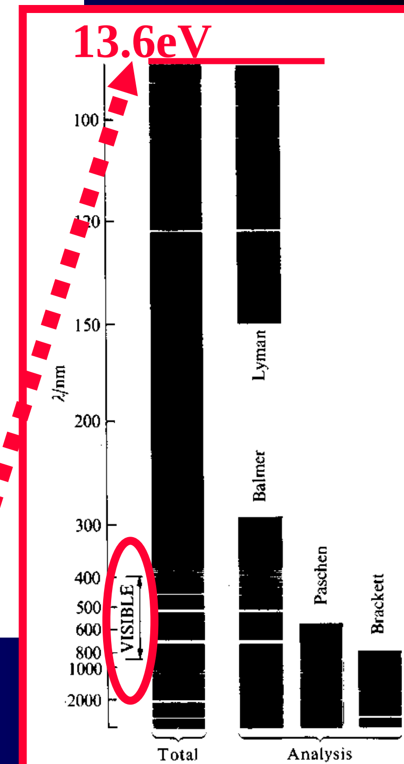

Fig. 15.1. The spectrum of atomic hydrogen. The spectrum is shown on the left, and is analysed into its overlapping series on the right. Note that the Balmer series lies in the visible region.

13.6eV x 8065,5 cm^{-1} → 109000 cm^{-1} → 91nm

Energy levels H

5.2 **Atomic structure and atomic spectra**

Fig. 15.12. A *Grotrian diagram* which summarizes the appearance and analysis of the spectrum of atomic hydrogen. The thicker the line, the more intense the transition.

$$E_n = -\frac{Z^2 \mu e^4}{32\pi^2 \varepsilon_0^2 \hbar^2} \, x \, \frac{1}{n^2}$$

$$h\nu = 13.6\left(\frac{1}{n_f^2} - \frac{1}{n_i^2}\right)[eV]$$

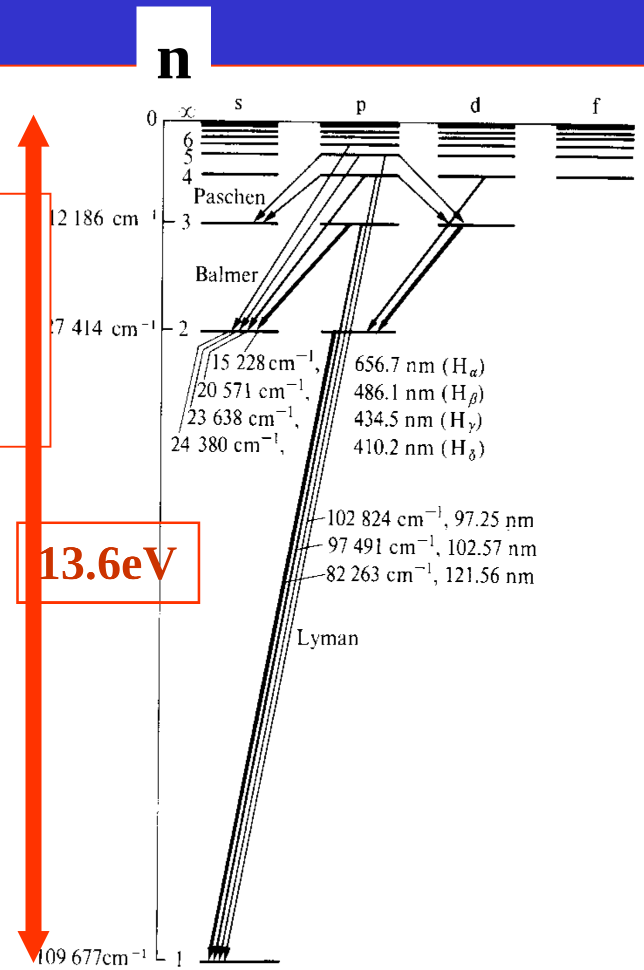

Fig. 15.12. A *Grotrian diagram* which summarizes the appearance and analysis of the spectrum of atomic hydrogen. The thicker the line, the more intense the transition.

13.6eV x 8065,5 cm^{-1} → 109000 cm^{-1} → 91nm

Rydberg

Energy levels He

Grotrian diagram He
Ionization energy He

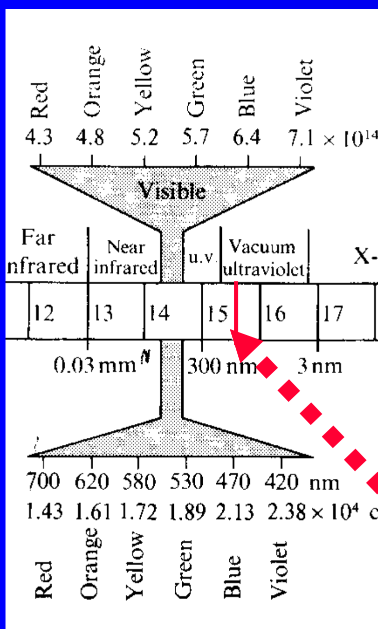

24.46eV

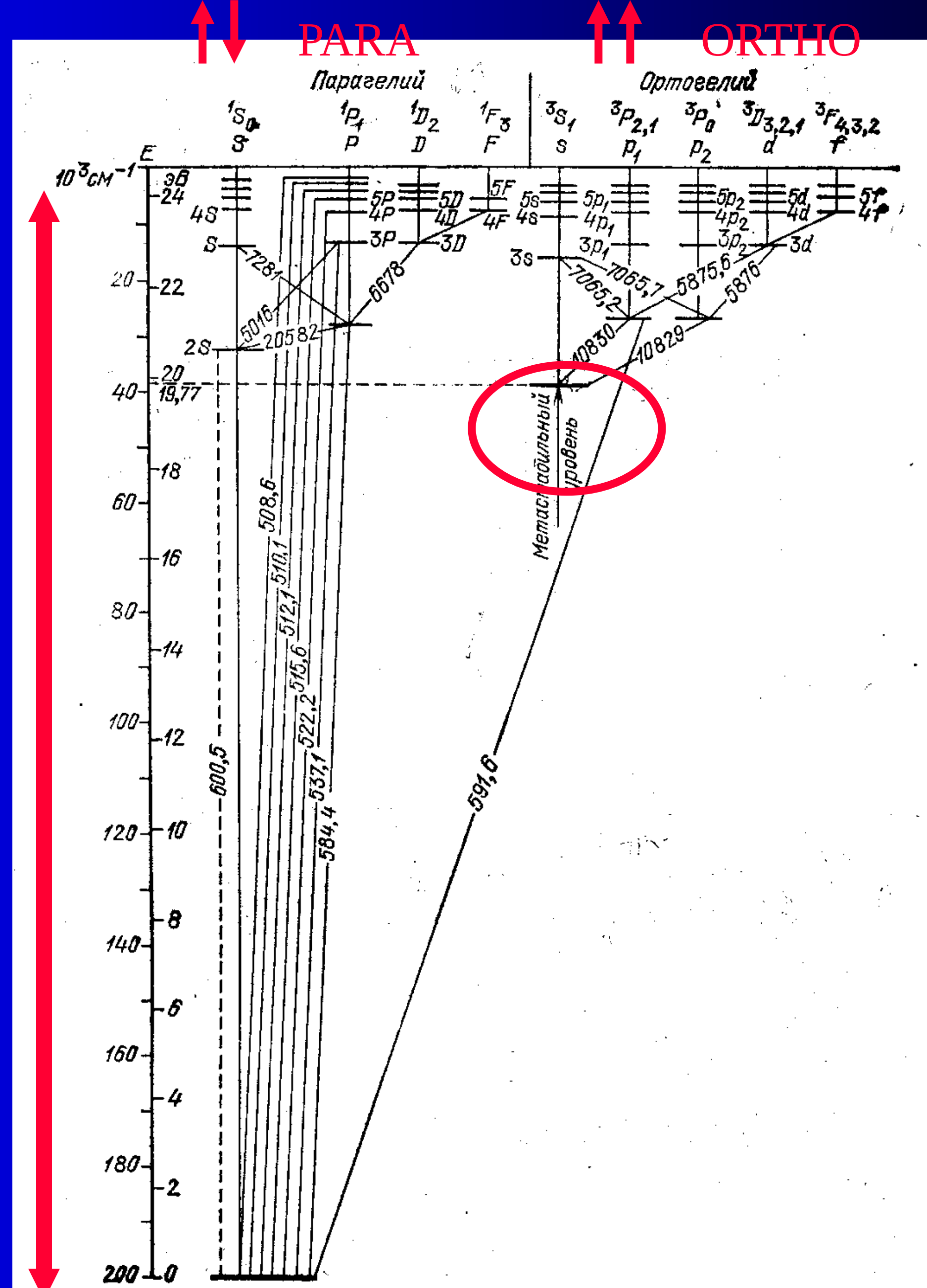

Рис. 3.8. Схема уровней атома He

24.46eV → ~198400 cm^{-1} → ~50nm
vacuum ultraviolet

Molecules

Time scale of interaction with electron

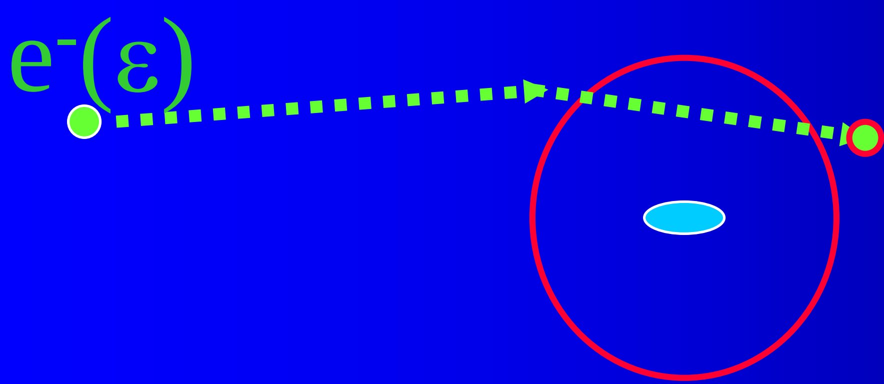

- What happens to the molecule when an electron goes by?
  - 70 eV electron => 5 x 10^6 m/s
  - Molecule = 10 A = 1 nm
    - Transit time = 2 x 10^{-16} s
    - Molecular vibrations > 10^{-12} s
    - Electronic time scale ~ 10^{-16} s
    - Frank-Condon principle: nuclei remain frozen in position

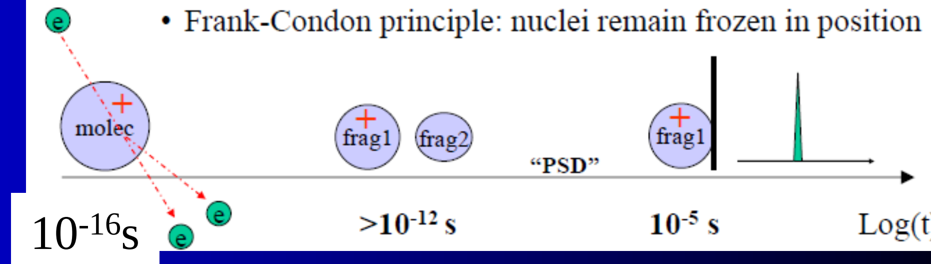

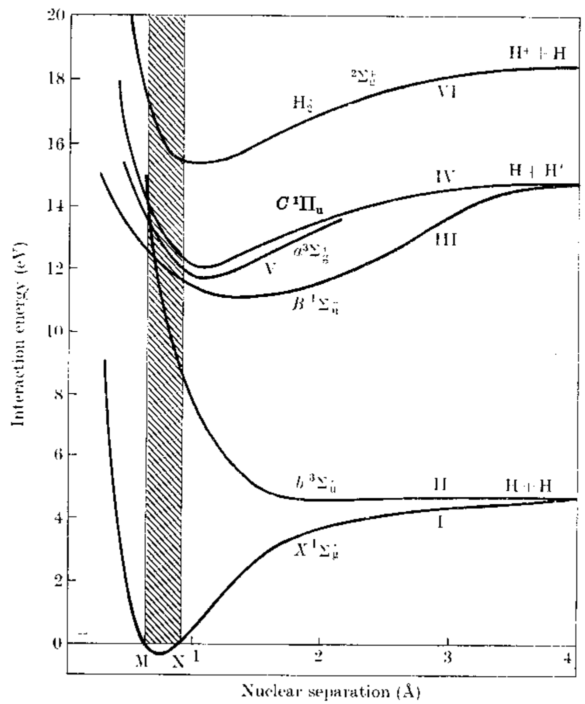

FIG. 13.1. Potential energy curves for electronic states of H_2 and H_2^+ lying within 20 eV of the ground state.

Interaction with molecules

Typical potential curves of diatomic molecules and H_2

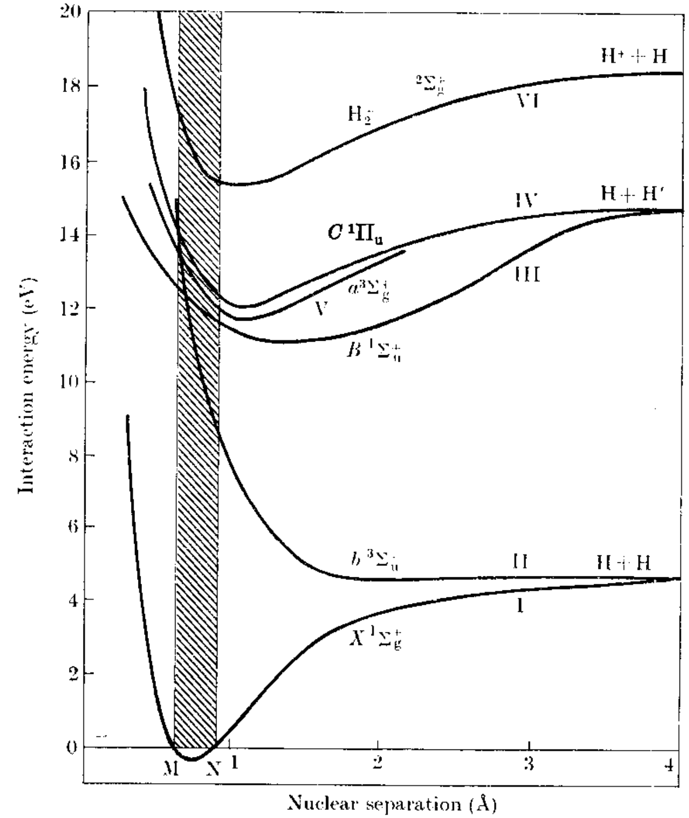

FIG. 13.1. Potential energy curves for electronic states of H_2 and H_2^+ lying within 20 eV of the ground state.

Franck-Condon Principle

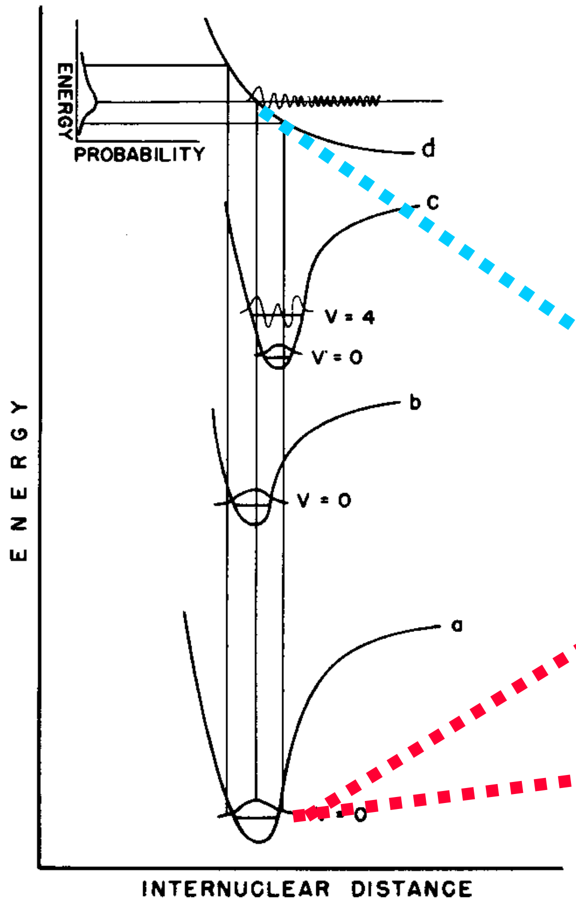

FIG. 21. Illustrative diatomic molecule and molecule-ion potential energy curves. The actual energy difference between curves a and b, c, and d is much greater than represented.

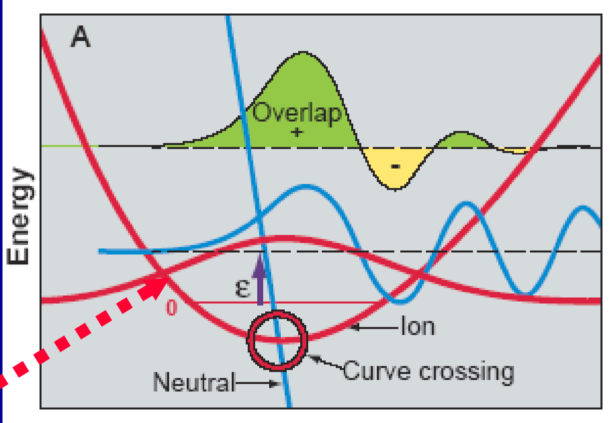

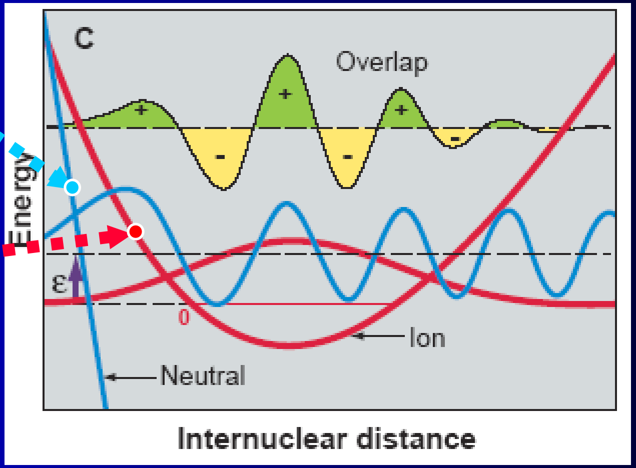

Franck-Condon Factors

$$P \sim <\psi_{initial.}\ \psi_{final}>^{2.}$$

Photoelectron spectrum H2

Franck-Condon Factors

$$P \sim \langle \psi_{initial.} \psi_{final} \rangle^{2.}$$

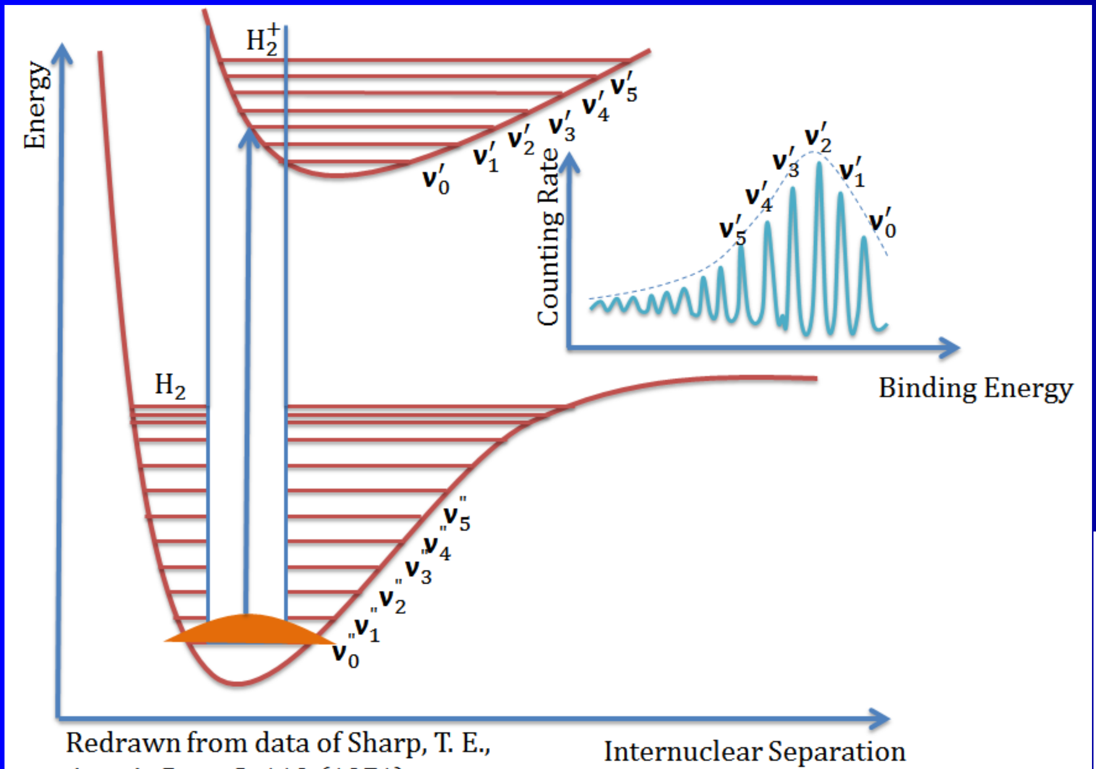

Fig. 3 Photoelectron spectrum of the ionization of H_2

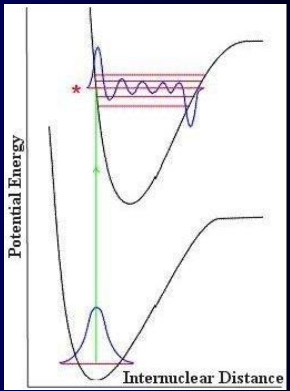

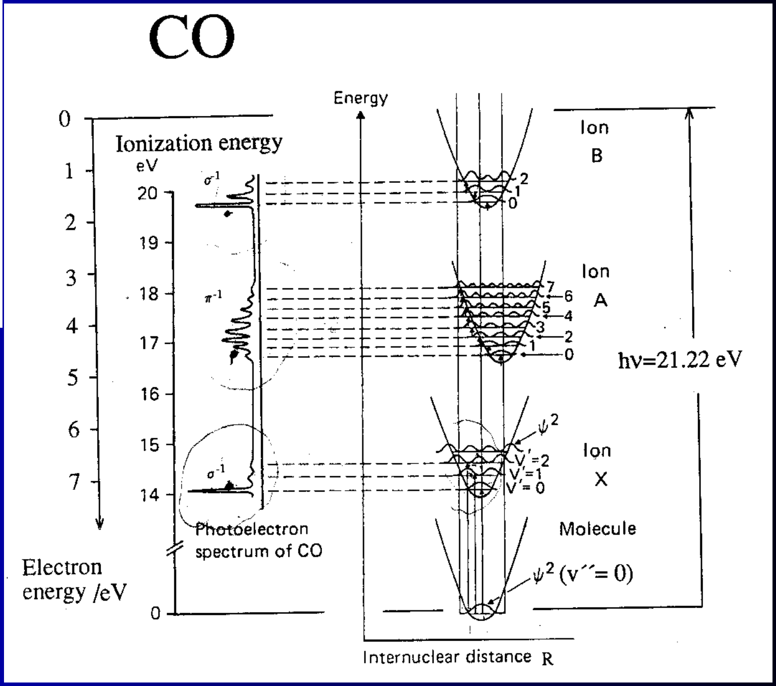

Cross sections for vibrational excitation, dissociation, ionization…H_2

H_2 + e	→ $H_2(v)$ + e …….	Vibrational excitation
	→ H + H +e…….	Dissociation
	→ H_2^* + hν + e …	Photon excitation
	→ H_2^+ +e + e…..	Ionization
	→ H^+ + H + e + e	Dissociative Ionization

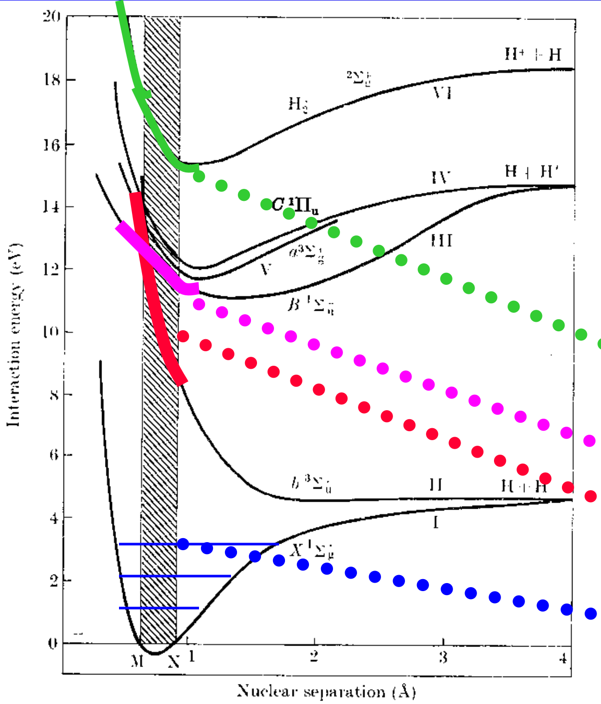

FIG. 13.1. Potential energy curves for electronic states of H_2 and H_2^+ lying within 20 eV of the ground state.

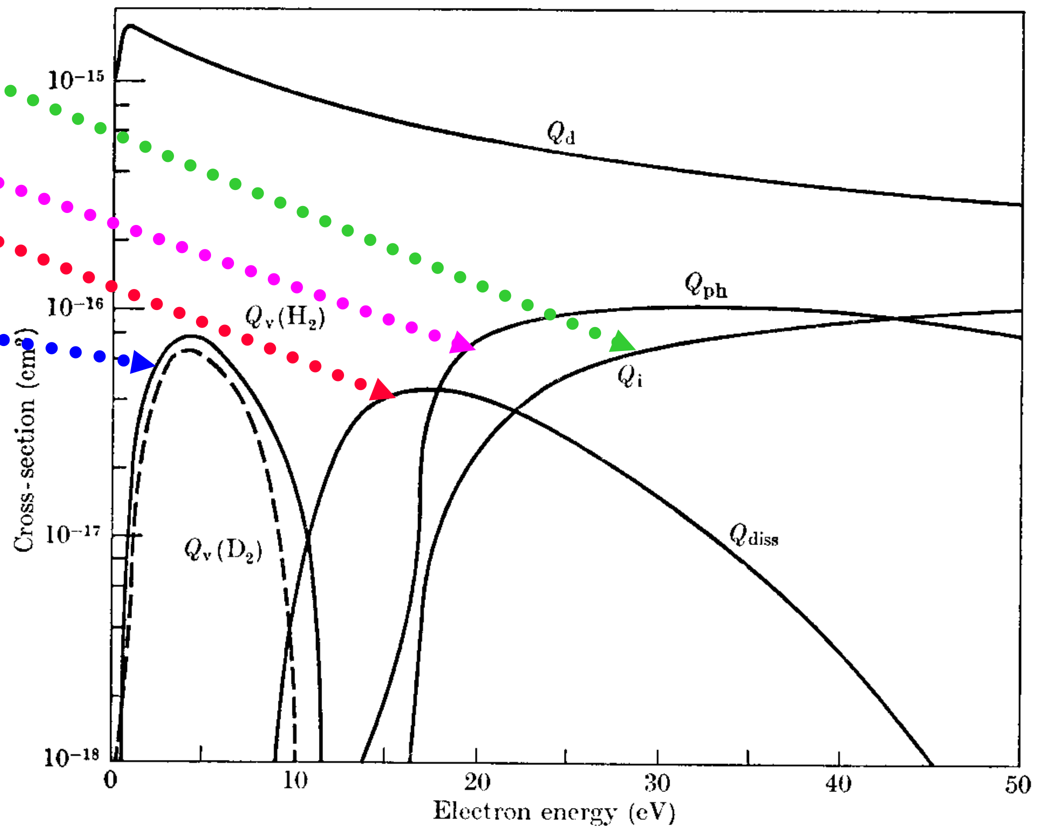

FIG. 13.37. Cross-sections assumed by Engelhardt and Phelps in their analysis of swarm data in H_2 and D_2 for electrons of characteristic energy greater than 1 eV. Q_d momentum-transfer cross-section, Q_i, ionization cross-section, Q_{diss} dissociation cross-section, Q_{ph} photon excitation cross-section, Q_v vibrational excitation cross-section (—— H_2, – – – D_2).

Details of interaction of electron with H_2 (1990)

CROSS SECTIONS FOR ELECTRON COLLISIONS WITH HYDROGEN 610

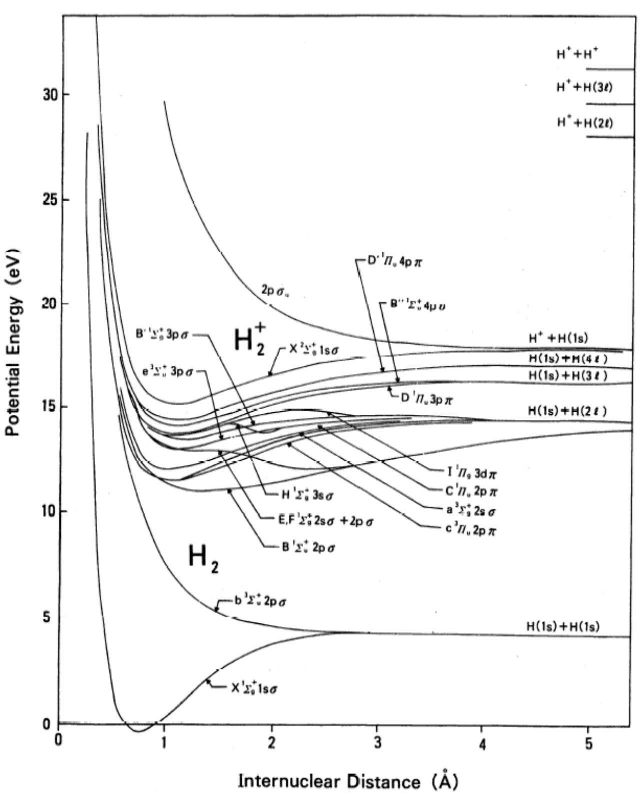

FIG. 1. Some important energy levels of molecular hydrogen and molecular ion (see Ref. 5).

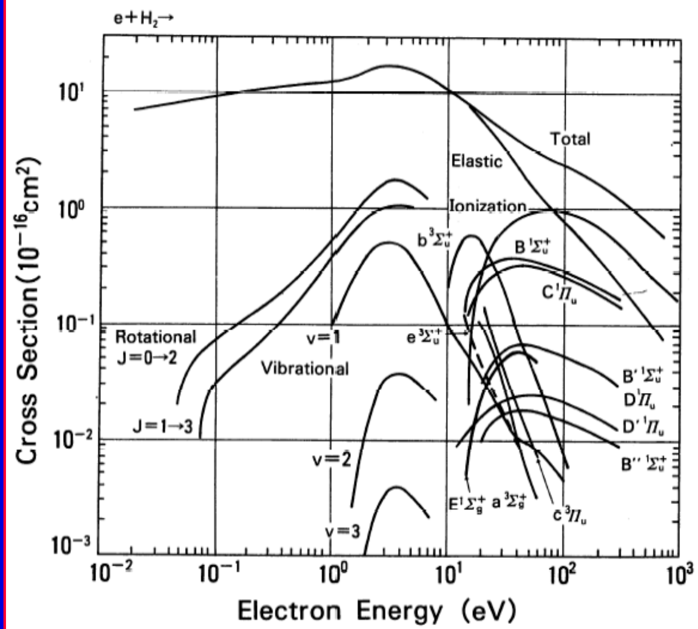

FIG. 2. Comparison of cross sections for various collision processes in neutral H_2. Also for comparison, cross sections of ionization of atomic hydrogen are shown. These data are taken at room temperatures.

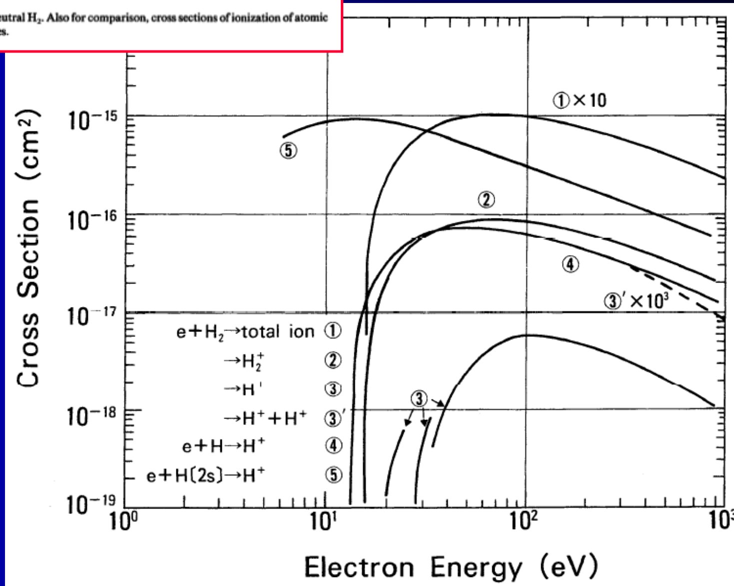

FIG. 16. Cross sections of the production for total ion, molecular hydrogen ions, protons and double protons. Those of proton production from H and H(2s) are also shown for comparison (see Ref. 125). Note that the short curves, for proton production at lower energies, correspond to the processes via $^2\Sigma_g$ (near-zero energy protons) and $^2\Sigma_u$ (repulsive state), respectively.

Cross Sections and Related Data for Electron Collisions with Hydrogen Molecules and Molecular Ions[a)]

H. Tawara, Y. Itikawa,[b)] H. Nishimura,[c)] and M. Yoshino[d)]

National Institute for Fusion Science,[e)] Nagoya 464-01, Japan

(Received July 5, 1989; revised manuscript received November 1, 1989)

Data are compiled and evaluated for collision processes of excitation, dissociation, ionization, attachment, and recombination of hydrogen molecules and molecular ions (H_2^+, H_3^+) by electron impact as well as for properties of their collision products.

Key words: electron impact; hydrogen molecule; hydrogen molecular ion; scattering; elastic integral; vibrational excitation; rotational excitation; dissociation; ionization; photon emission; cross section.

J. Phys. Chem. Ref. Data, Vol. 19, No. 3, 1990

Dissociative ionization $H_2 + e \rightarrow H^+ + H + e$

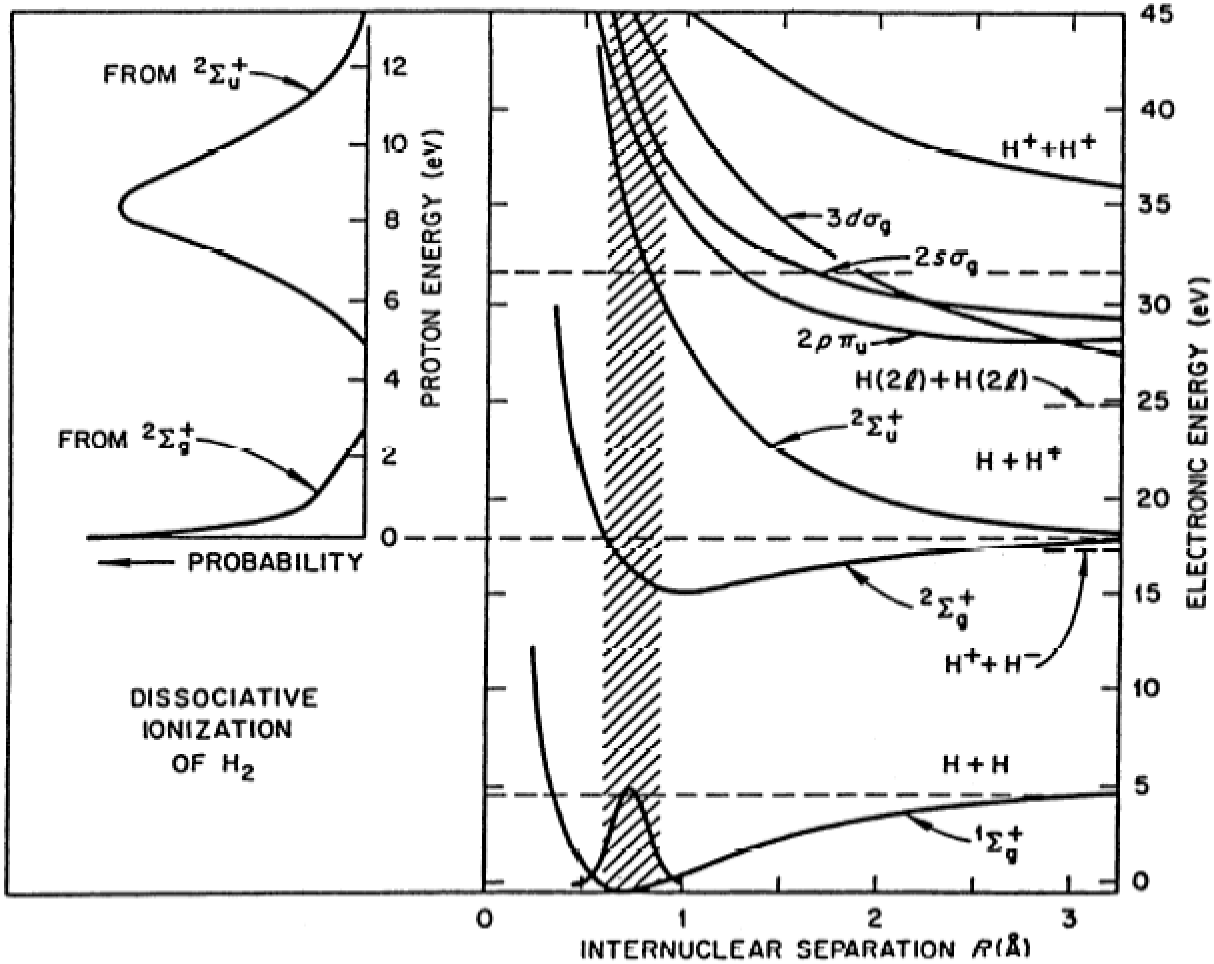

FIG. 21. Potential energy curves of H_2, H_2^+ and H_2^{2+} and the expected energy distributions of protons produced via $^2\Sigma_g^+$ and $^2\Sigma_u^+$ states of H_2^+ in dissociative ionization of H_2 (see Ref. 115).

Rotational excitation N_2

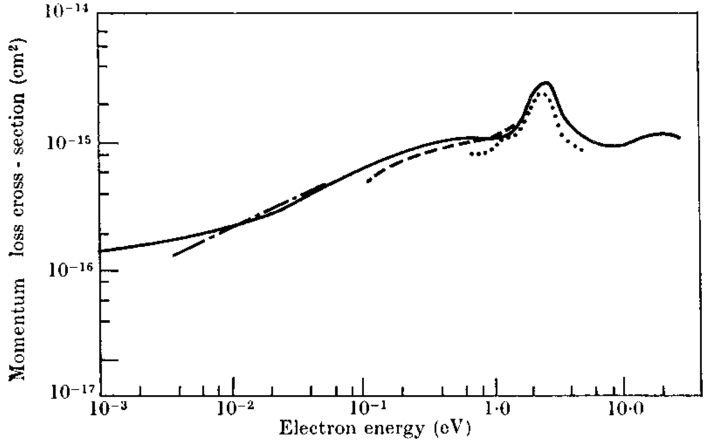

FIG. 11.30. Momentum-transfer cross-section for electrons in N_2. —— derived by Engelhardt, Phelps, and Risk from analysis of swarm data. —·—·— derived by Pack and Phelps from analysis of their drift velocity observations. — — — derived from drift velocity observations of Crompton and Sutton. · · · · total cross-section measured by Ramsauer method.

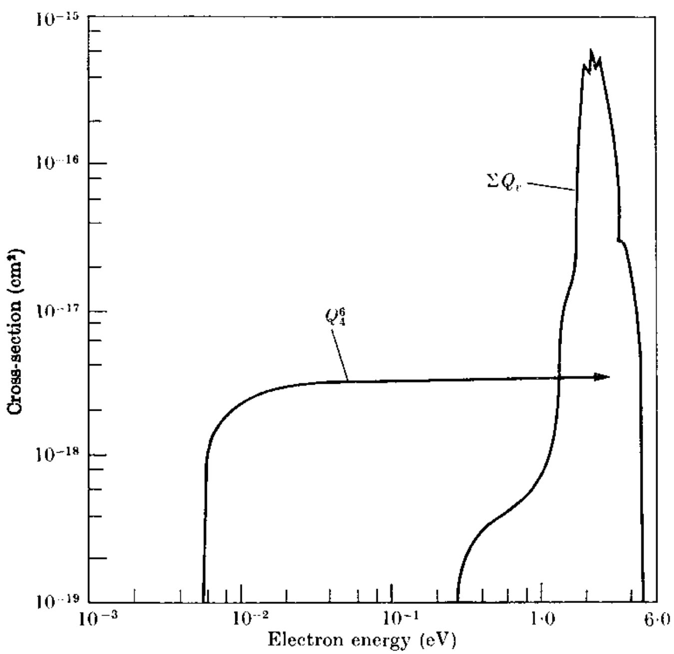

FIG. 11.31. Cross-sections for rotational and vibrational excitation of nitrogen. Q_4^6 is the cross-section for the rotational excitation $J = 4 \rightarrow J = 6$. $\Sigma_v Q_v$ is the sum of the cross-sections for vibrational excitation consistent with the swarm data.

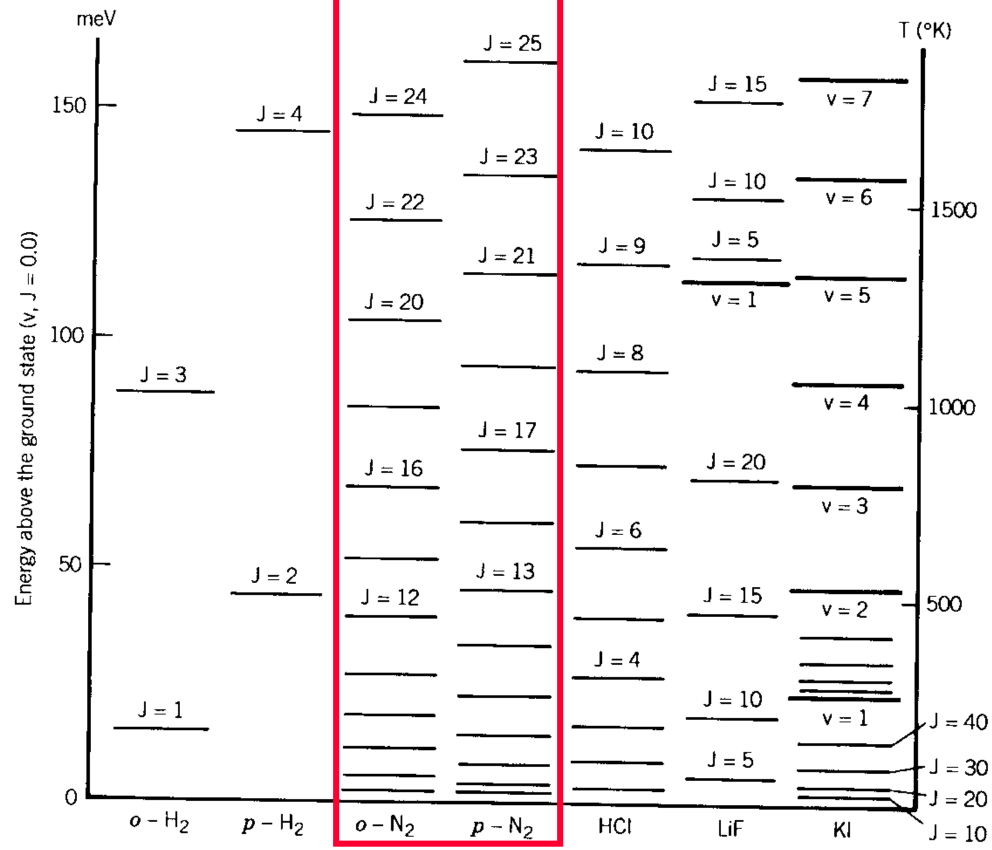

Figure 2-2-1. Vibrational–rotational levels (quantum numbers v and J) of a few diatomic molecules. The ($v = 1$, $J = 0$) level of H_2 lies 0.54 eV above the ground state ($v = 0$, $J = 0$). Rotational level spacings for H_2 are uniquely large, about 15J meV, where J is the quantum number for the upper level. For the ortho species of H_2(o-H_2), the nuclear spins are parallel; for the para version (p-H_2), the nuclear spins are antiparallel. [From Shimamura (1984).]

Vibr. excitation of N_2 fine structure

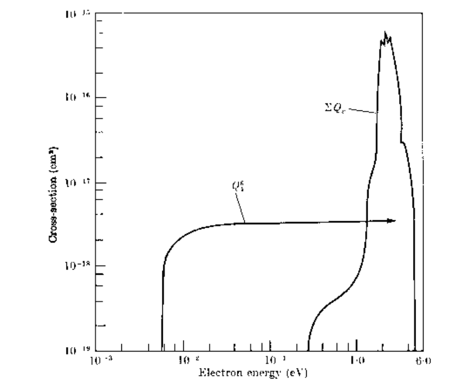

Fig. 11.31. Cross-sections for rotational and vibrational excitation of nitrogen. Q_4^6 is the cross-section for the rotational excitation $J = 4 \rightarrow J = 6$. $\Sigma_v Q_v$ is the sum of the cross-sections for vibrational excitation consistent with the swarm data.

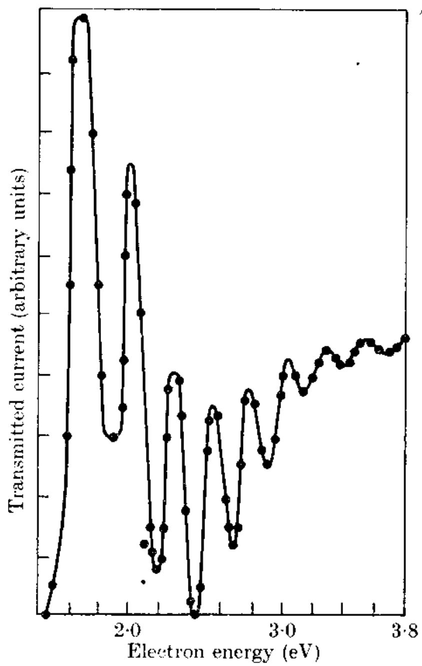

Fig. 10.32. Fine structure observed by Golden and Nakano in the transmission of electrons through N_2. The points are obtained from a number of plots of the transmitted current. Because of electron optical effects no significance attaches to the relative magnitudes of peaks and troughs.

of a theory such as that outlined above. Haas suggested that we must regard the collisions as taking place in two stages—the incident electron is first captured to form a negative ion N_2^- that is energetically unstable but has a lifetime greater than a vibrational period. It eventually breaks up, becoming a neutral molecule that may be in an excited vibrational state—in other words, the process is regarded as a resonance one of the same type as that found in elastic scattering of electrons by helium and other atoms and molecules (see Chap. 9).

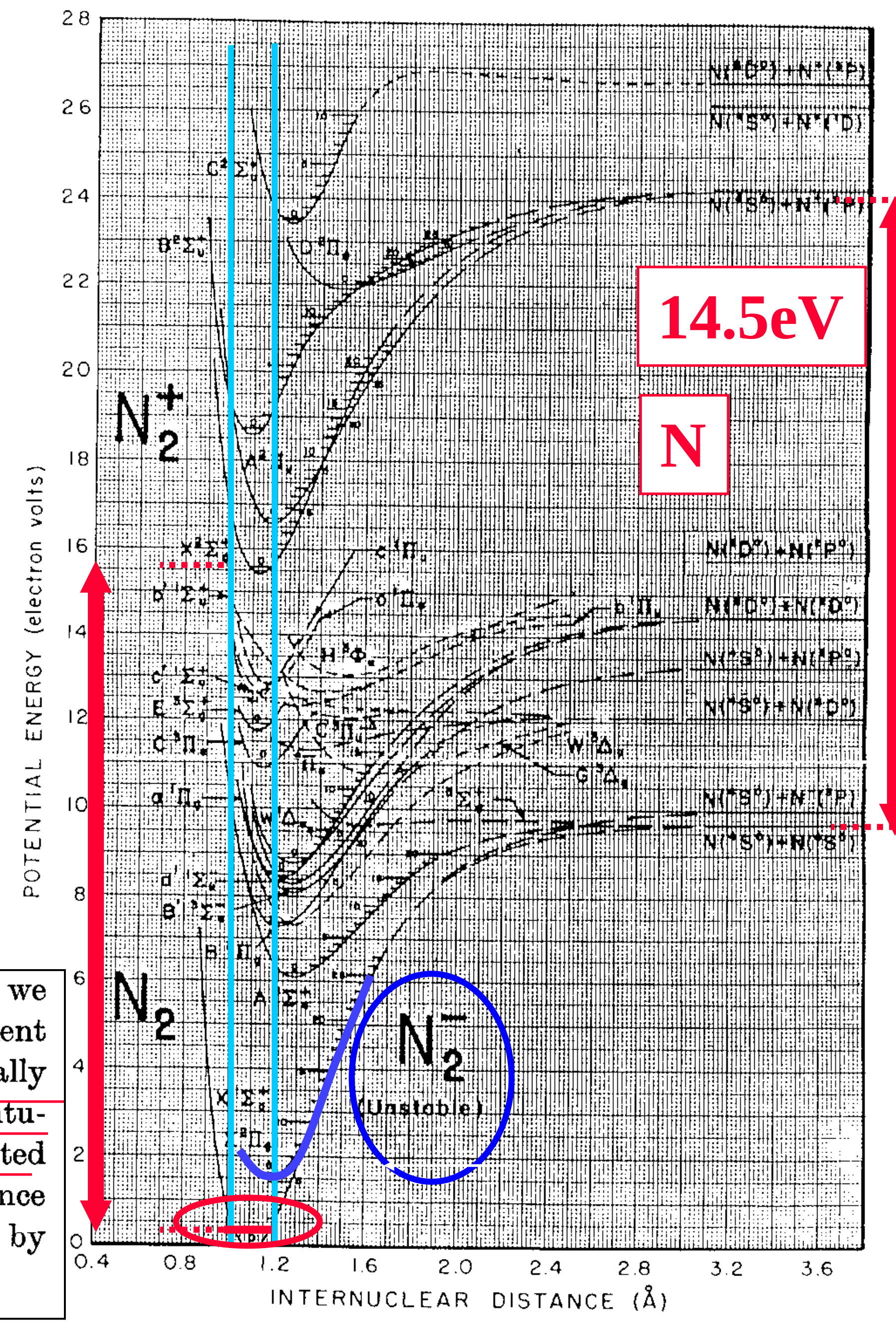

FIGURE 1. Potential energy curves for N_2 and N_2^+.*

Next → IONIZATION

Time scale of ionization

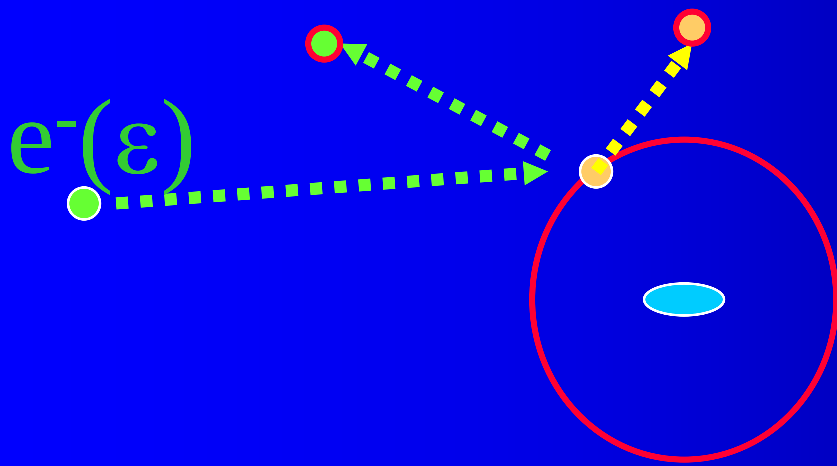

- What happens to the molecule when an electron goes by?
  - 70 eV electron => 5 x 10^6 m/s
  - Molecule = 10 A = 1 nm
    - Transit time = 2 x 10^{-16} s
    - Molecular vibrations > 10^{-12} s
    - Electronic time scale ~ 10^{-16} s
    - Frank-Condon principle: nuclei remain frozen in position

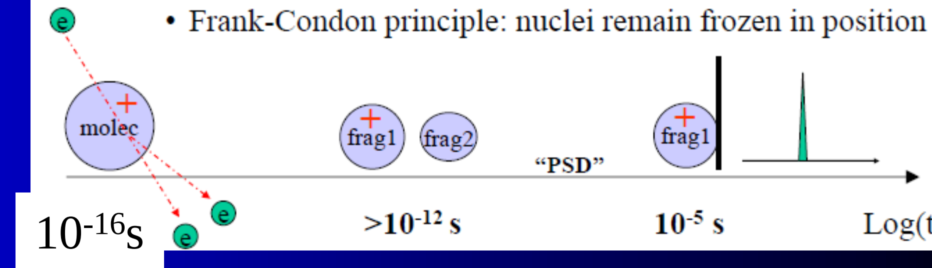

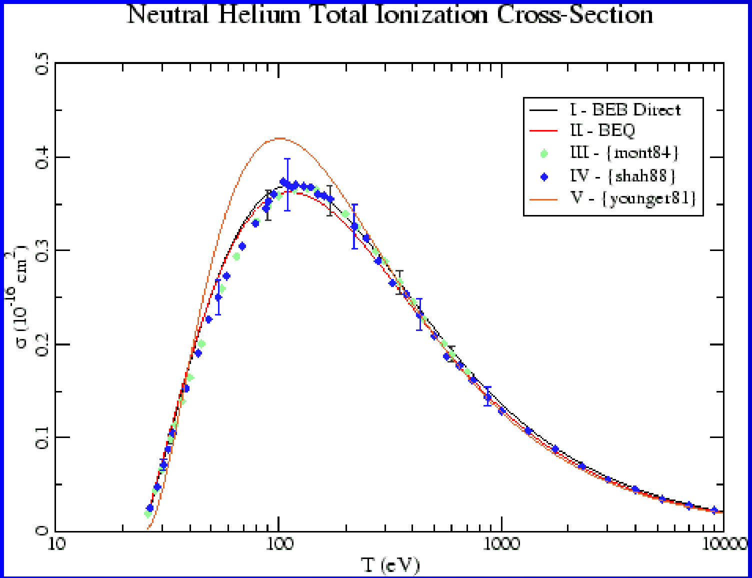

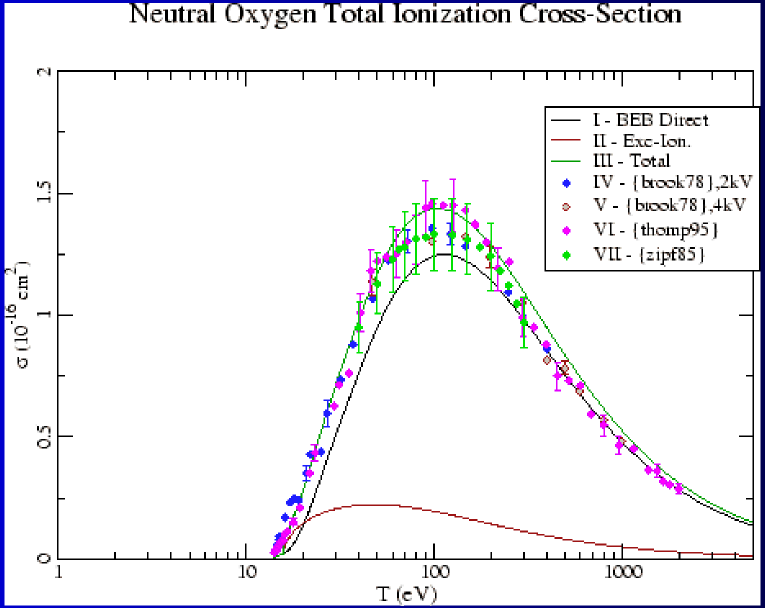

http://physics.nist.gov/cgi-bin/Ionization/ion_data.

Table of Ionization Cross Sections at Specific Energies (tab-delimited ASCII)

Atomic Orbital Constants for BEB Calculation of the Direct Cross Section

Total Ionization Cross Section

Ionization cross section

Ionization

Simple

$$Ar + e^-(\varepsilon_0) \rightarrow Ar^+ + e_1^-(\varepsilon_1) + e_2^-(\varepsilon_2)$$

Complicated

$N_2(\nu,j) + e^-(\varepsilon_0)$ $\rightarrow N_2^+(\nu,j) + e_1^-(\varepsilon_1) + e_2^-(\varepsilon_2)$

$\rightarrow N^+(\varepsilon_{KIN}) + N(\varepsilon_{KIN}) + e_1^-(\varepsilon_3) + e_2^-(\varepsilon_4)$

$NH_3 + e^-(\varepsilon_0) \rightarrow$ **…..to many channels**

Ionization energies

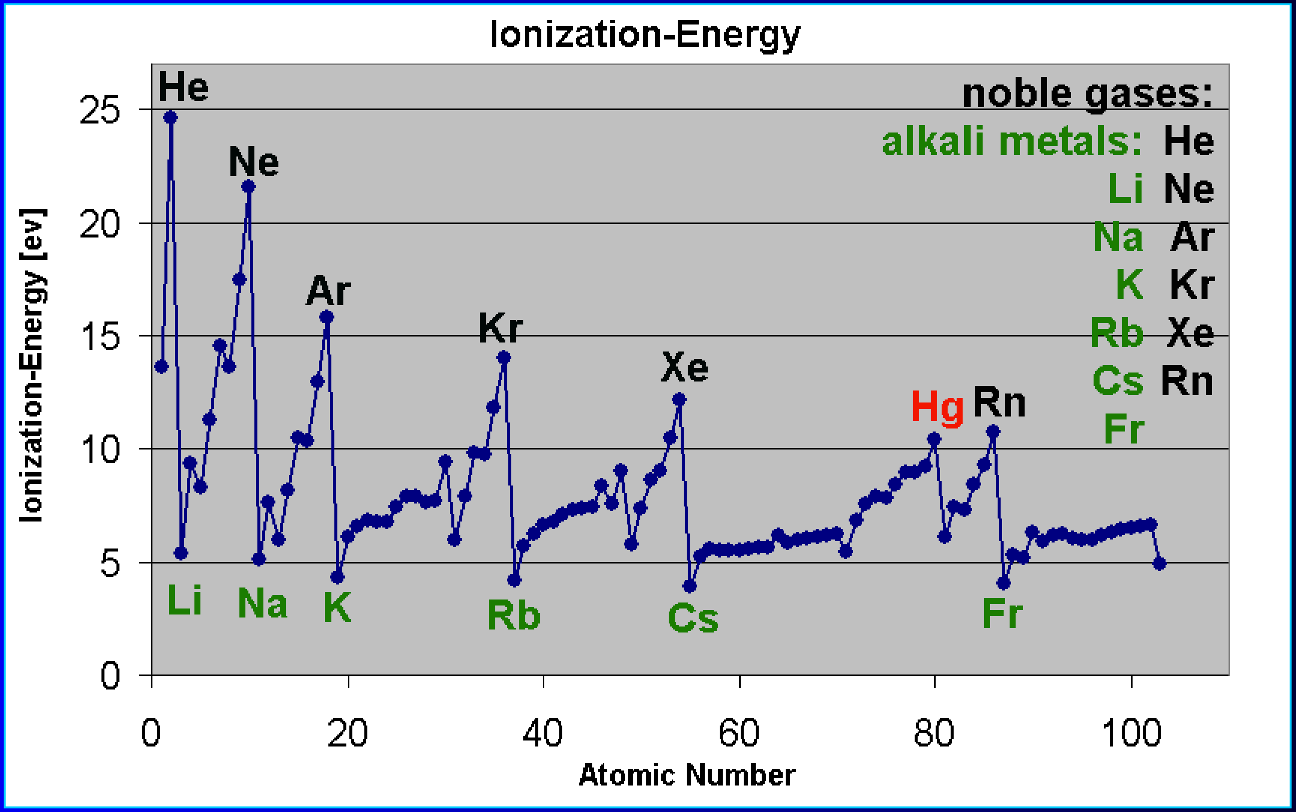

$Ar + e^{-}(\varepsilon_0) \rightarrow Ar^{+} + e_1^{-}(\varepsilon_1) + e_2^{-}(\varepsilon_2)$

$N_2 + e^{-}(\varepsilon_0) \rightarrow$ ion

Ionization energies

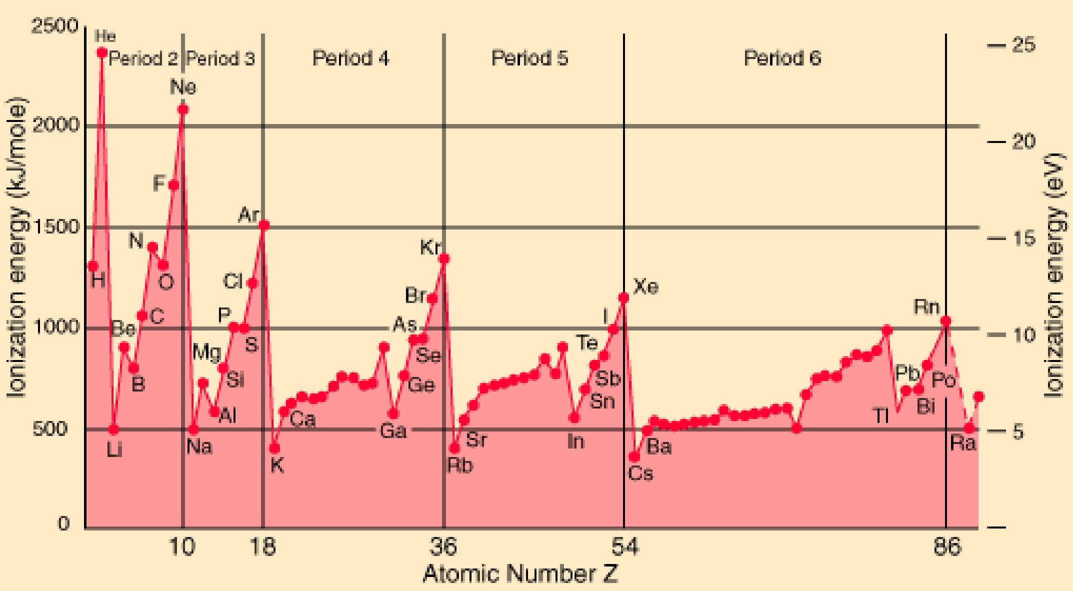

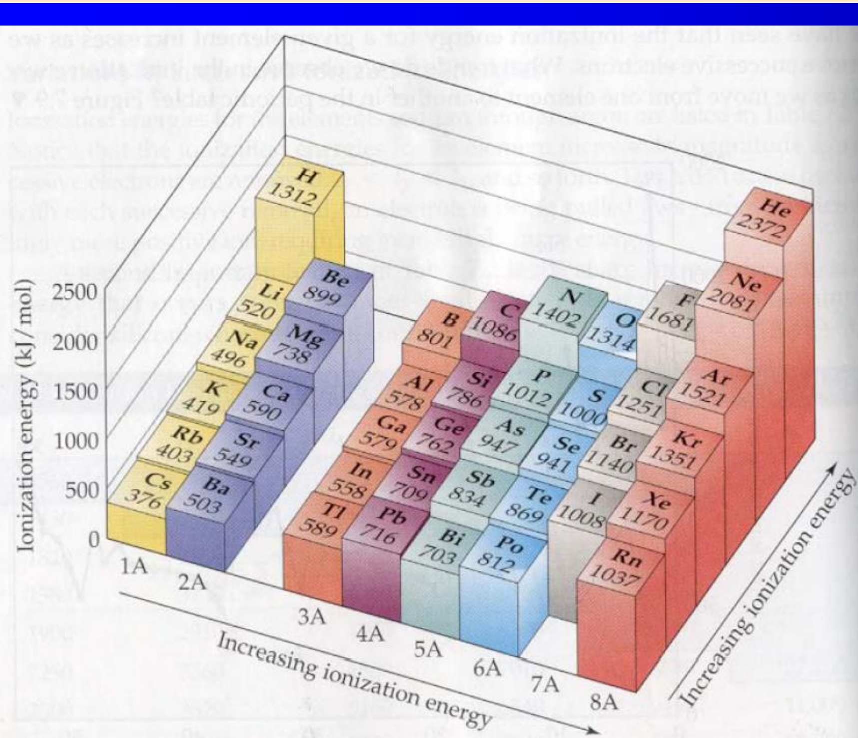

Ionization Energy

- **First ionization energy (IE_1)**

The minimum amount of energy required to remove the most loosely bound electron from an isolated gaseous atom to form a 1+ ion.

$$\text{atom}_{(g)} + \text{energy} \rightarrow \text{ion}^{+}_{(g)} + e^{-}$$

Element/Compound	Ionization Potential (Volts or eV)
He	24.6
Ar	15.8
H_2	15.4
N_2	15.6
O_2	12.1
CO_2	13.8
CO	14.1
C	11.3
Si	8.2
Fe	7.9
Ni	7.6
Na	5.1
K	4.3
Cs	3.9

Electron affinity

$$A + e^{-}(\varepsilon_0) \rightarrow A^{-}$$

Electron Affinity

- Electron affinity is the amount of energy ***absorbed*** when an electron is added to an isolated gaseous atom to form an ion with a -1 charge.
- Electron affinity is a measure of an atom's ability to form negative ions.

$$\text{atom(g)} + e^{-} + \text{EA} \rightarrow \text{ion}^{-}\text{(g)}$$

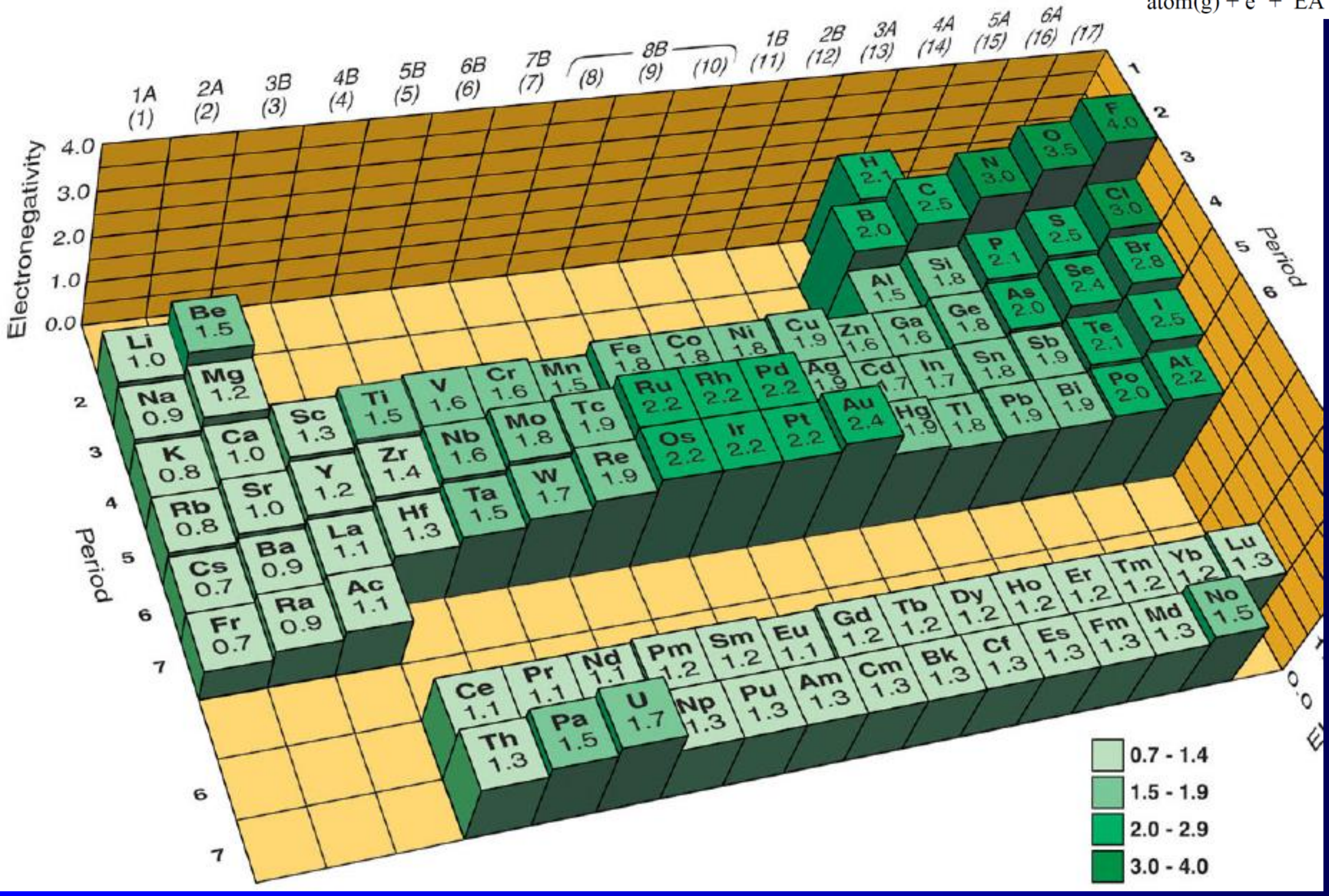

Ionization energies

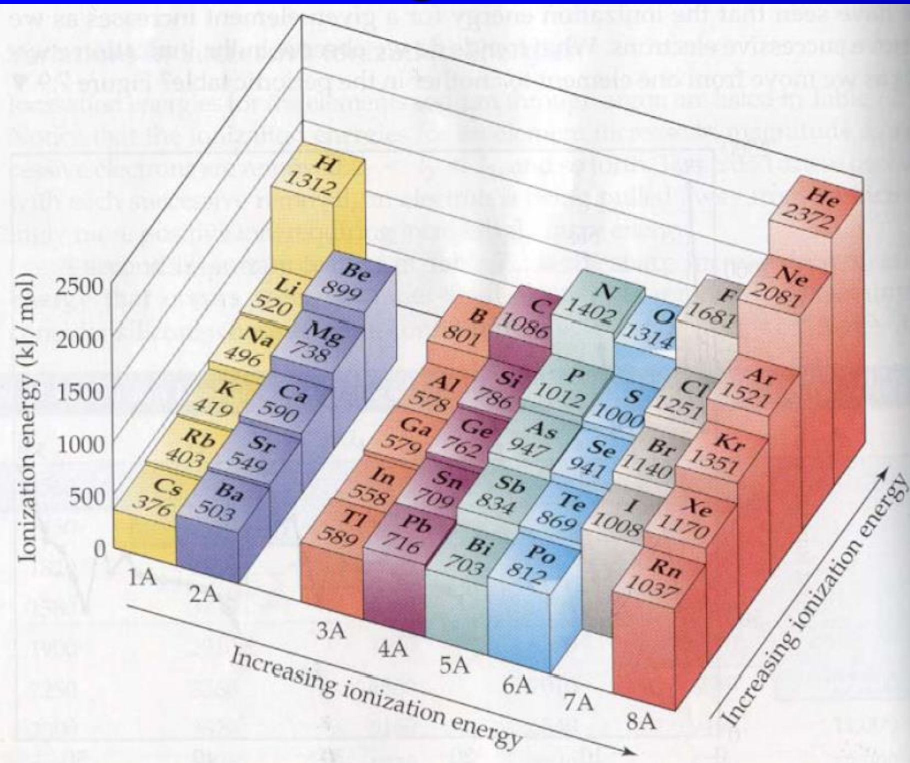

Electron affinity

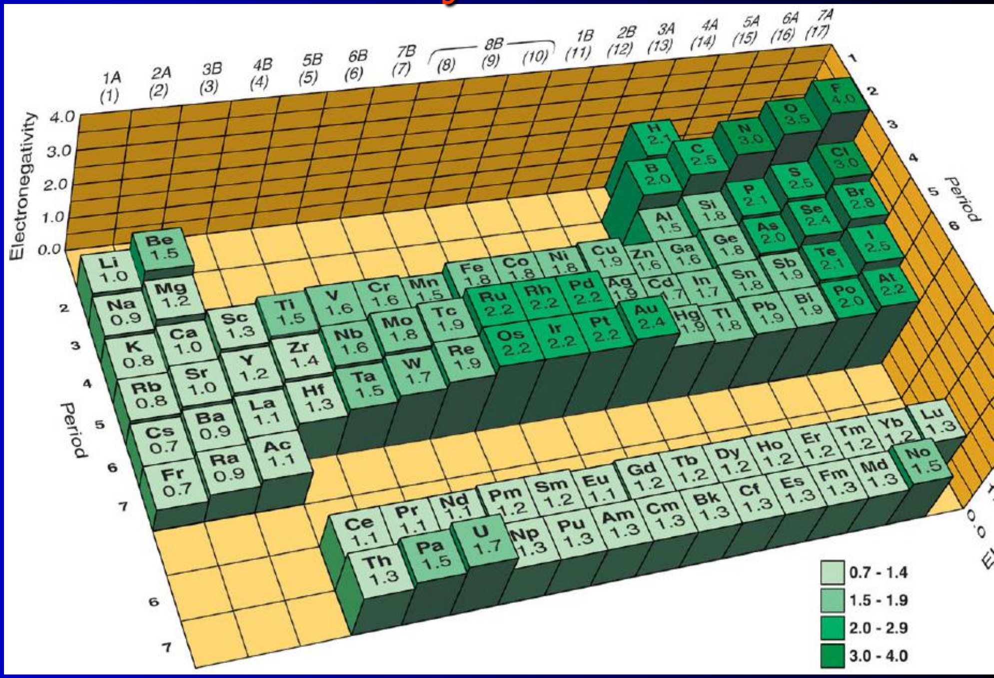

$$A + e^-(\varepsilon_0) \rightarrow A^+ + 2e$$

$$A + e^-(\varepsilon_0) \rightarrow A^-$$

Ionization of molecules

Potential Energy Surface Description of the Ionization of Dihydrogen

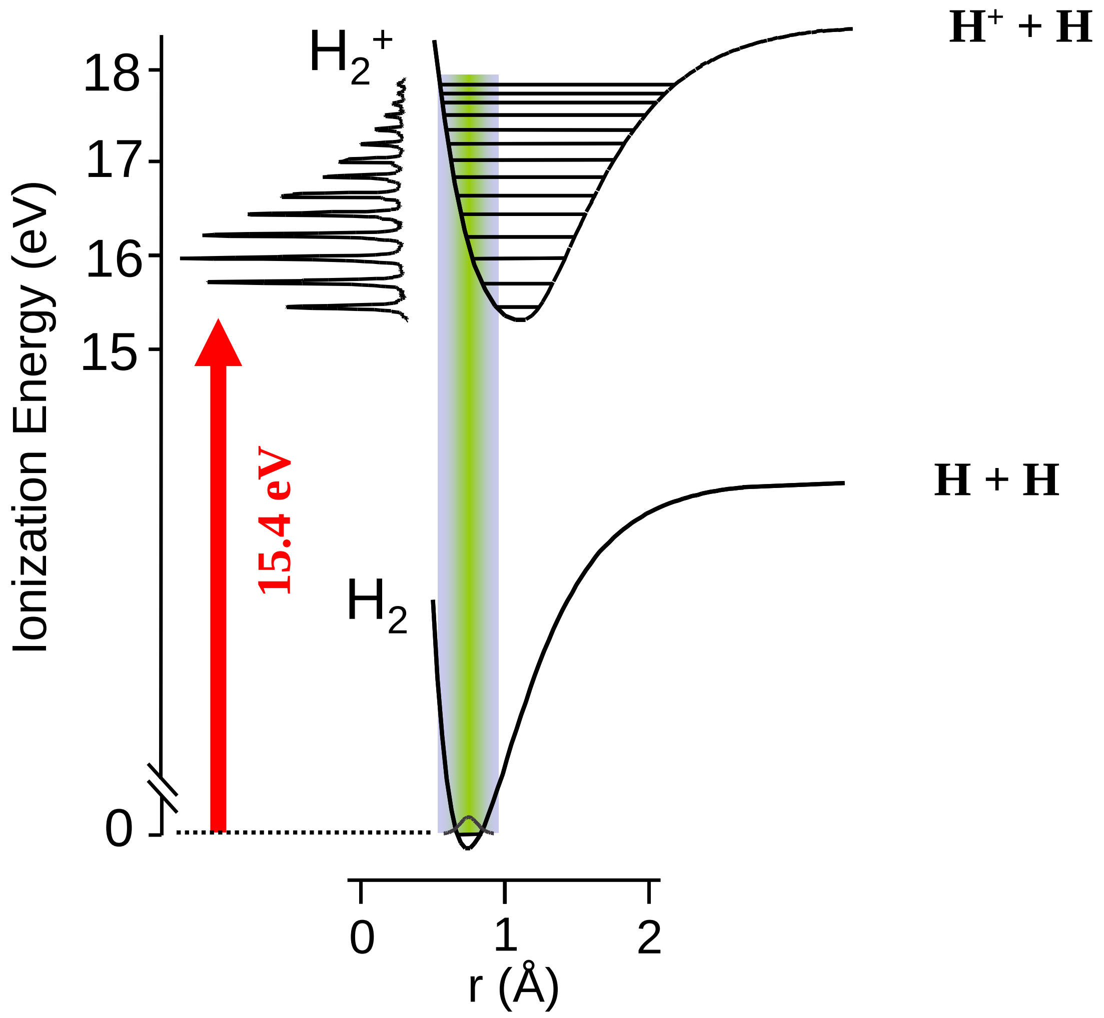

Ionization of molecules

Potential Energy Surface Description of the Ionization of Dihydrogen

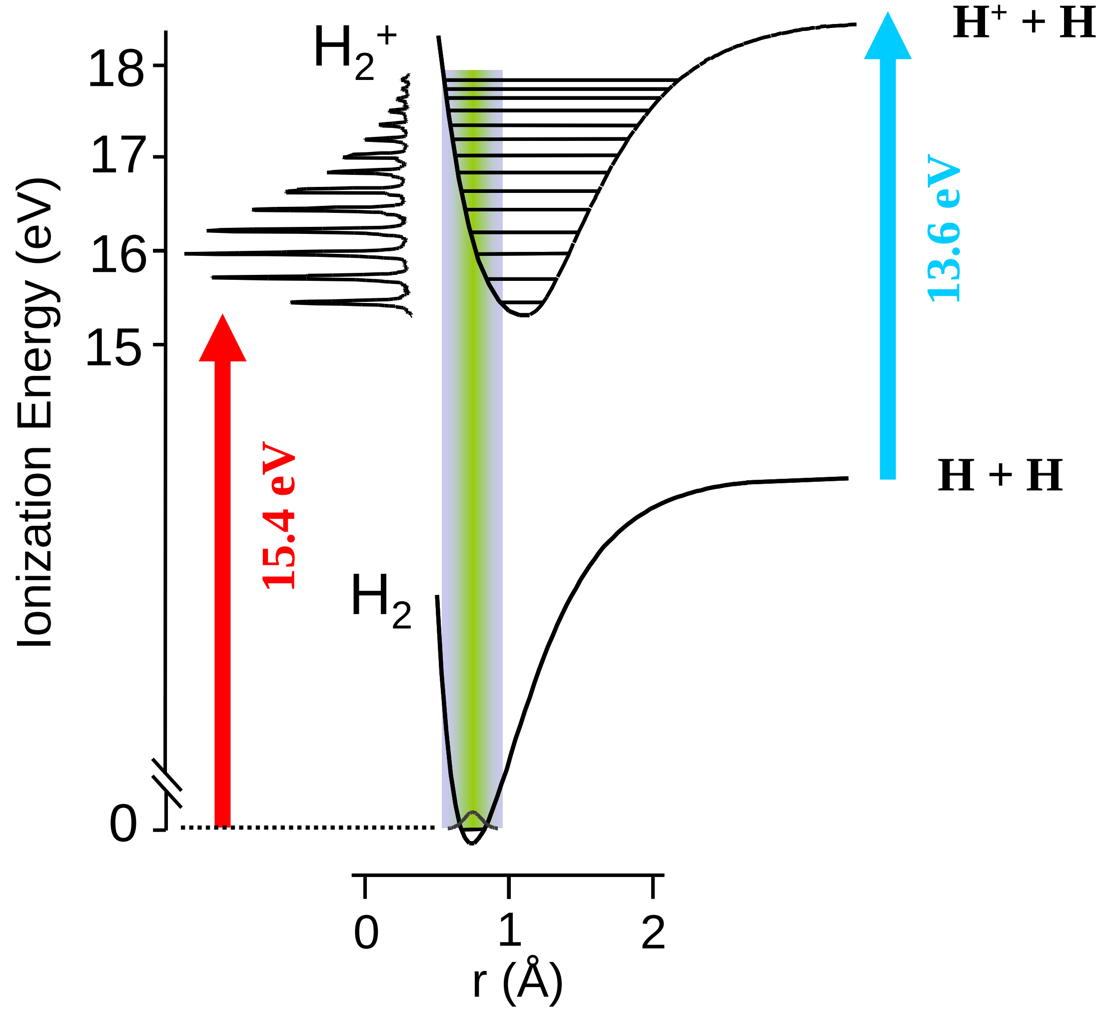

Ionization energies of molecules

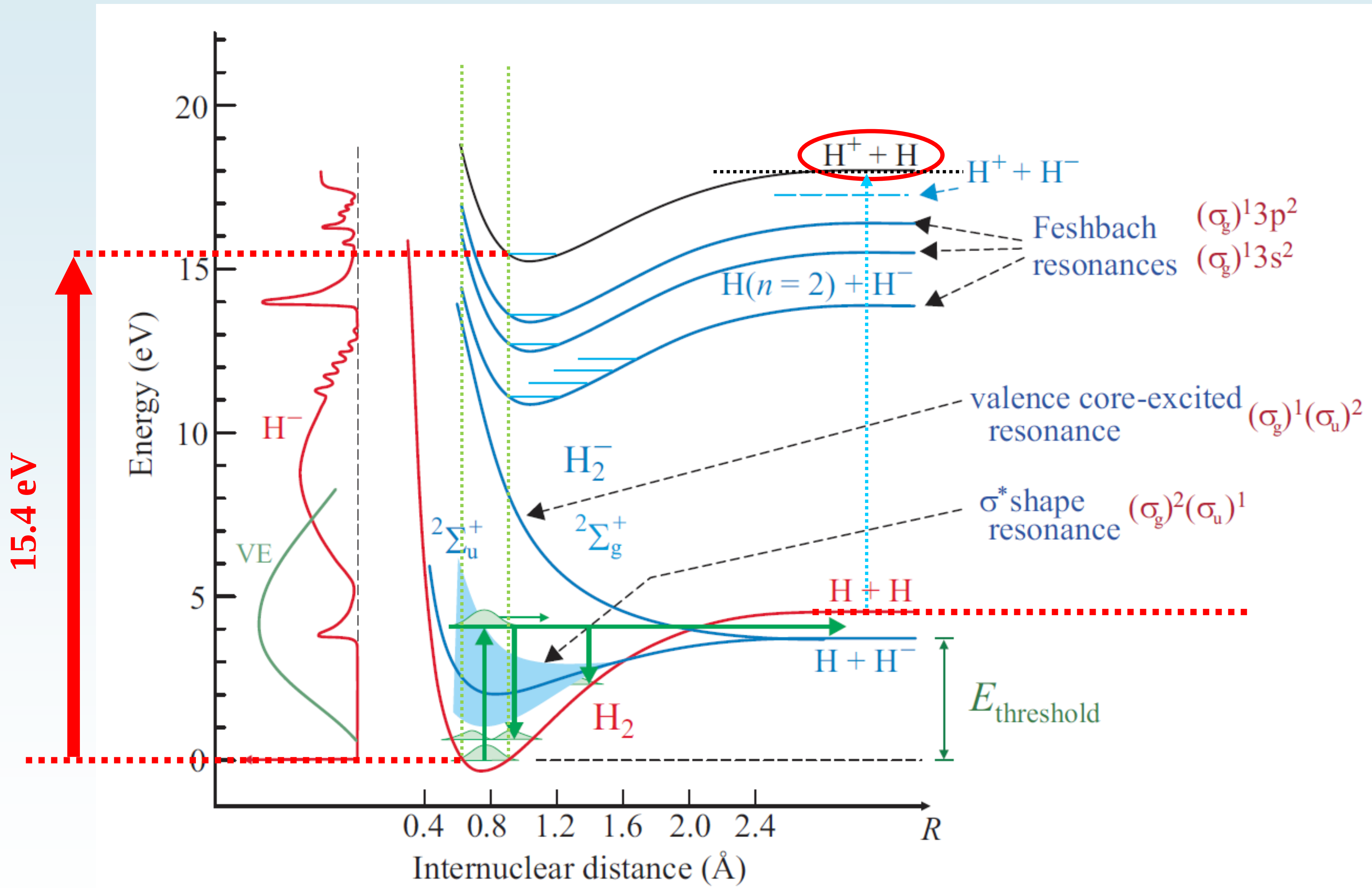

Ionization energies of molecules

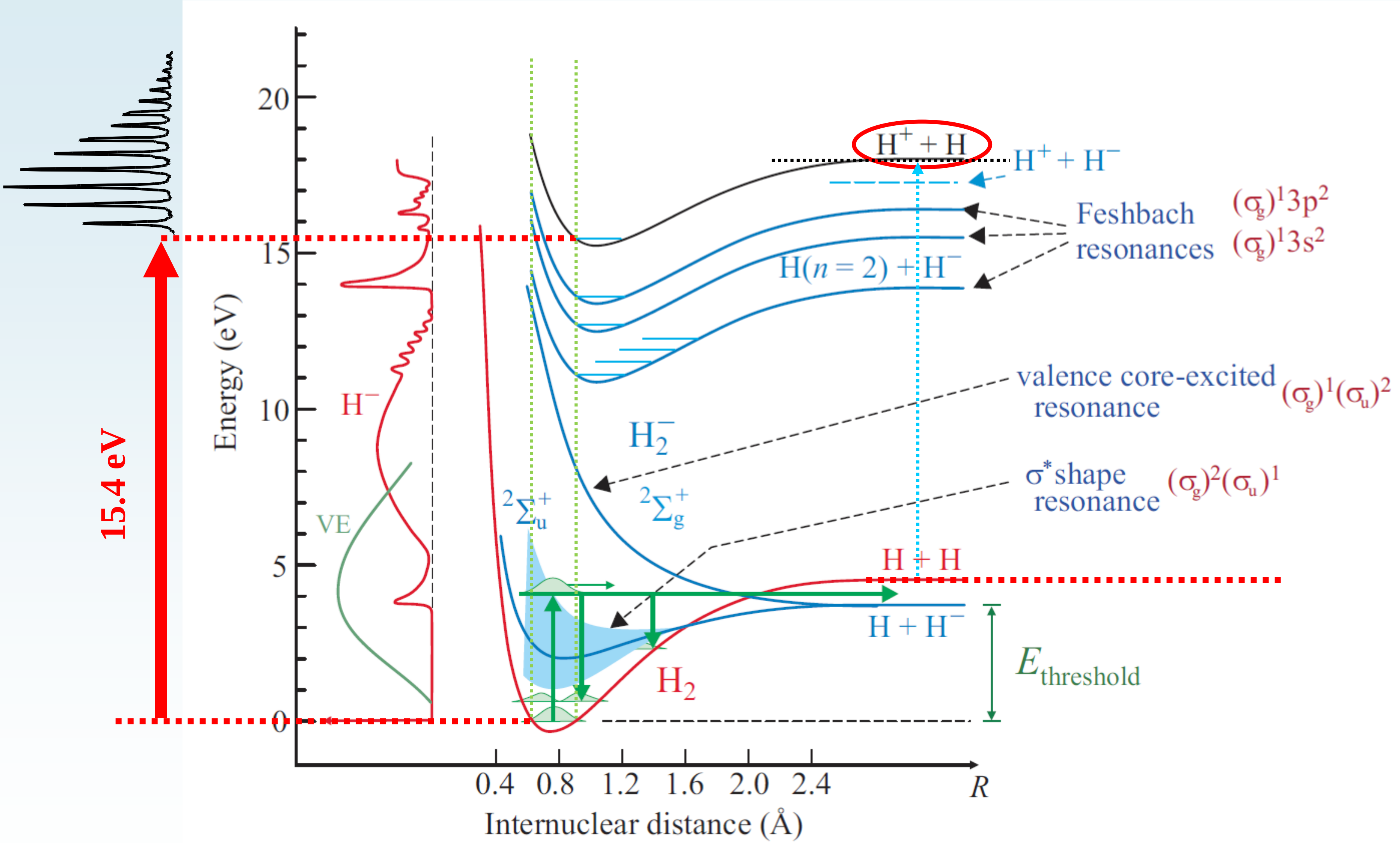

Photoelectron spectrum H2

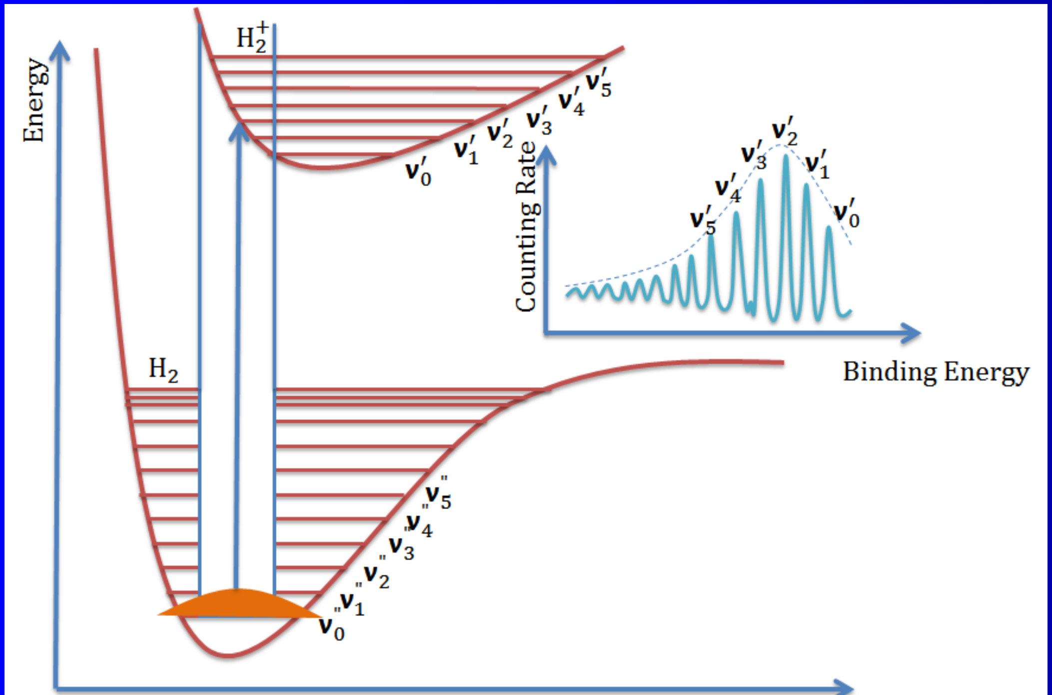

Redrawn from data of Sharp, T. E., *Atomic Data*, **2**, 119 (1971)

Fig. 3 Photoelectron spectrum of the ionization of H_2

$$P \sim \langle \psi_{initial.}\, \psi_{final} \rangle^{2.}$$

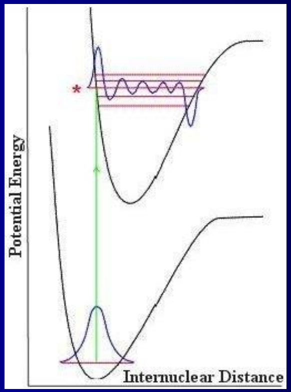

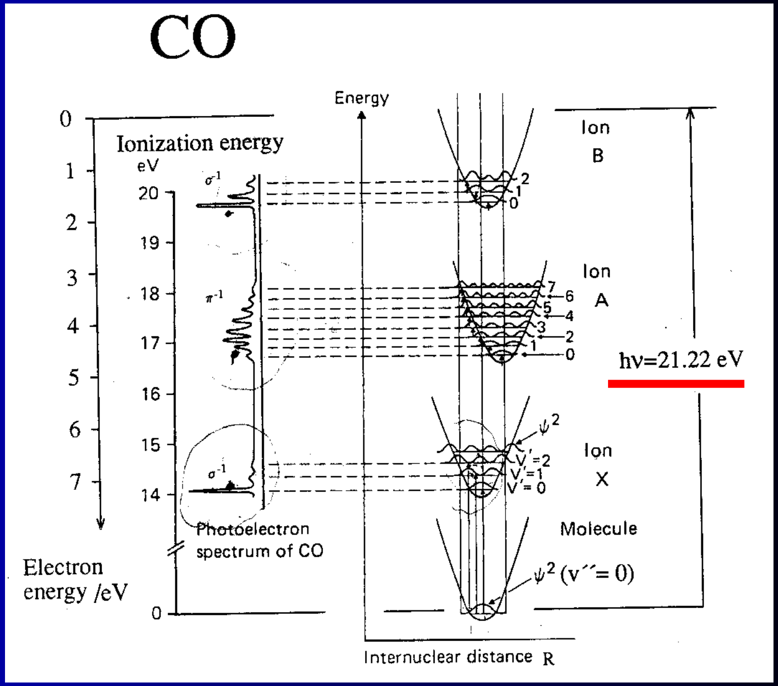

Ionization cross section He and N_2

Electron impact

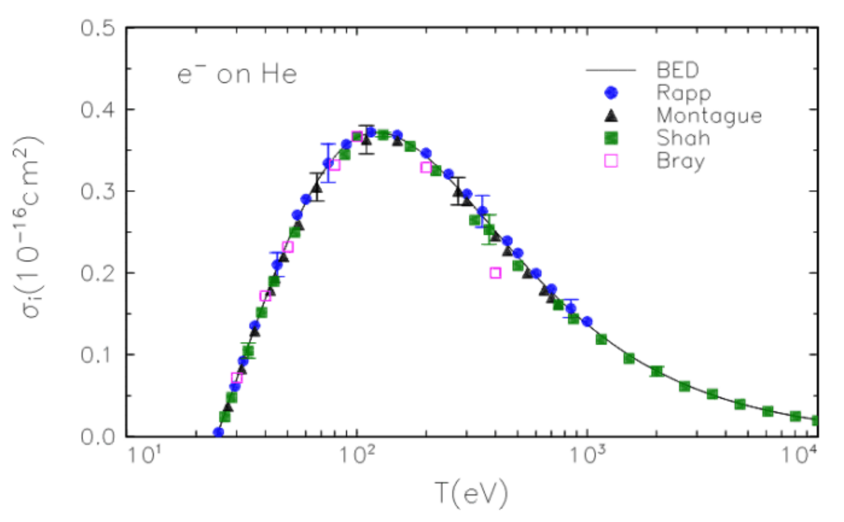

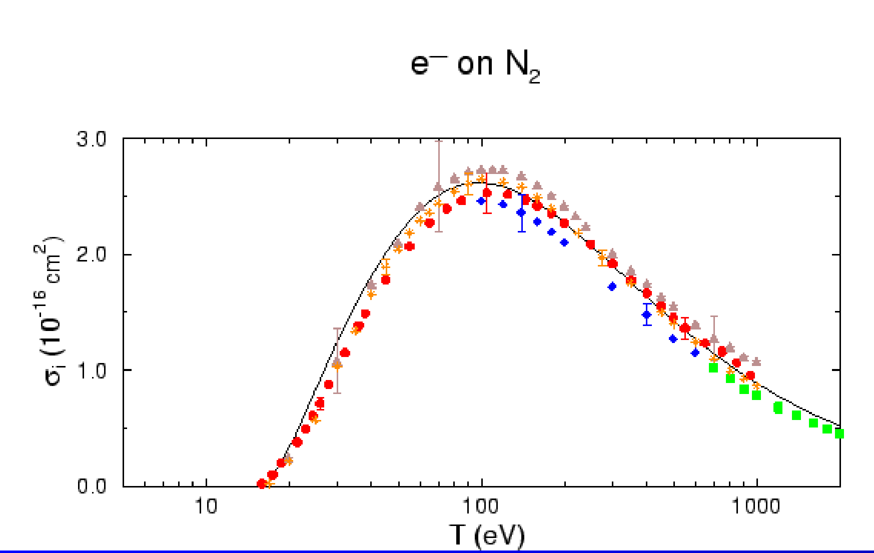

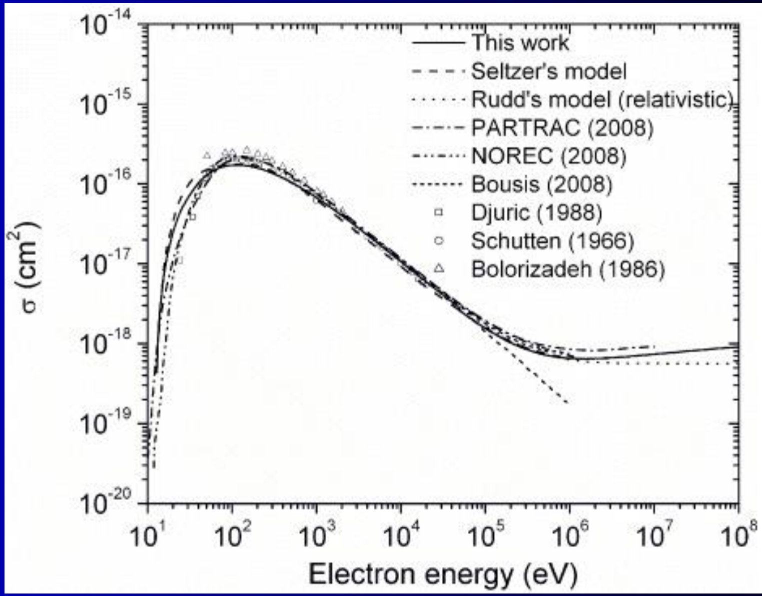

BEB W. Hwang, Y.-K. Kim and M.E. Rudd, J. Chem. Phys. **104**, 2956 (1996).

New J. Phys. **11** (2009) 063047
doi:10.1088/1367-2630/11/6/063047

Cross sections for the interactions of 1 eV–100 MeV electrons in liquid water and application to Monte-Carlo simulation of HZE radiation tracks

Ianik Plante[1,2] and Francis A Cucinotta[1]

Ionization cross section He and N_2

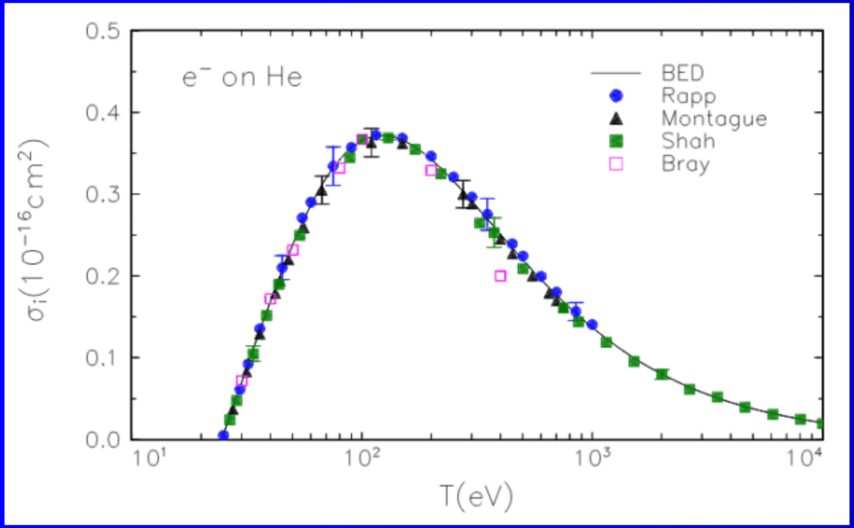

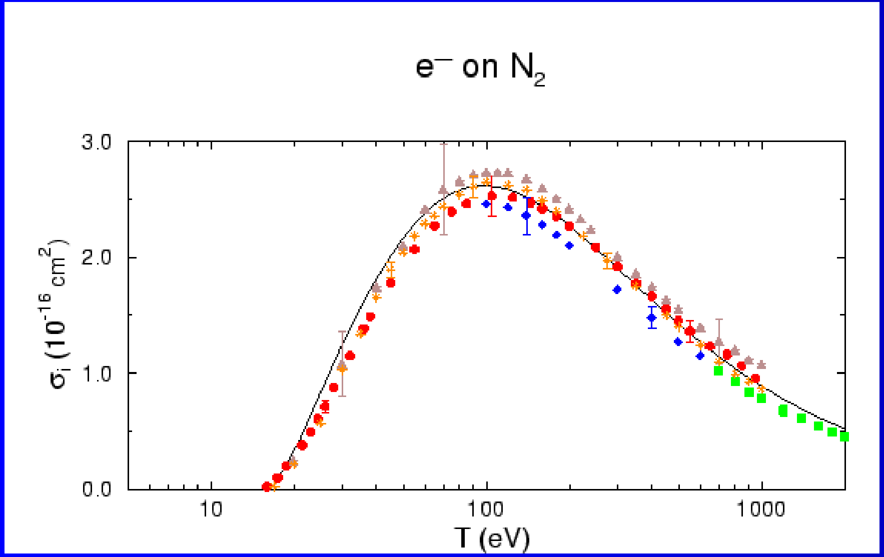

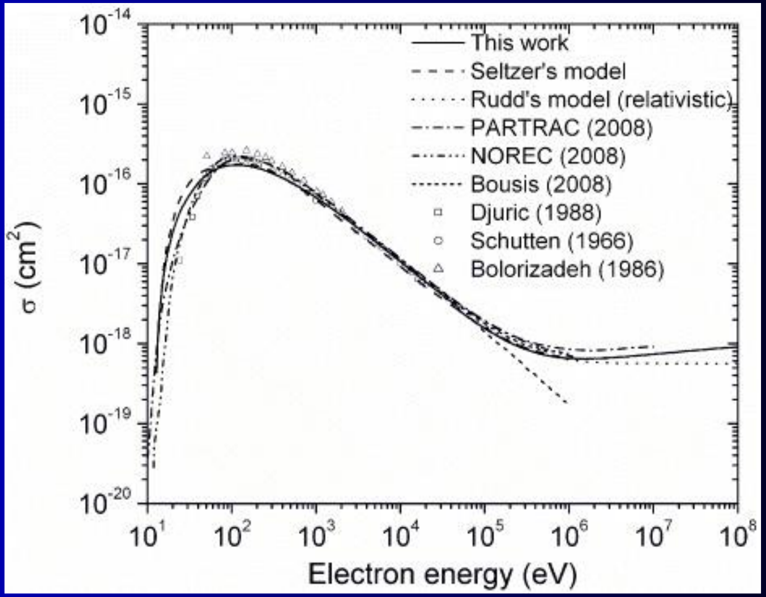

BEB W. Hwang, Y.-K. Kim and M.E. Rudd,
J. Chem. Phys. **104**, 2956 (1996).

New J. Phys. **11** (2009) 063047
doi:10.1088/1367-2630/11/6/063047
Cross sections for the interactions of 1 eV–100 MeV electrons in liquid water and application to Monte-Carlo simulation of HZE radiation tracks

Ianik Plante[1,2] and Francis A Cucinotta[1]

2.3. Electron impact ionization

The electron impact ionization is the most fundamental ionization process for the operation of ion sources.

Why?

- The cross section for the impact ionization is by orders of magnitudes higher than the cross section for the photo ionization.
- The cross section depends on the mass of the colliding particle. Since the energy transfer of a heavy particle is lower, a proton needs for an identical ionization probability an ionization energy three orders of magnitudes higher than an electron

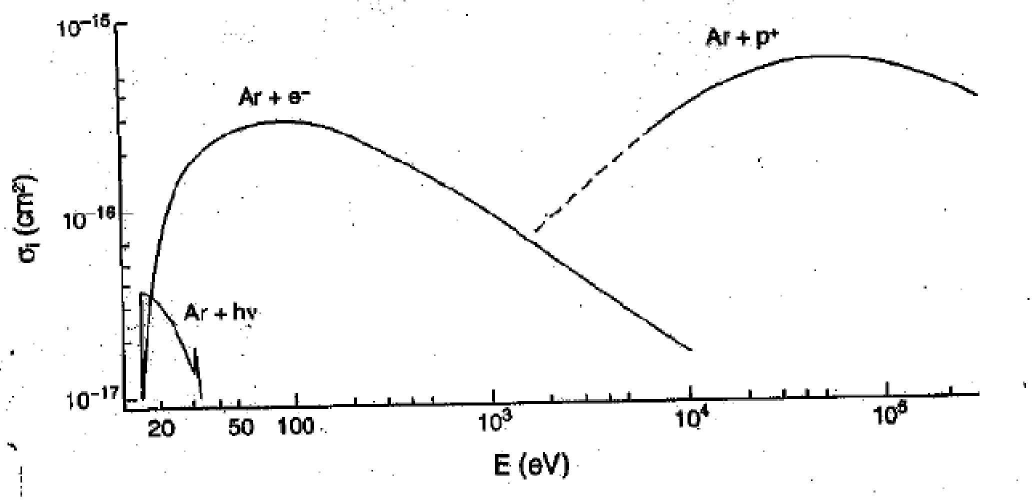

FIGURE 4
Ionization cross sections as functions of energy for ionizing collisions with fast electrons, protons, and photons. (From Winter, H., in *Experimental Methods in Heavy Ion Physics*, Springer-Verlag,

Ionization by electron impact

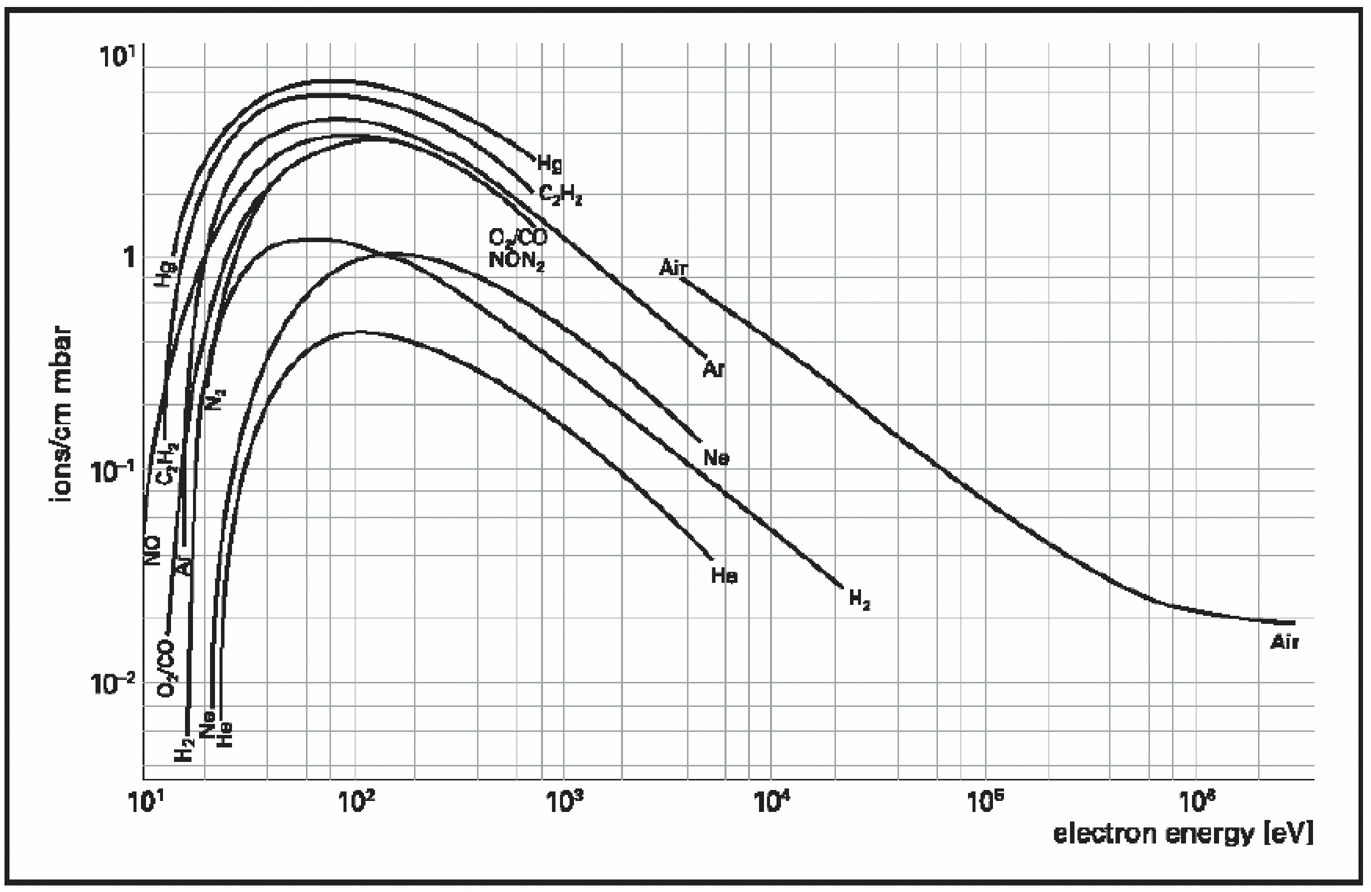

Thomson's formula

$$\sigma_j = C_j(\varepsilon - E_{ION})$$

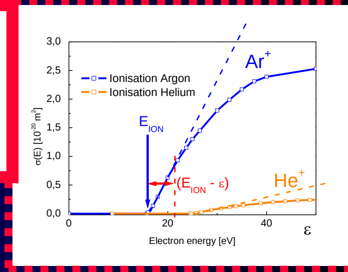

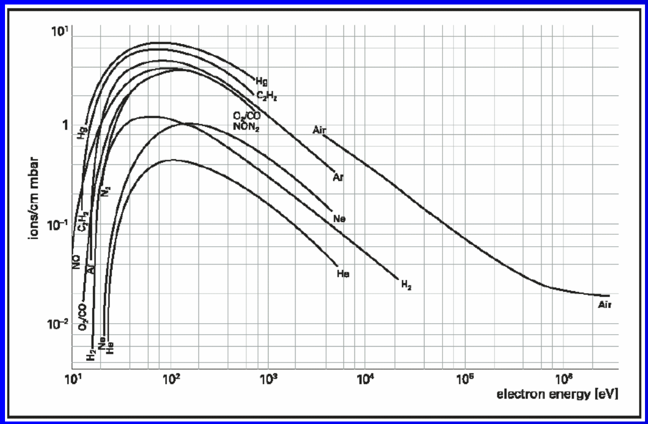

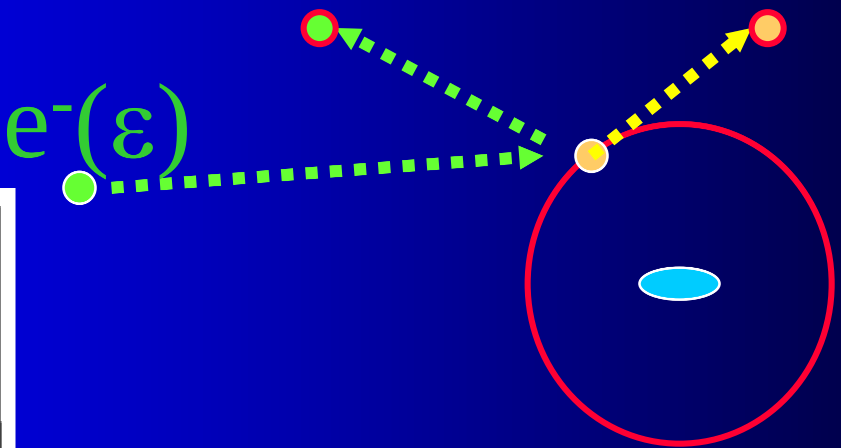

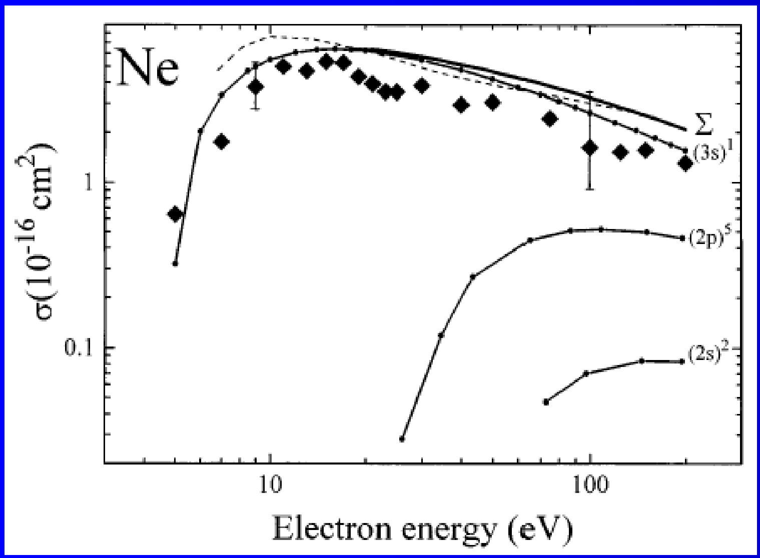

Calculated ionization cross section of the $^3P_0$ state in Ne using the DM formalism. The full curves refer to the contributions from the various subshells and have been labeled appropriately. The sum of the various subshell contributions has been labeled by the symbol*6*. Also shown is the Born calculation of Ton-That and Flannery (broken curve, see text for details). The experimental data points (diamonds) are those of Johnston *et al* . Two typical error bars (combined systematic and statistical uncertainty) are shown for the experimental data.

Ionization if $\Delta\varepsilon > I$

Formula of Rutherford for coulomb force

$d\sigma = e^4 d\Theta / 4\varepsilon^2 \sin^4(\phi/2)$….. $\sigma_i = \pi e^4/I \cdot (\varepsilon - I)/\varepsilon^3$

$$\sigma_i = 4\pi a_0^2 (I_H/\varepsilon)^2 \cdot (\varepsilon - I)/I$$

→ $\sigma_i = 4\pi a_0^2 (I_H/\varepsilon)^2 \cdot (\varepsilon/I - 1) = f_{function}(\varepsilon/I)$

$\sigma_i = \Sigma\, \sigma_{in}$ sum of the various subshell contributions

Near the threshold ➔ linear approximation

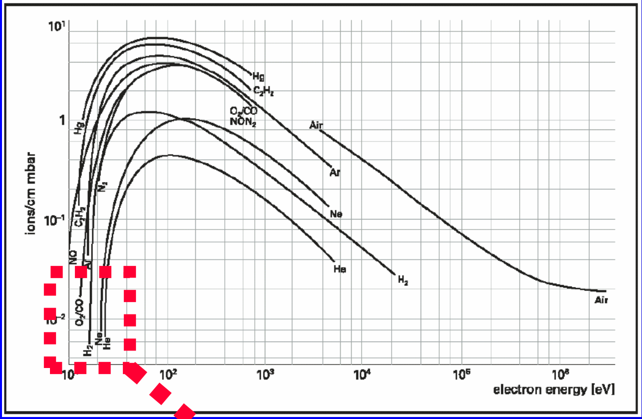

$$\sigma_i = 4\pi a_0^2 (I_H/\varepsilon)^2 \cdot (\varepsilon - I)/I$$

➔ $\sigma_i = 4\pi a_0^2 (I_H/\varepsilon)^2 \cdot (\varepsilon/I - 1) = f_{function}(\varepsilon/I)$

$$\sigma_j = C_j(\varepsilon - E_{ION})$$

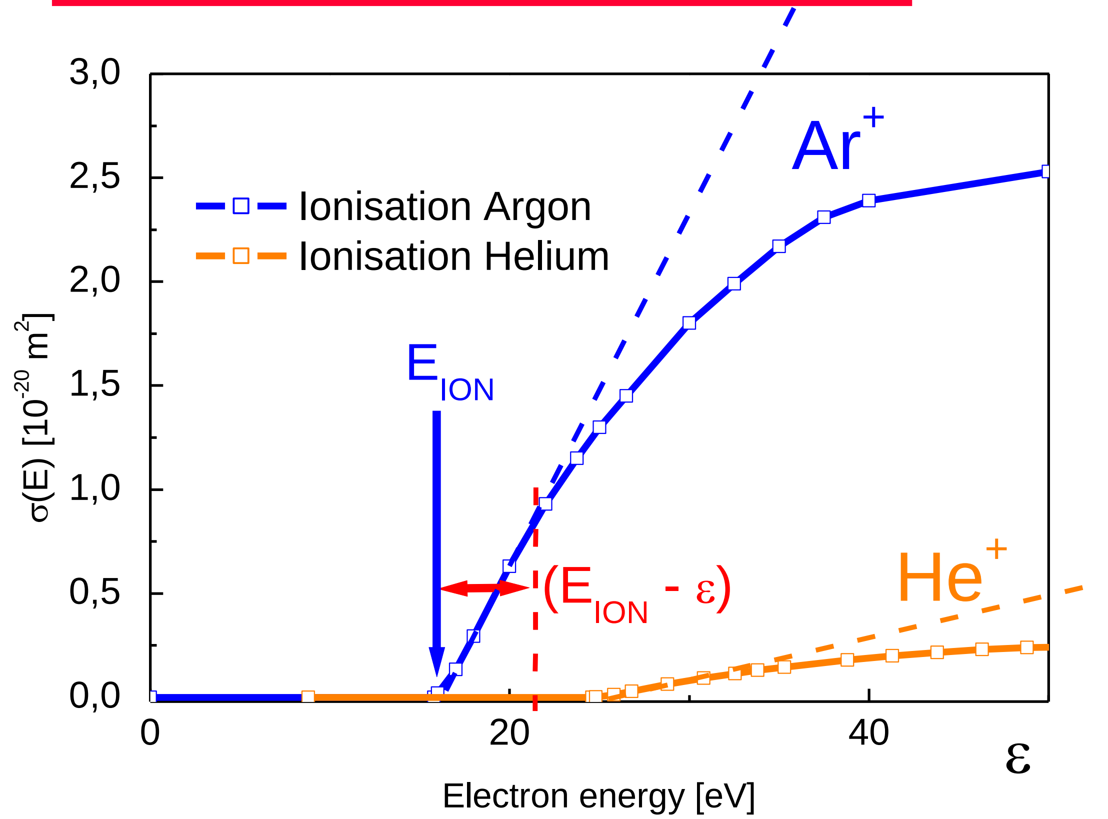

Ionization cross section – idea of experiment

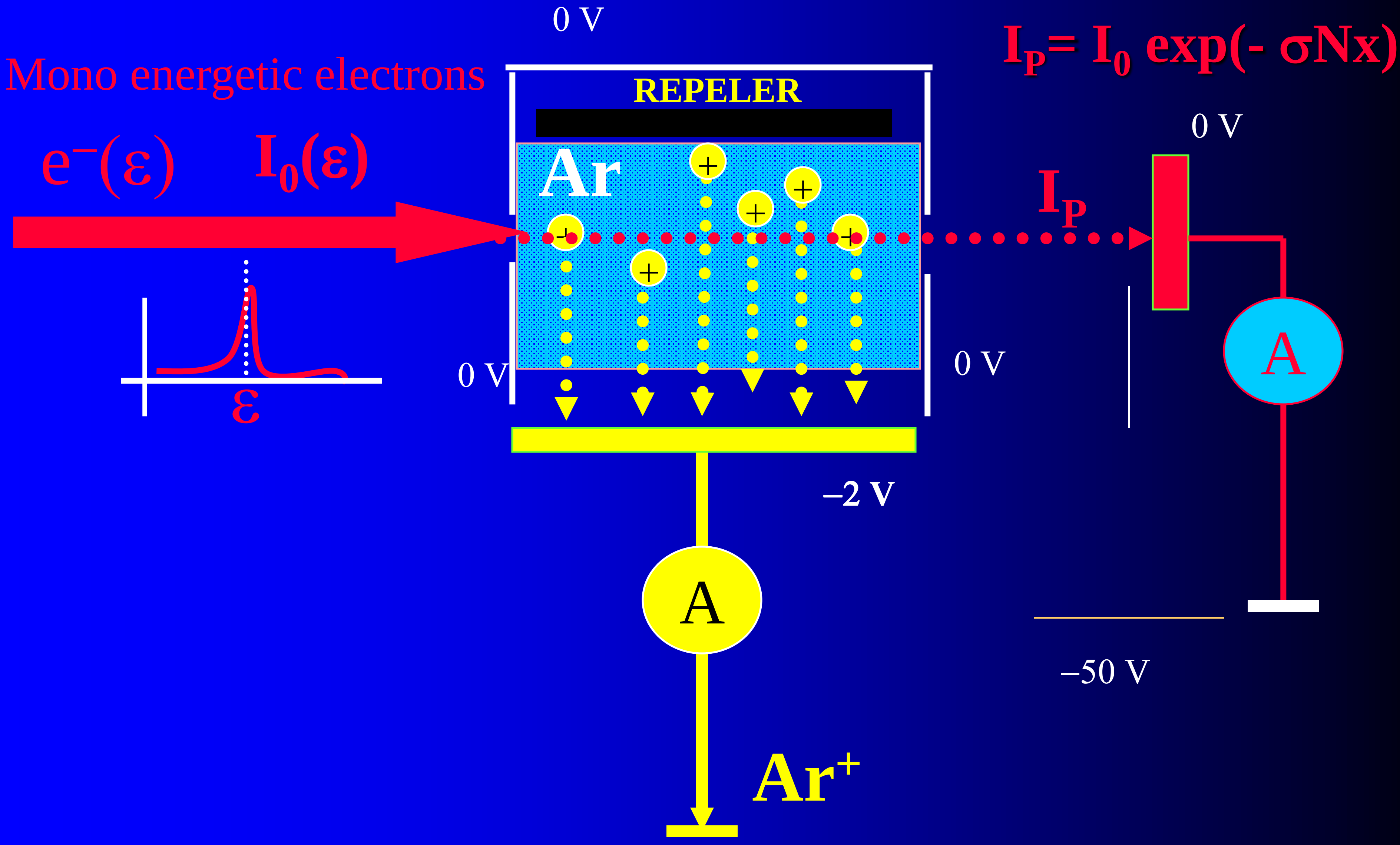

Electron impact ion source – ion source of mass spectrometer

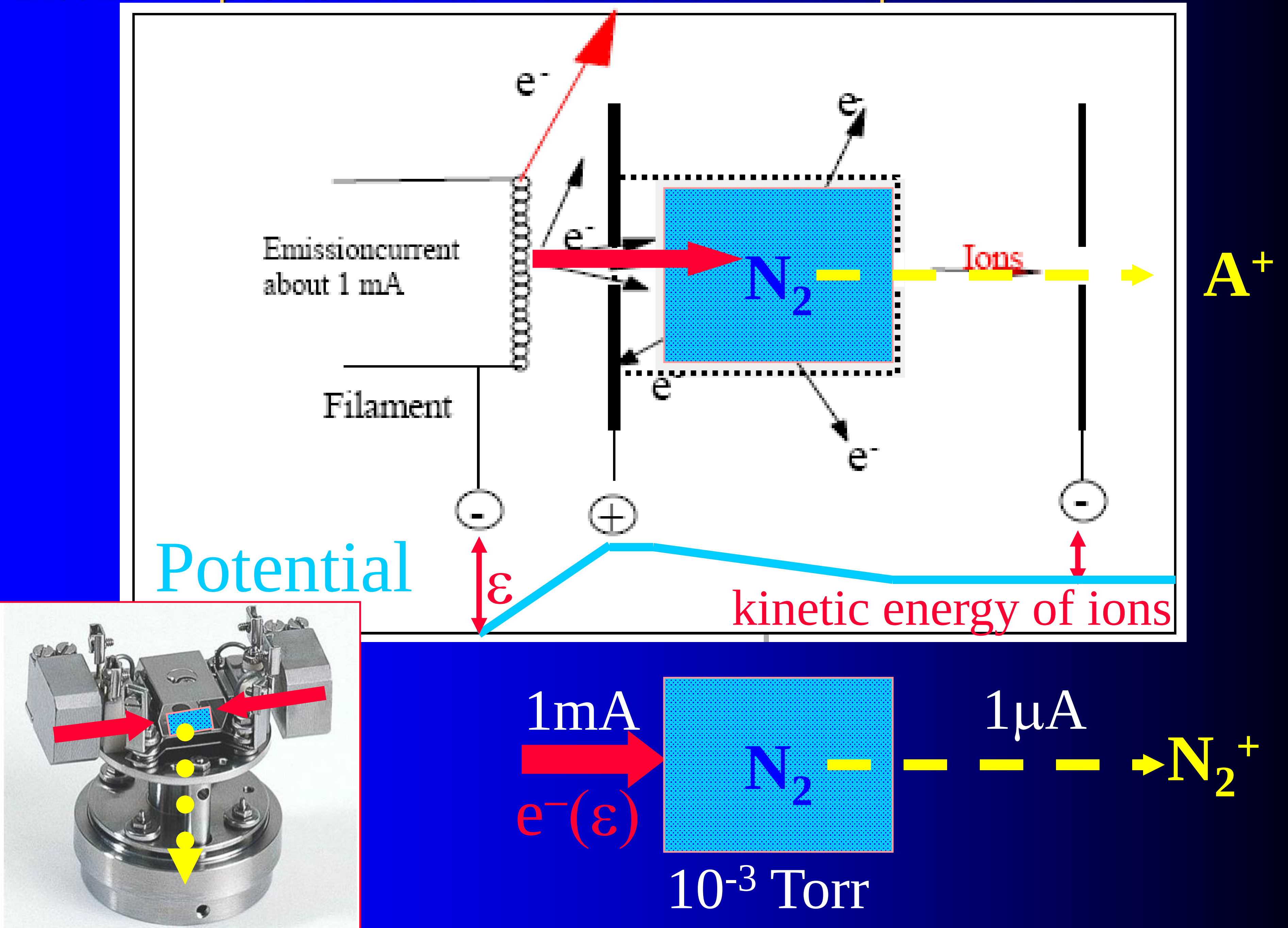

Electron impact ionization

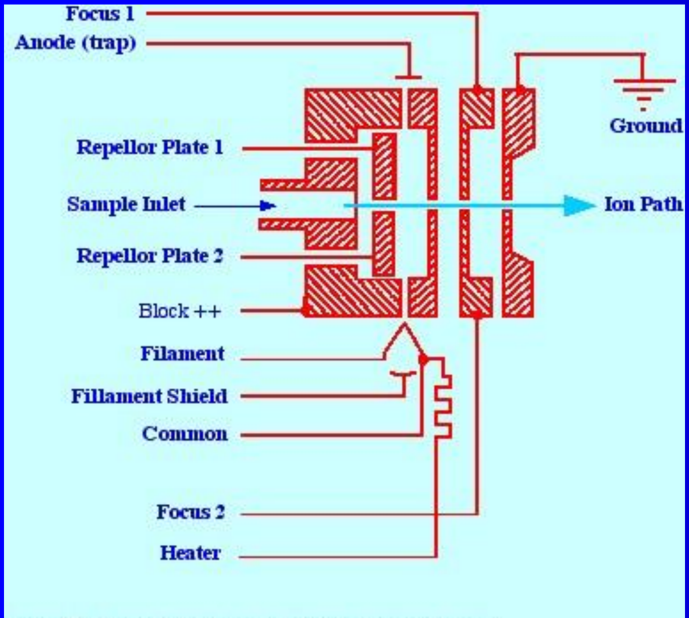

Figure 3. Cross Section of an Electron Impact Source

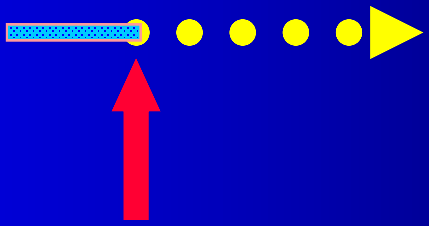

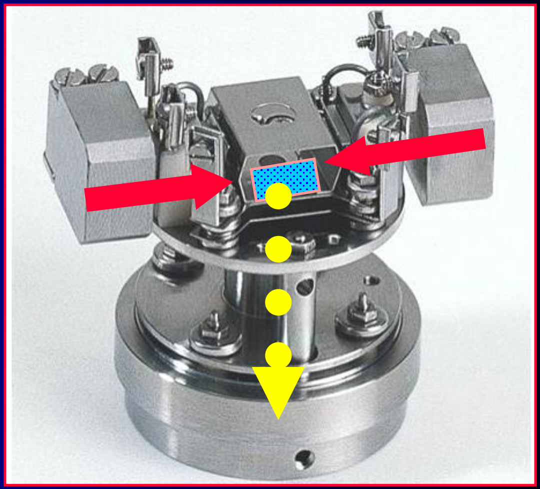

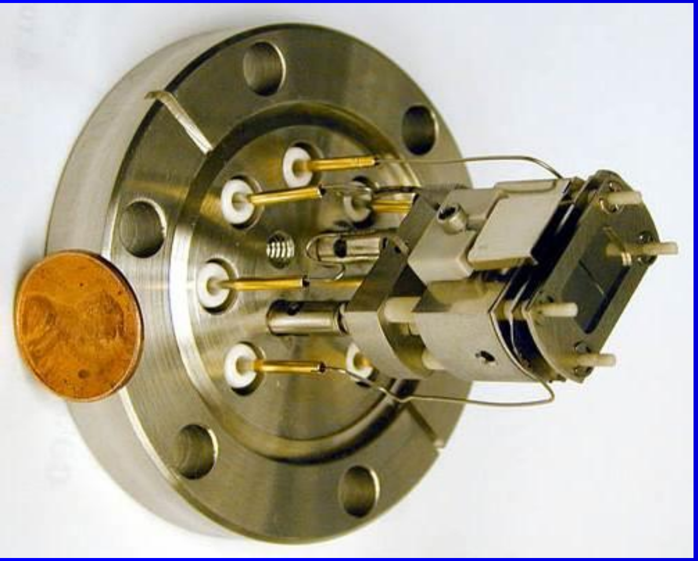

Ionization cross section N_2

BEB
W. Hwang, Y.-K. Kim and M.E. Rudd, J. Chem. Phys. **104**, 2956 (1996).

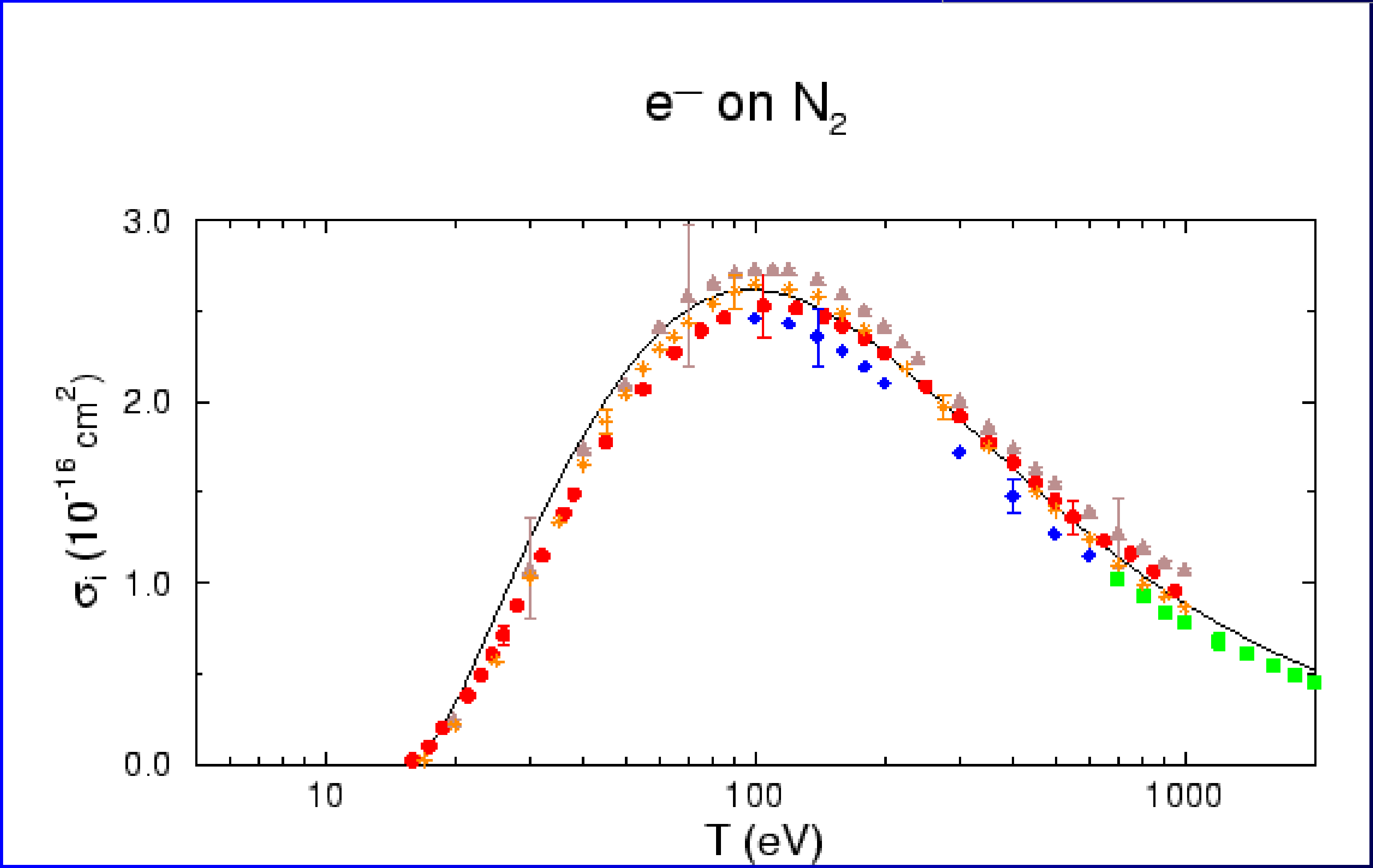

Ionization cross section -acetylene C_2H_2
Product channels

Pragmatic approach

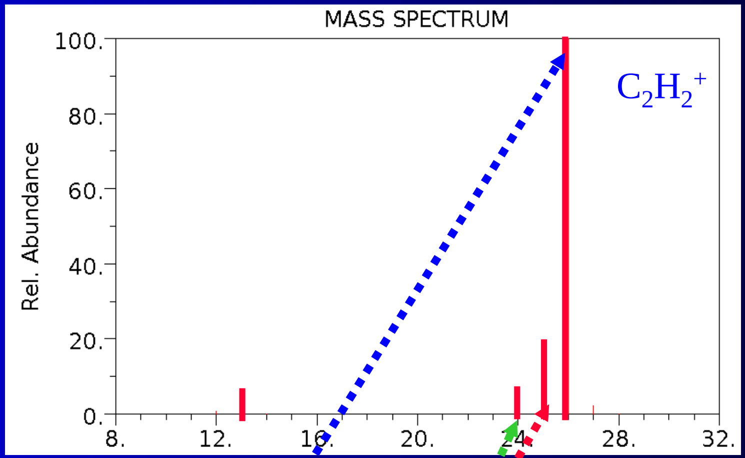

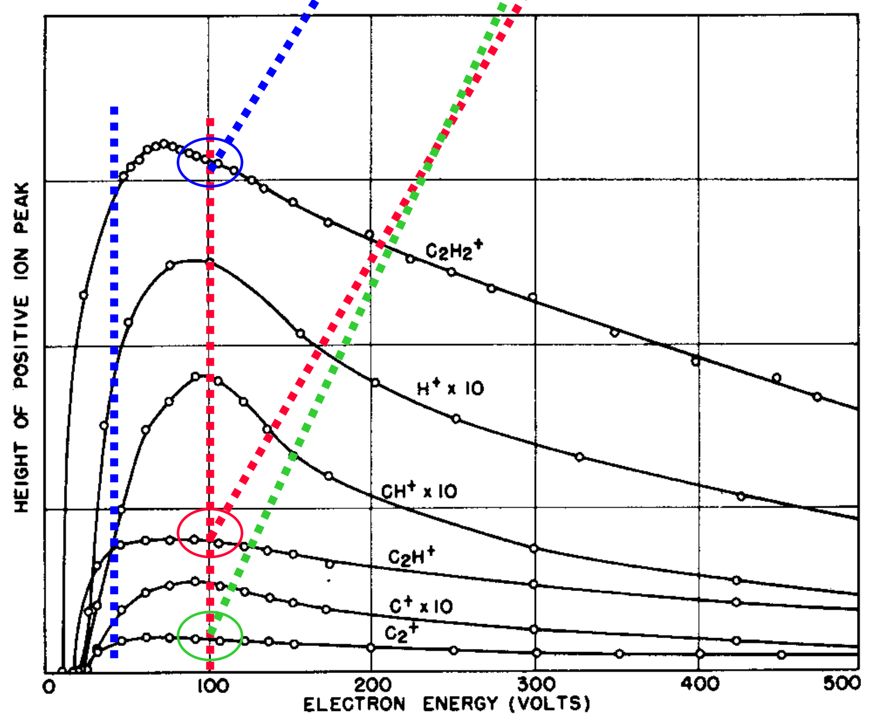

FIG. 6. Ionization efficiency curves for several ions from acetylene (493).

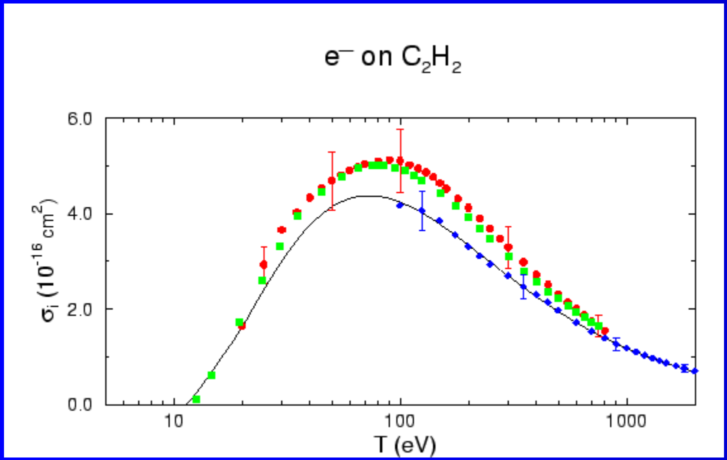

Ionization cross section data from http://webbook.nist.gov

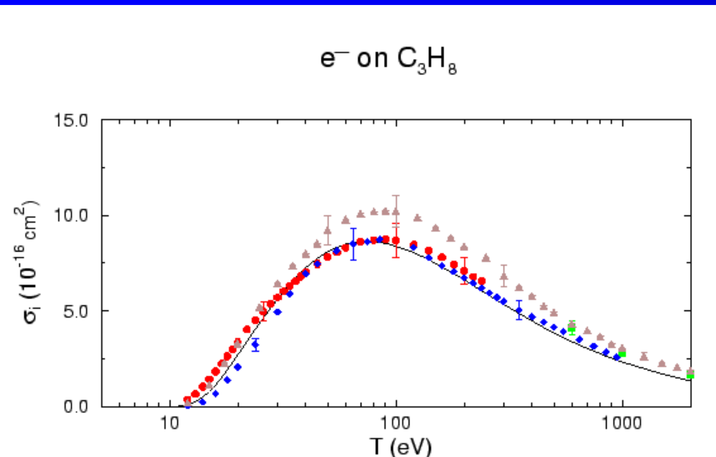

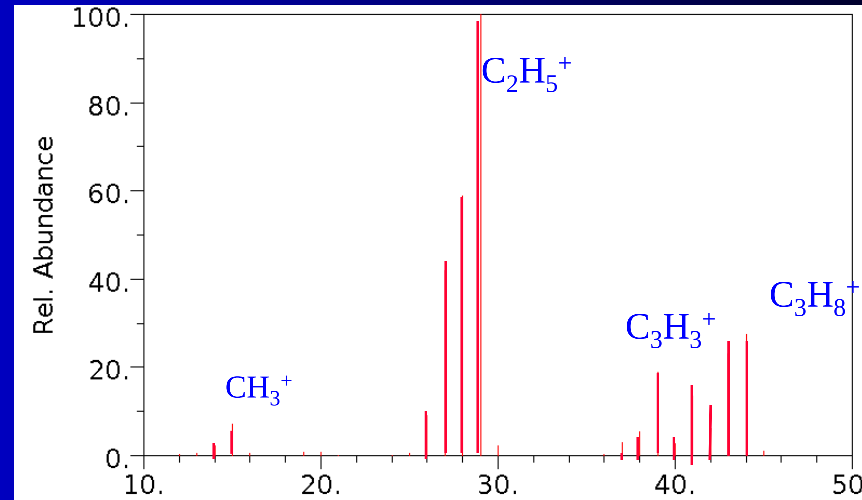

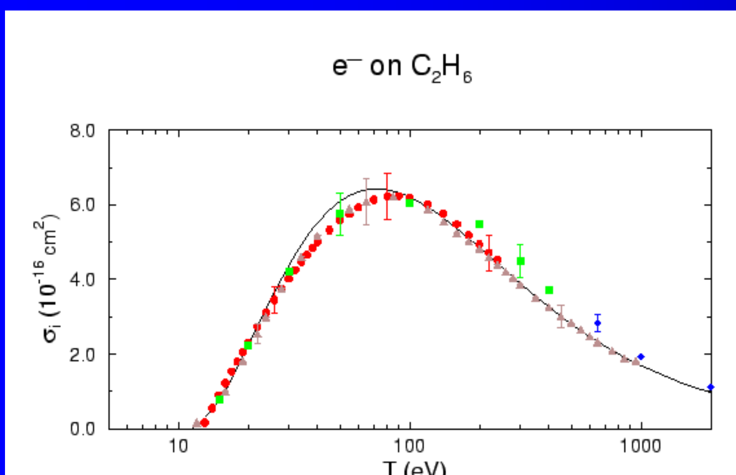

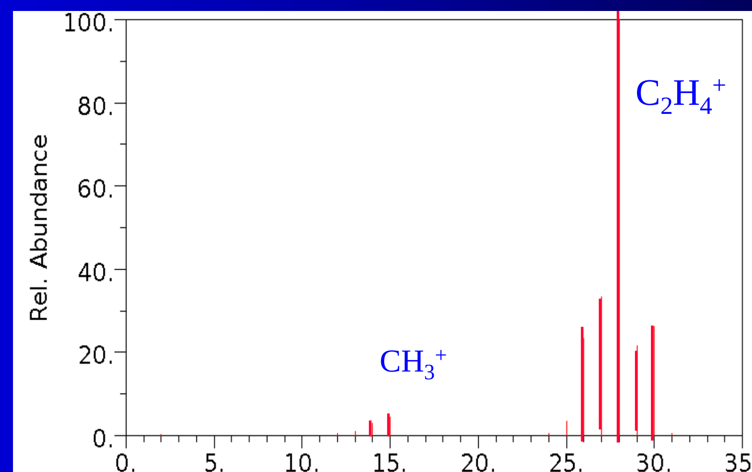

How to recognize spectra ???

Ionization - EII of CH_4

Determination of ionization energies (IEs)

for EII of CH_4 for the following reactions:

e $+CH_4$	$\rightarrow CH^+_4 + 2e$	(1)
	$\rightarrow CH^+_3 + H + 2e$	(2*a*)
	$\rightarrow CH^+_3 + H^- + e$	(2*b*)
	$\rightarrow CH^+_2 + H_2 + 2e$	(3)
	$\rightarrow CH^+ + H + H_2 + 2e$	(4*a*)
	$\rightarrow CH^+ + H^- + H_2 + e$	(4*b*)
	$\rightarrow C+ + 2H_2 + 2e.$	(5)

$\sigma w(E, \mathbf{p}) =$	0	for $E < IE_1(Ar)$
	$A_1(E - IE1)^{d1}$	for $E > IE_1$ and $E < IE_2$
	$A_1(E - IE1)^{d1} + A_2(E - IE2)^{d2}$	for $E > IE_2$

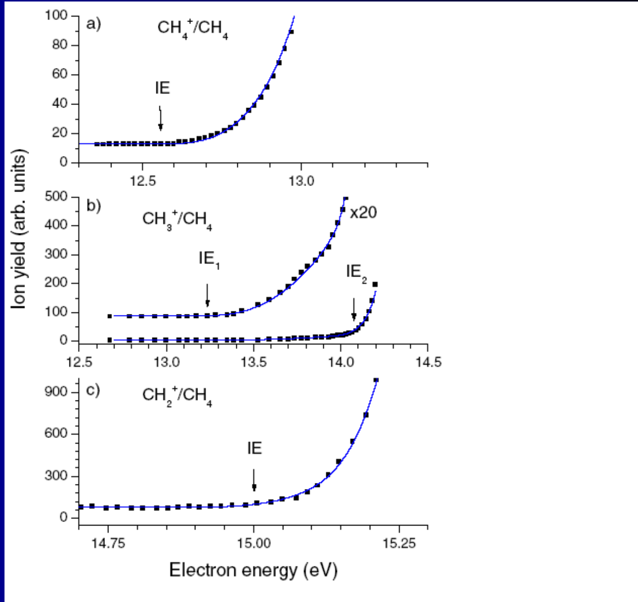

Figure A.1. Ion yield curve for CH_4^+, CH_3^+ and CH_2^+/CH_4 obtained through digitalization of the data from [3]. Full curves present fits through these data. Arrows indicate the estimated IEs derived by the fitting procedure.

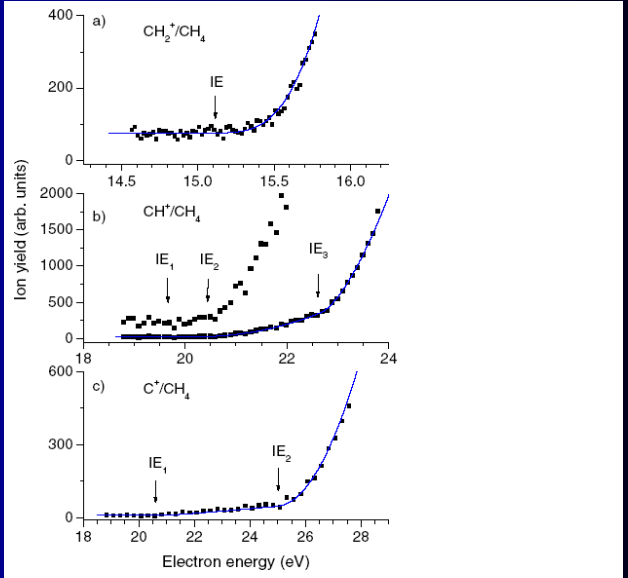

Figure 5. Ion yield curve for CH_2^+, CH^+ and C^+/CH_4 as measured at 293 K. Full curves present fits through the experimental data. Arrows indicate the IEs derived by the fitting procedure. Note that for the case of CH^+ only IE_2 and IE_3 have been derived from the present data; IE_1 has been calculated from the known EA of H (see text).

Multiple ionization

Multiple ionization of helium and krypton by electron impact close to threshold: appearance energies and Wannier exponents

J. Phys. B: At. Mol. Opt. Phys. **35** (2002) 4685–4694

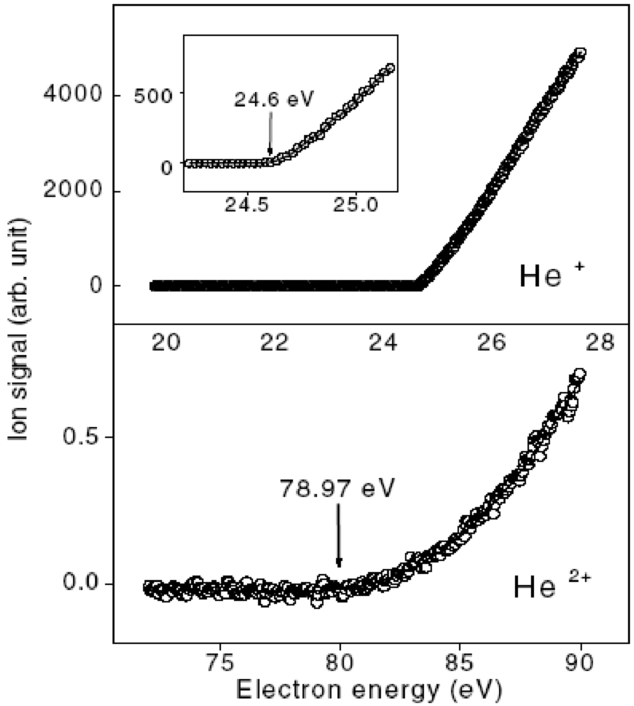

Figure 1. Ion signal as a function of electron energy for the formation of He^{+} ions (top) and He^{2+} ions (bottom) in the near-threshold region. The measured data are shown as open circles, the fits are shown as solid curves. The AEs, which are indicated, are the AEs for the individual data sets shown and may differ from the AE values listed in table 1 which were obtained from a comprehensive analysis of many individual data sets.

Table 1. AE values in eV for the formation of He^{+} and He^{2+} ions in comparison with other measured or calculated AE values.

	Spectroscopic value [1]	Redhead [45]	This work
He^{+}	24.59	—	24.6 ± 0.15
He^{2+}	79.00	77.58	79.05 ± 0.3

Ionization of He

Single-ionisation: He + e → He^{+} + 2e

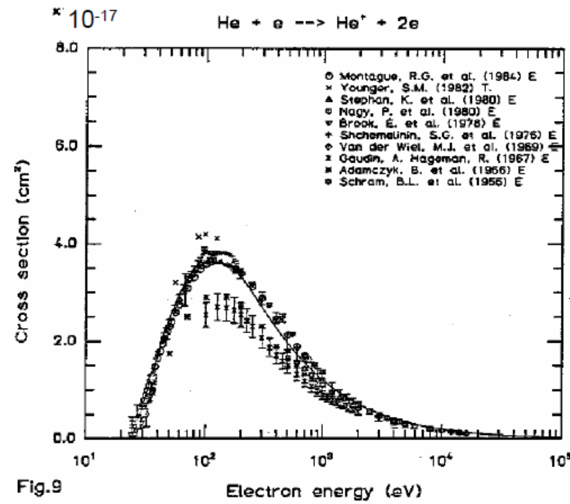

Fig.9

Multi-ionisation: He + e → He^{2+} + 3e

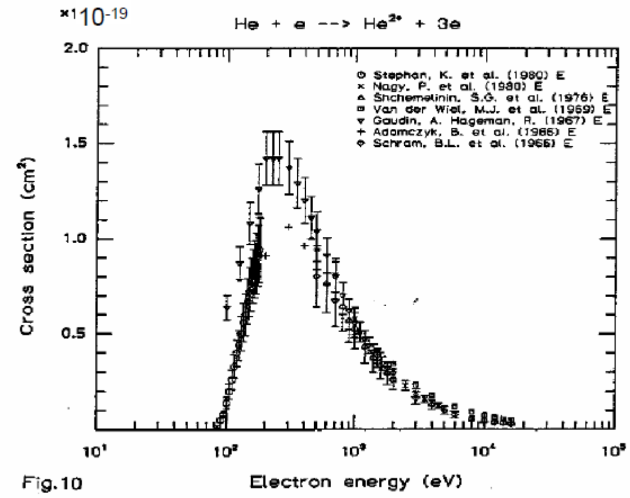

Fig.10

Ionization of the excited state

He (2s) + e → He^{+} + 2e

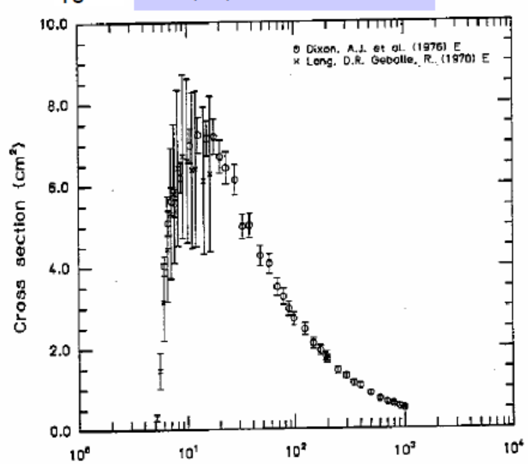

Fig.11

Ionization of singly charged He

He^{+} + e → He^{2+} + 2e

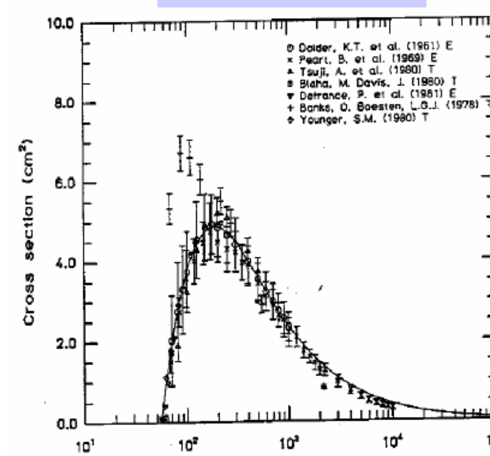

Fig.12

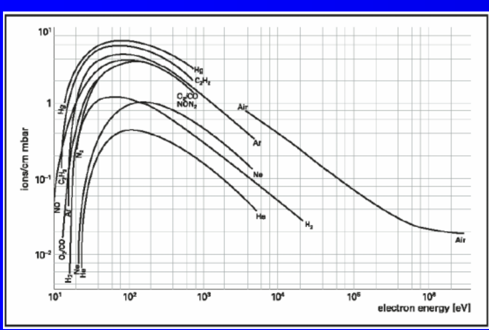

Multiple ionization

Multiple ionization of helium and krypton by electron impact close to threshold: appearance energies and Wannier exponents

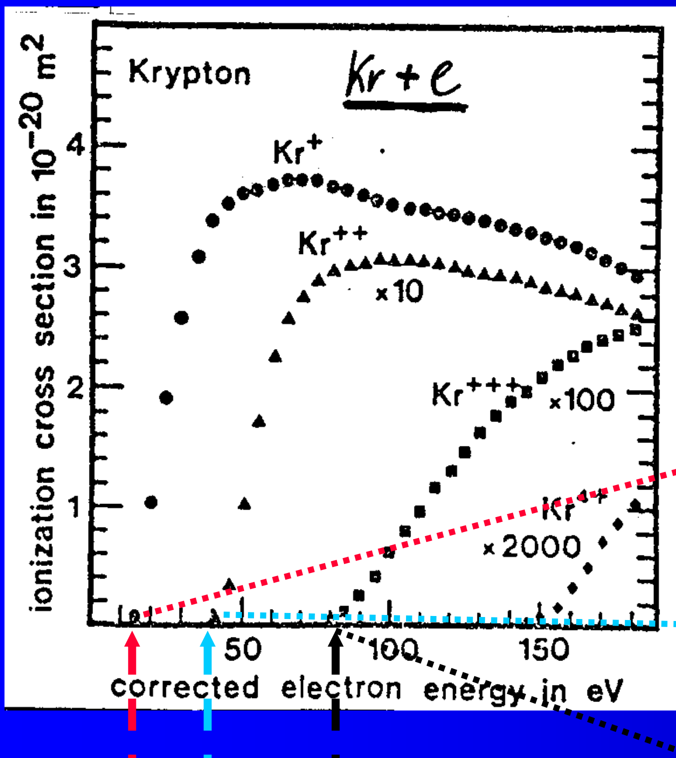

J. Phys. B: At. Mol. Opt. Phys. **35** (2002) 4685–4694

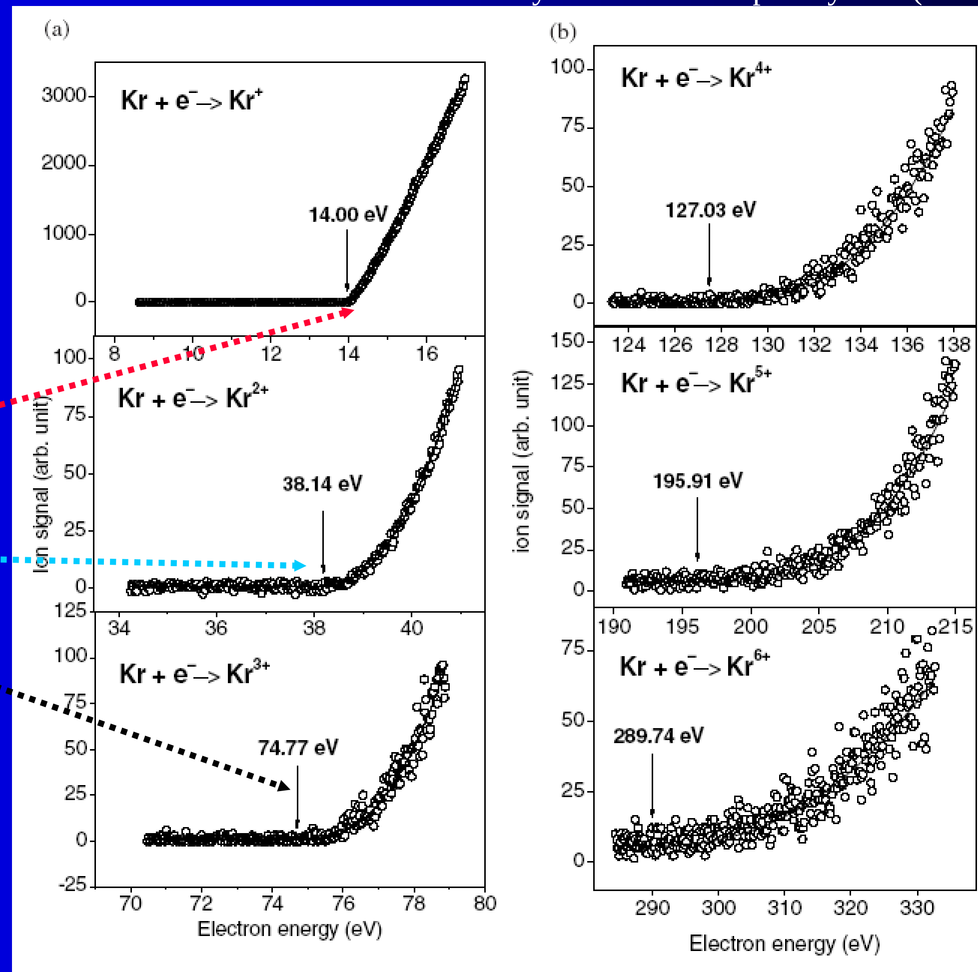

Figure 2. Ion signal as a function of electron energy for the formation of Kr^{n+} ions ($n = 1$–6) in the near-threshold region. The measured data are shown as open circles, the fits are shown as solid curves. The AEs, which are indicated, are the AEs for the individual data sets shown and may differ from the AE values listed in table 2 which were obtained from a comprehensive analysis of many individual data sets.

Multiple ionization

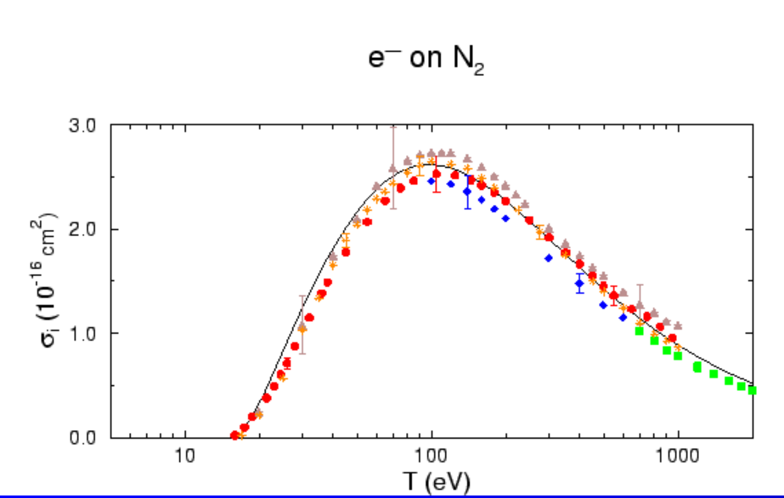

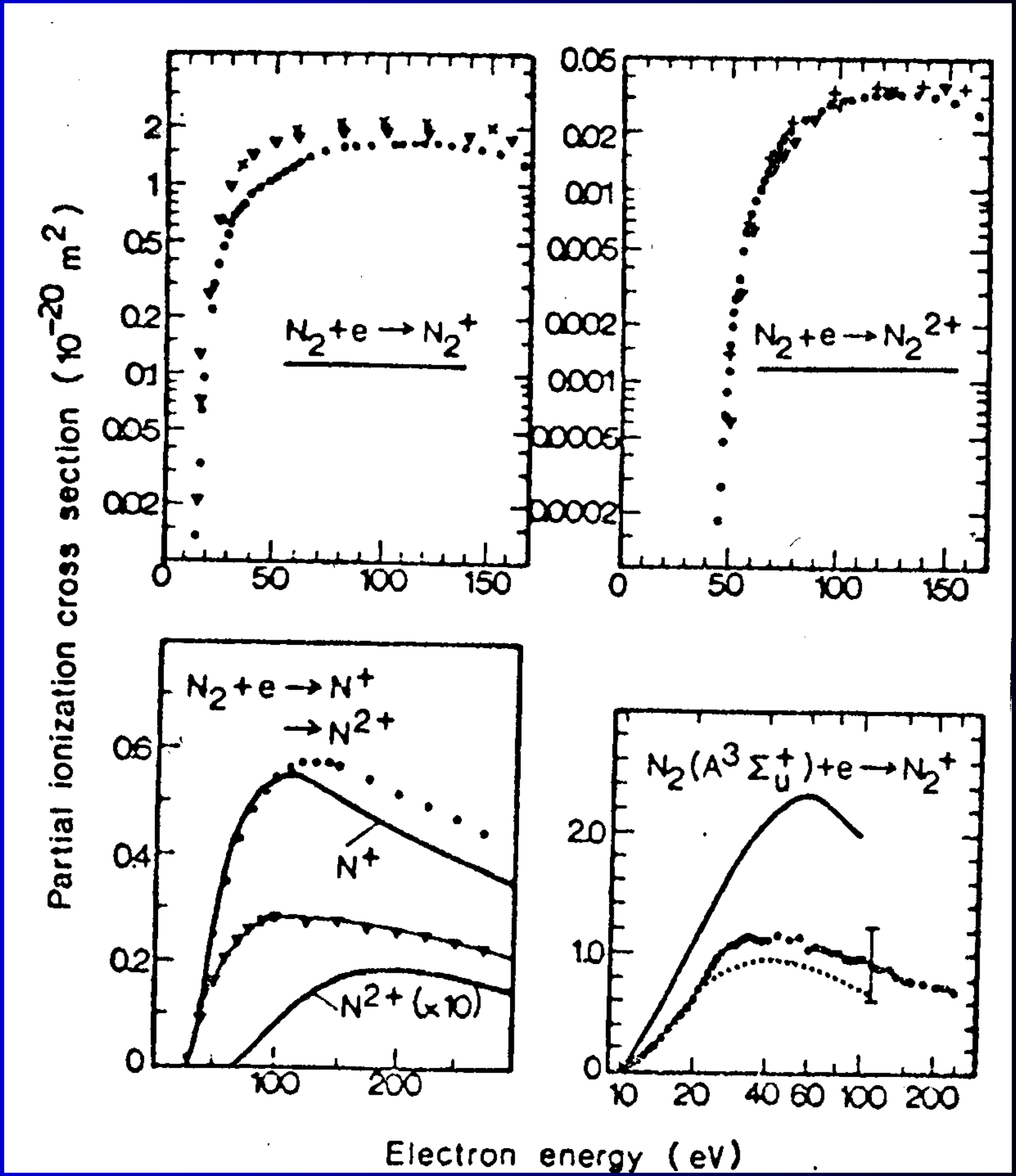

High efficiency
Grid ion source

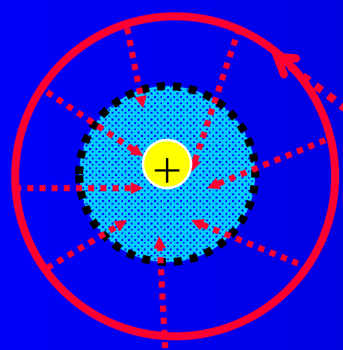

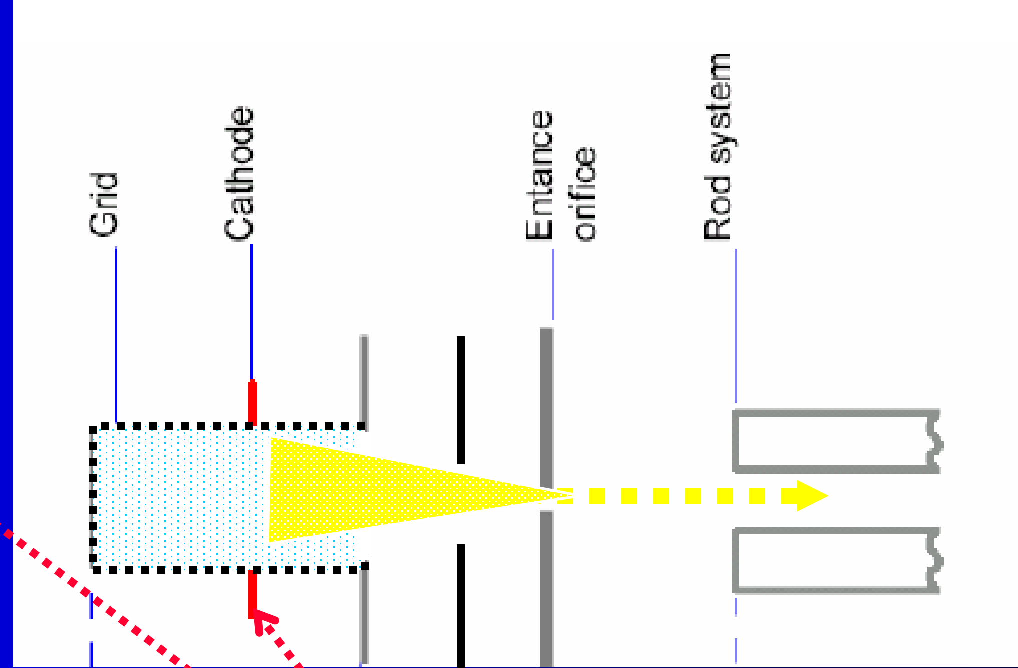

Ion optics **Mass filter**

Filament

Grid ion source

- Open design
- Two filaments (W)
- Low degassing rate
  - mimimum amount of material
  - Pt-Ir wires for formation chamber
  - Molybdenum filament holders
- Easy to degas via electron bombardment
- Filaments on positive potential

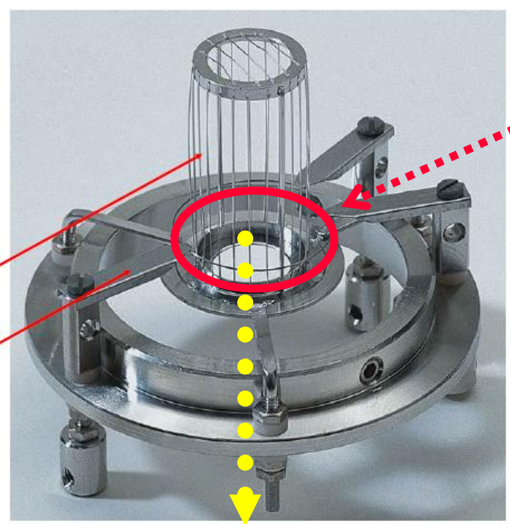

Flight paths of electrons

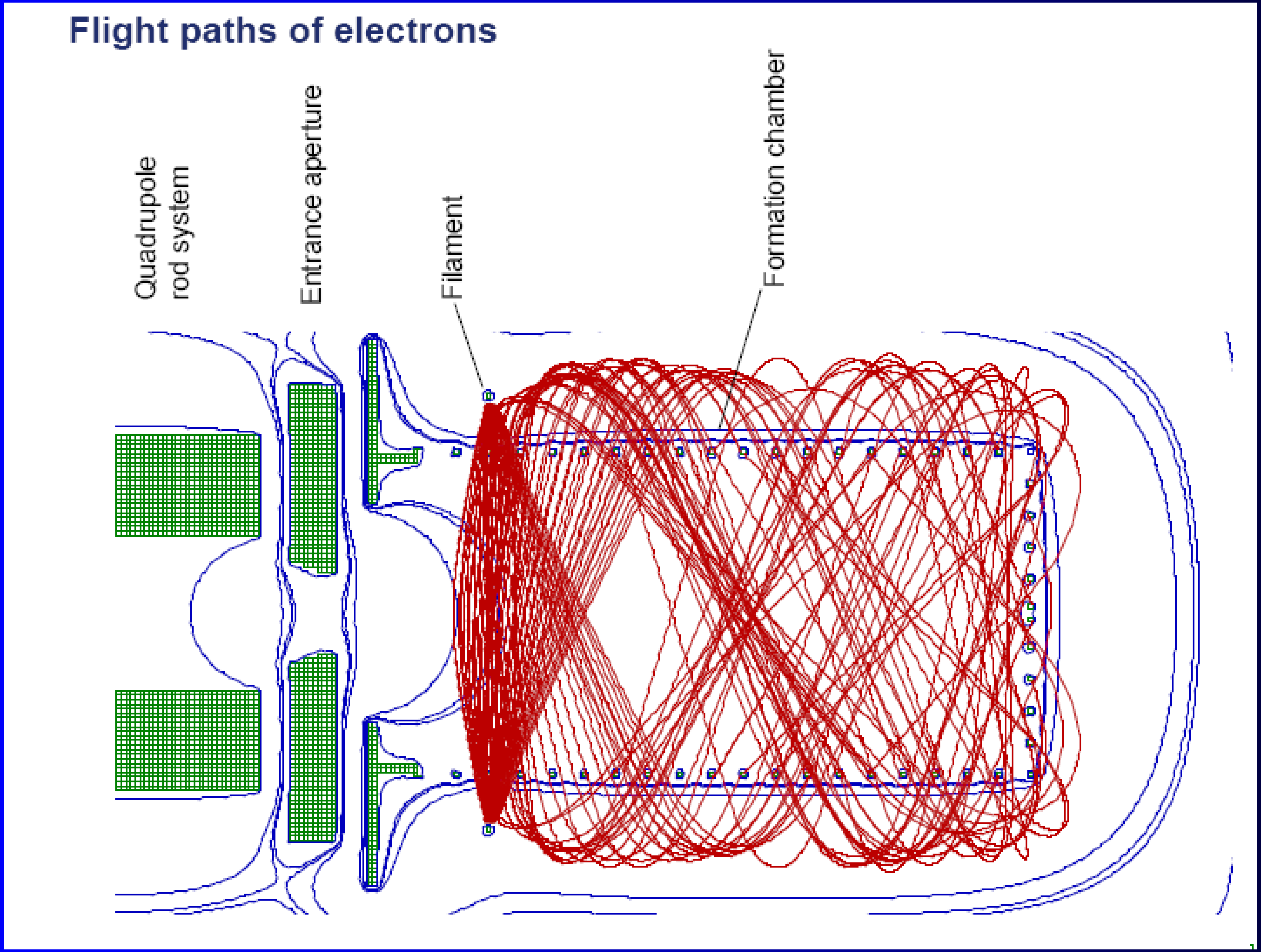

Flight paths of electrons 3D

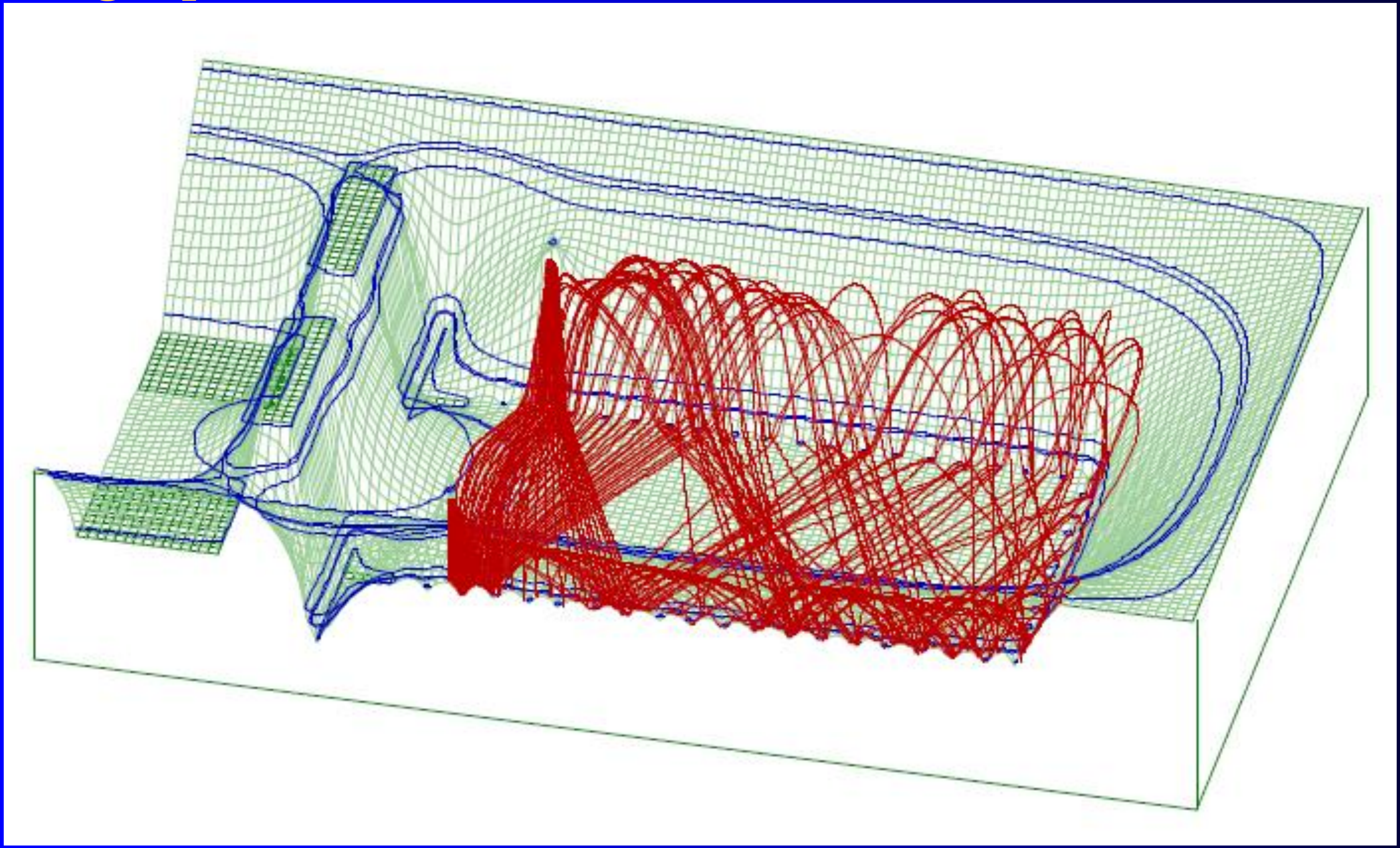

Flight paths of positive ions

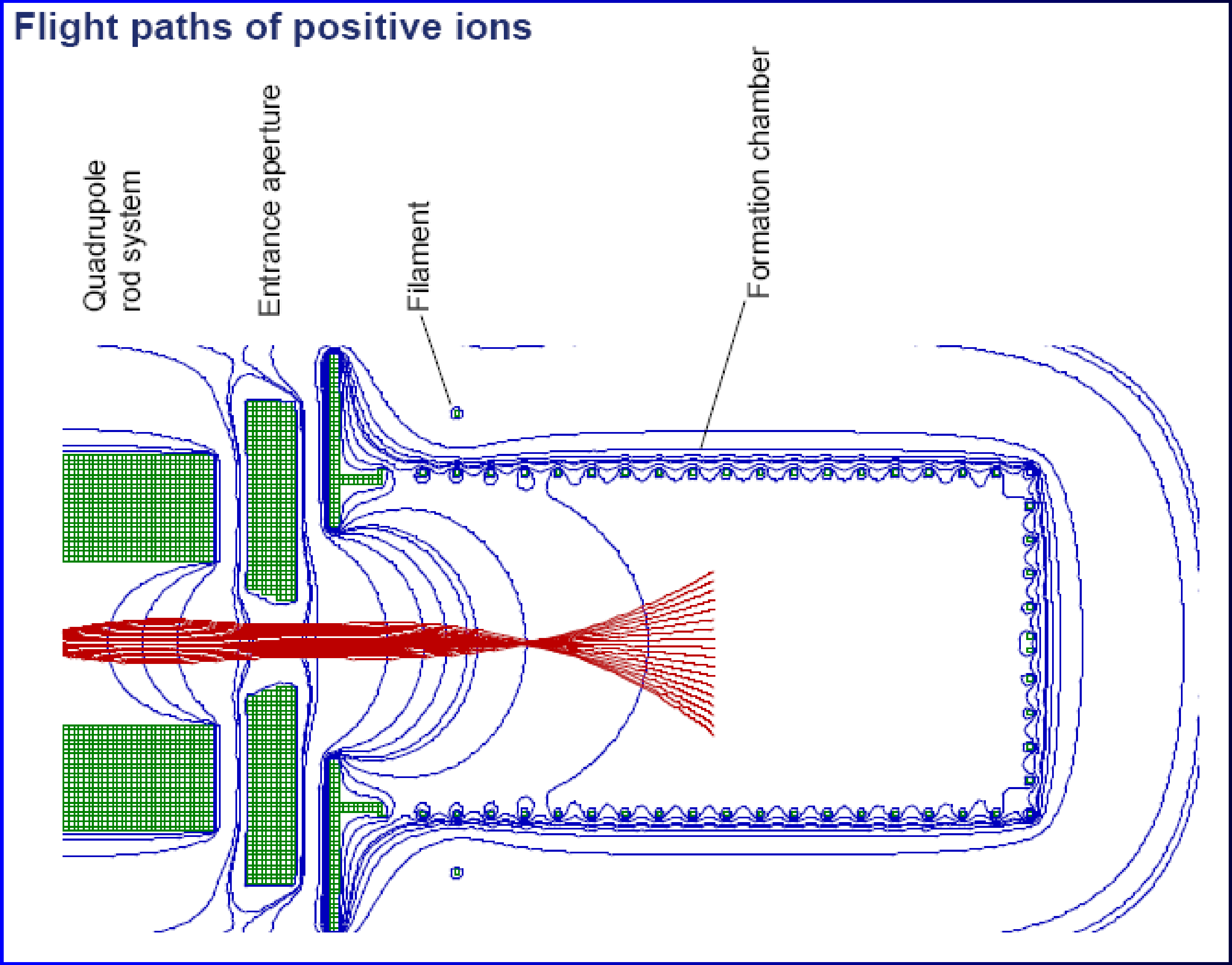

Flight paths of ions 3D

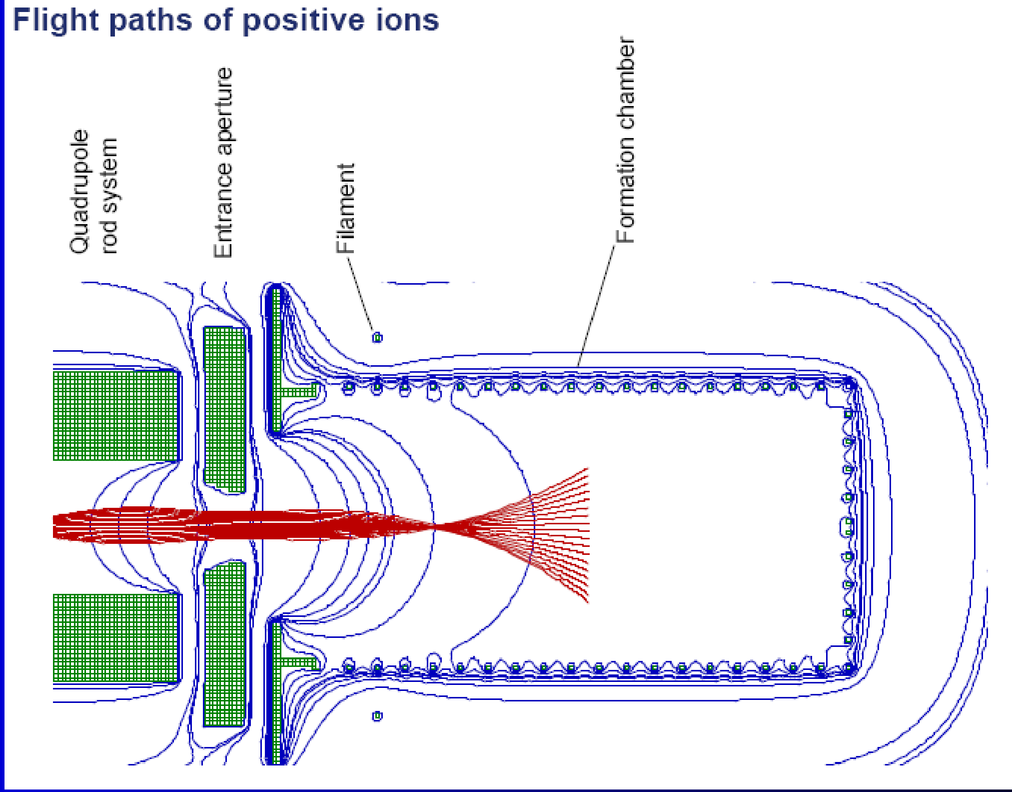

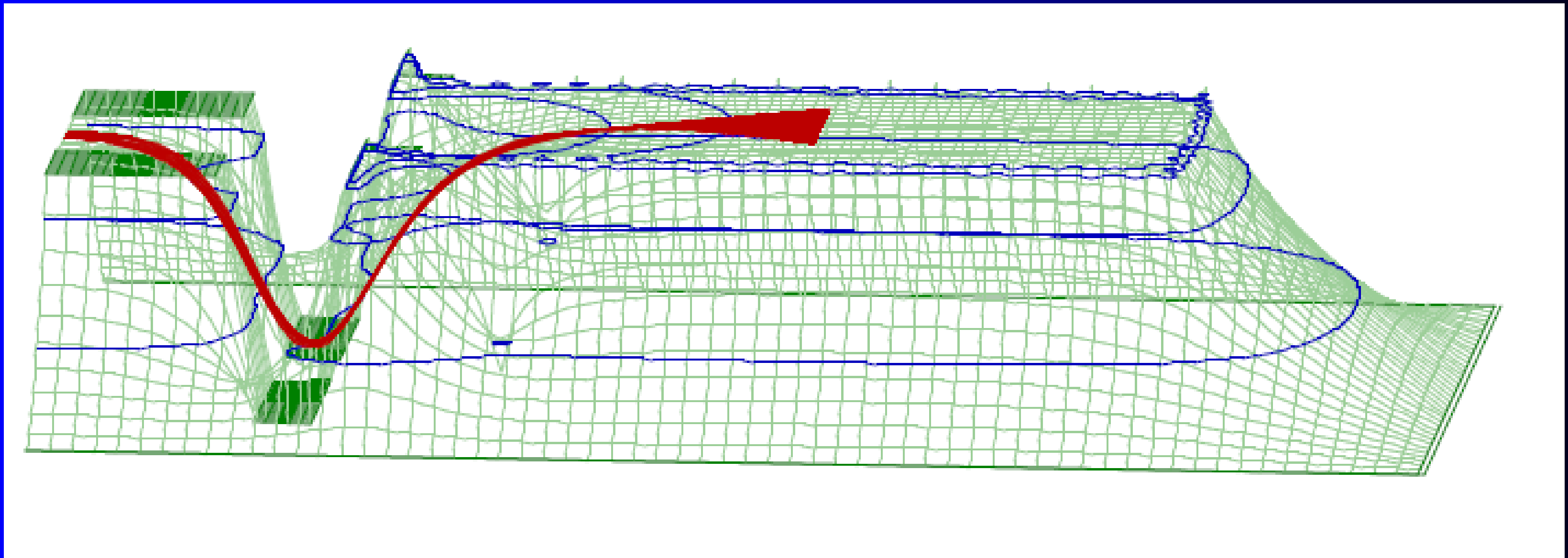

Cross Beam ion Source, calculations

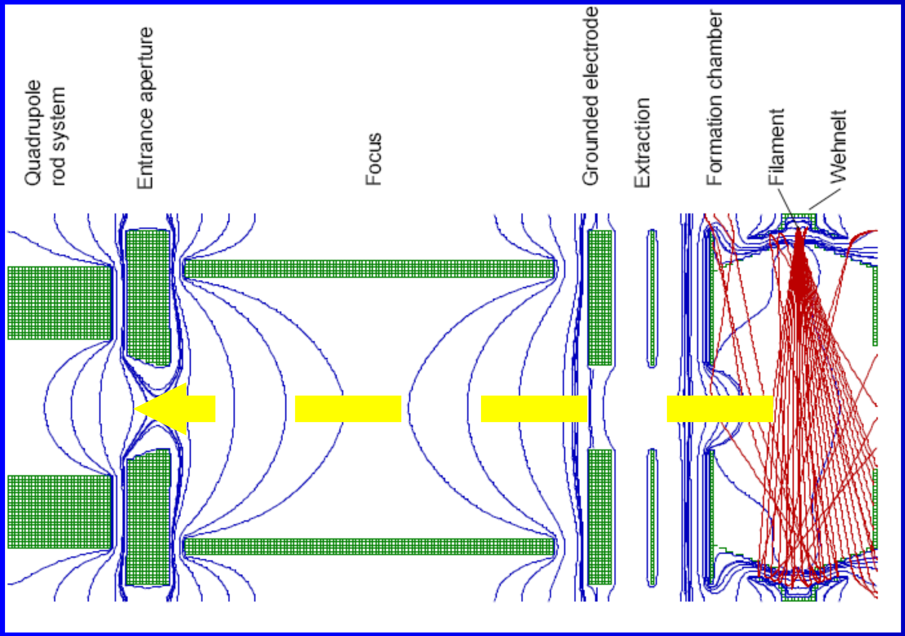

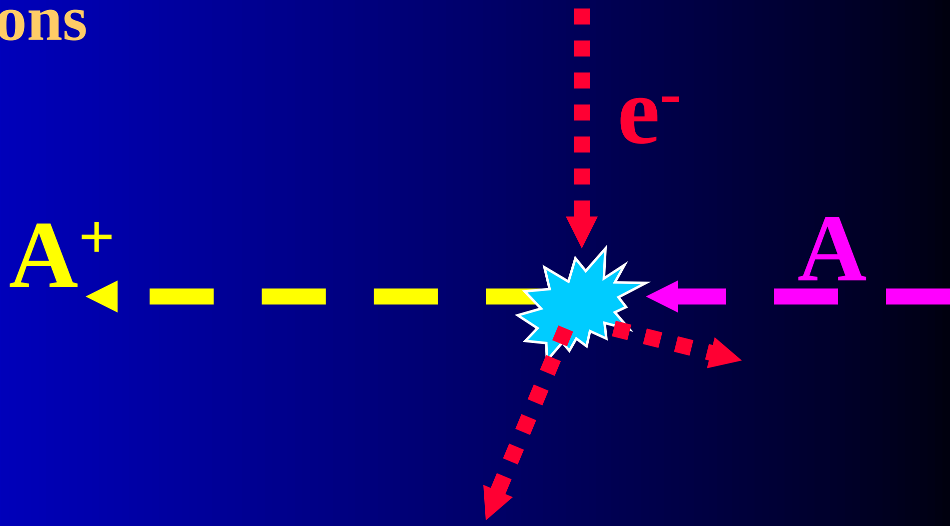

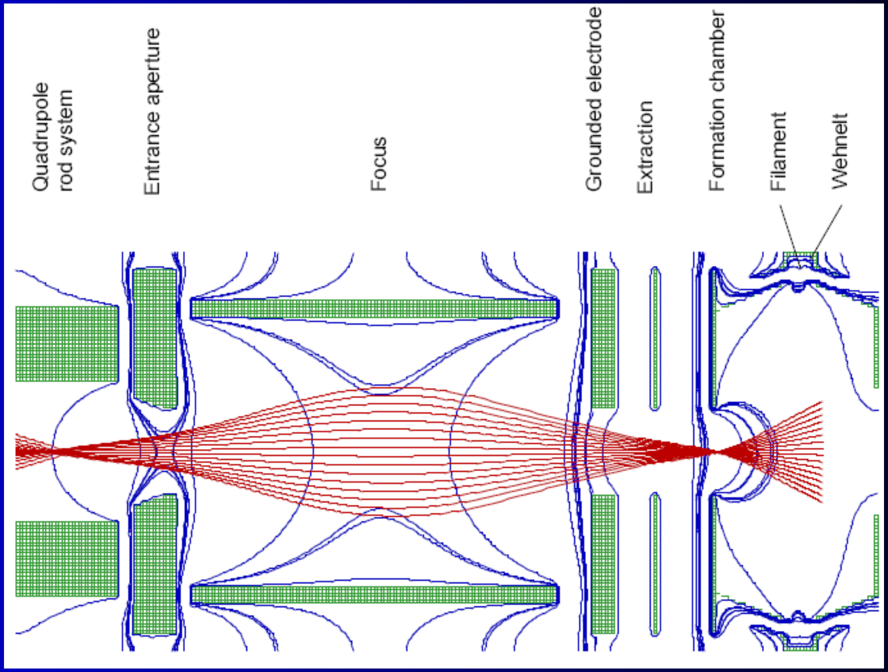

Flight paths of ions

Cross Beam ion Source

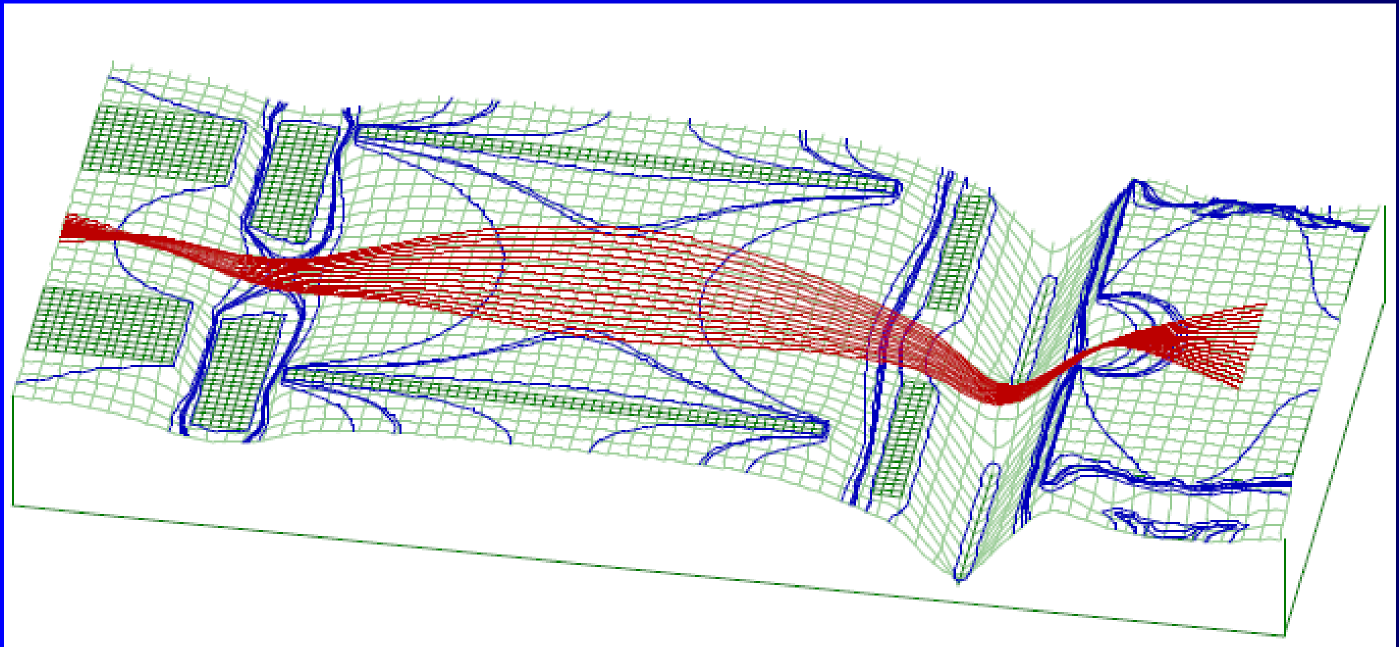

Cross Beam ion source
with magnets

- Two filaments
- Easy to degas
- Good ion focussing
- Bakeable to 300°C

Mass spectrometer

16 mm rod system for highest resolution, stability and transmission (e.g. He/D_2 separation)

8 mm rod system for High-End RGA and analytical applications

6 mm rod system for common RGA

90° off axis arrangement

efficient suppression of

- photons
- fast neutral particles
- stray ions

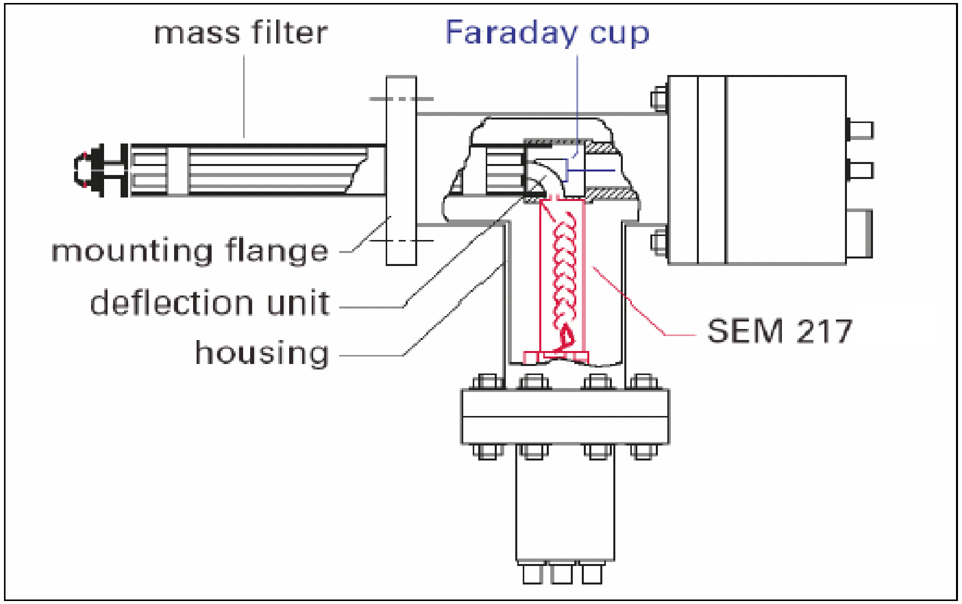

Ion detector – Discrete dynode SEM

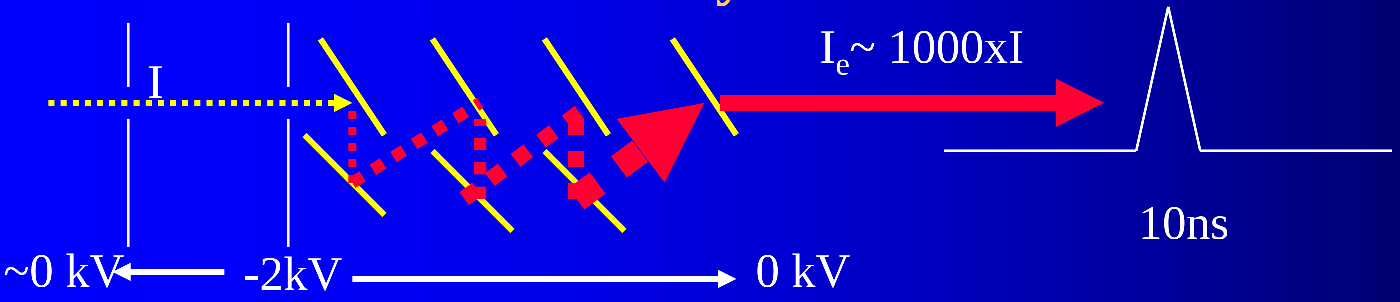

- Ion Detection
  - Discrete Dynode SEM
  - Bakeable to 400°C
  - for analog amplification and for pulse counting
  - Low noise (< 0.1 cps)

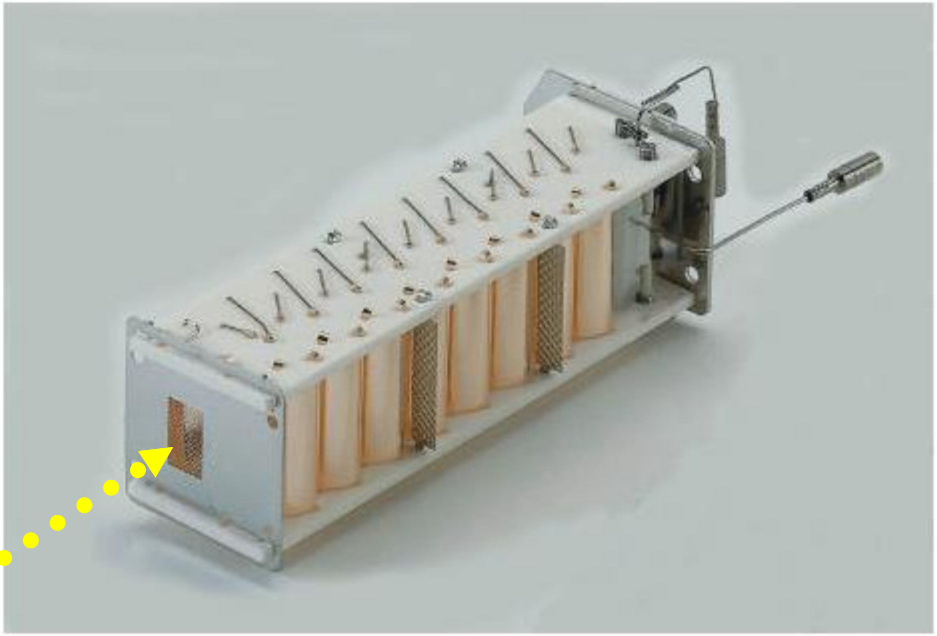

IONS

QMA

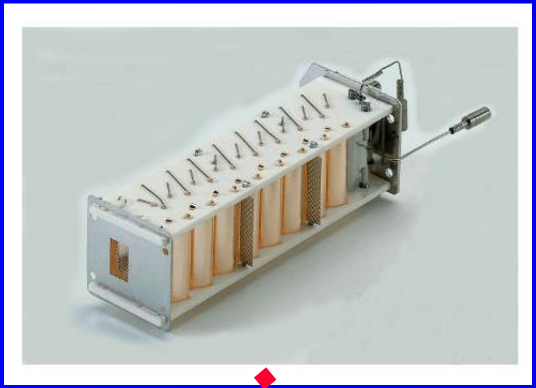

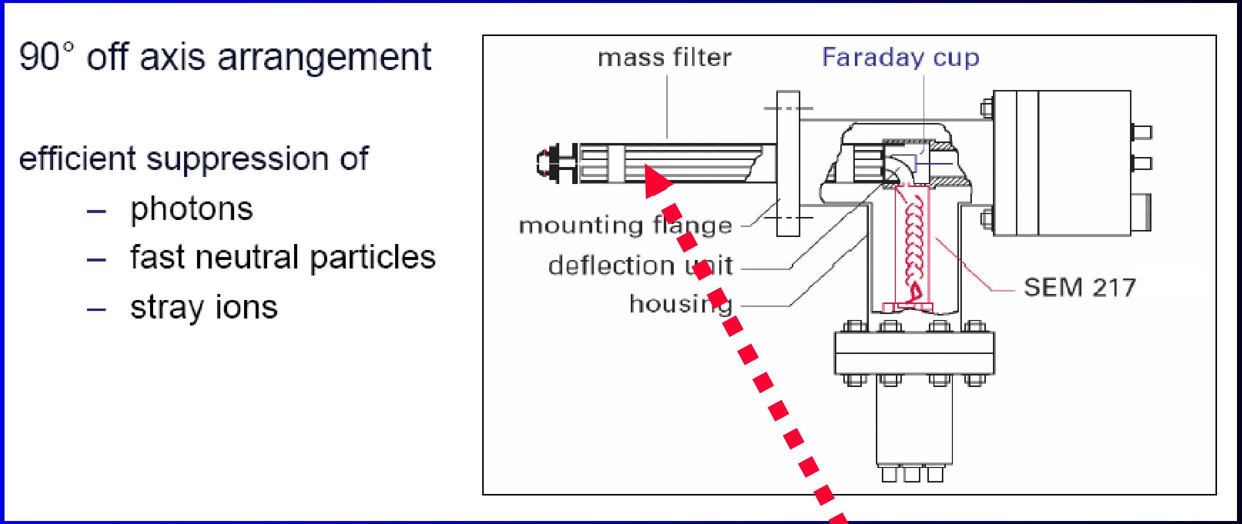
90° off axis arrangement
efficient suppression of
– photons
– fast neutral particles
– stray ions
mass filter
Faraday cup
mounting flange
deflection unit
housing
SEM 217

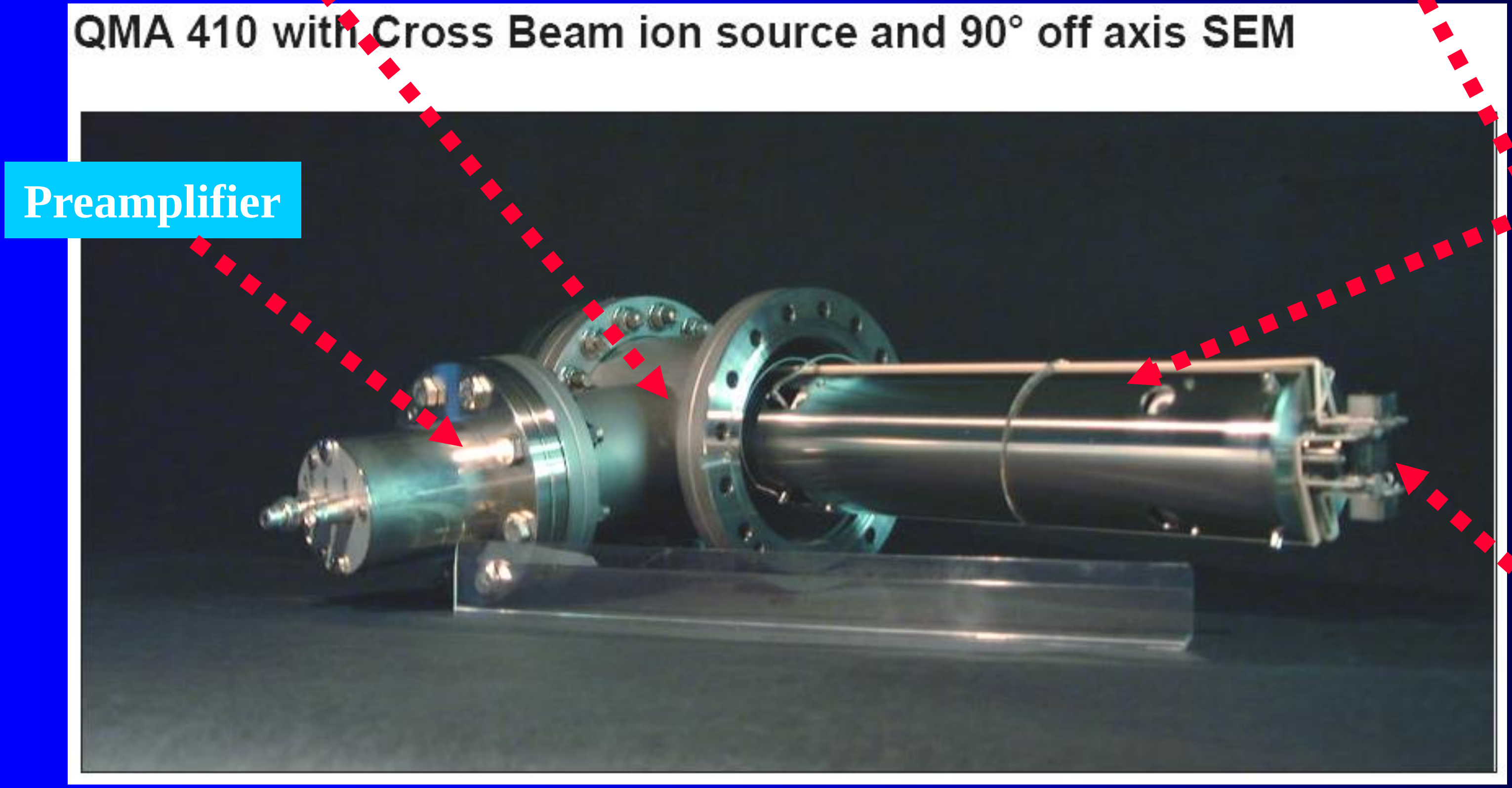
QMA 410 with Cross Beam ion source and 90° off axis SEM
Preamplifier
Cross Beam SOURCE

Mass spectrum

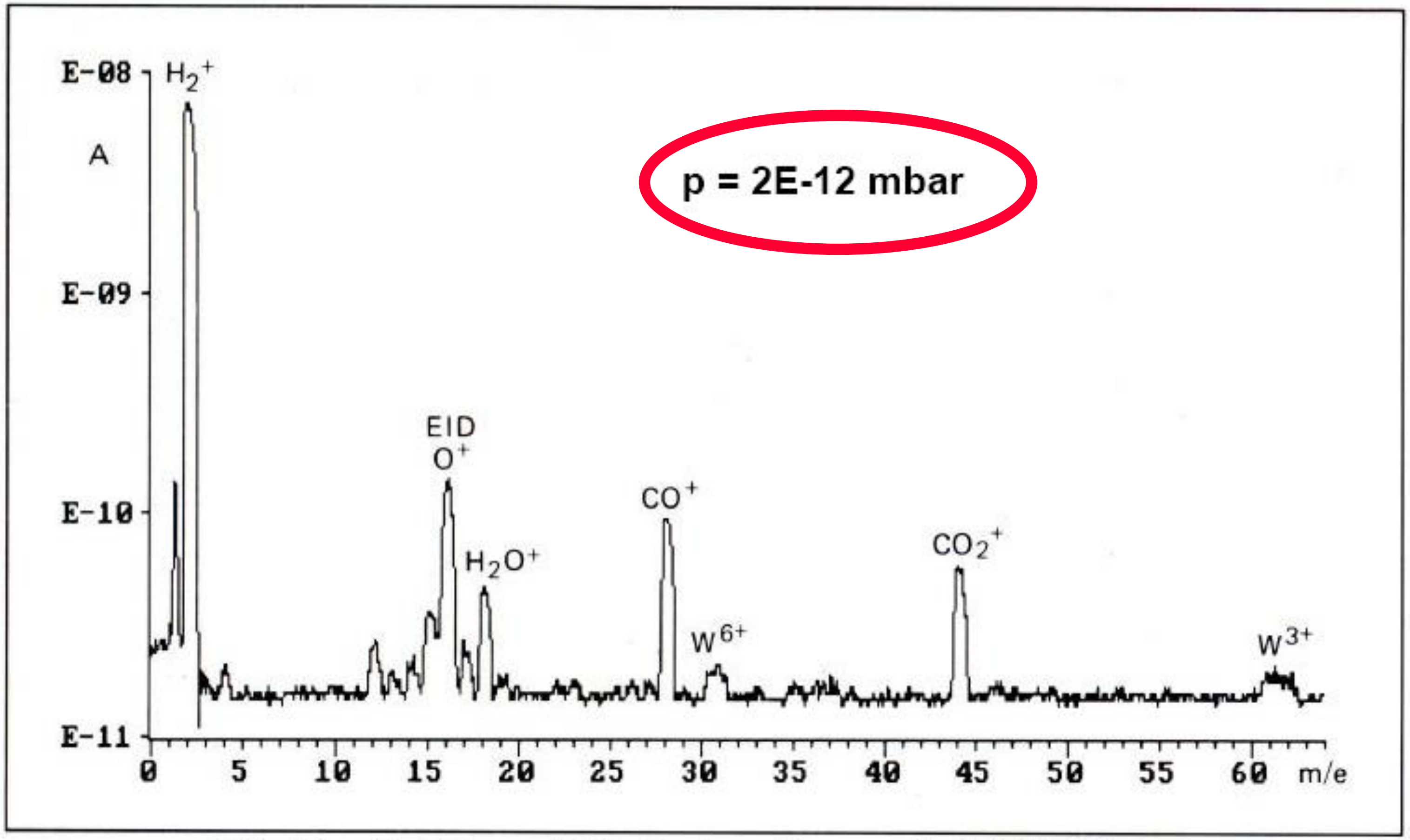

W.K. Huber, N. Müller, and G.Rettinghaus, Vacuum, 41, 2103 (1990)

Typical UHV spectrum

Ionization of clusters

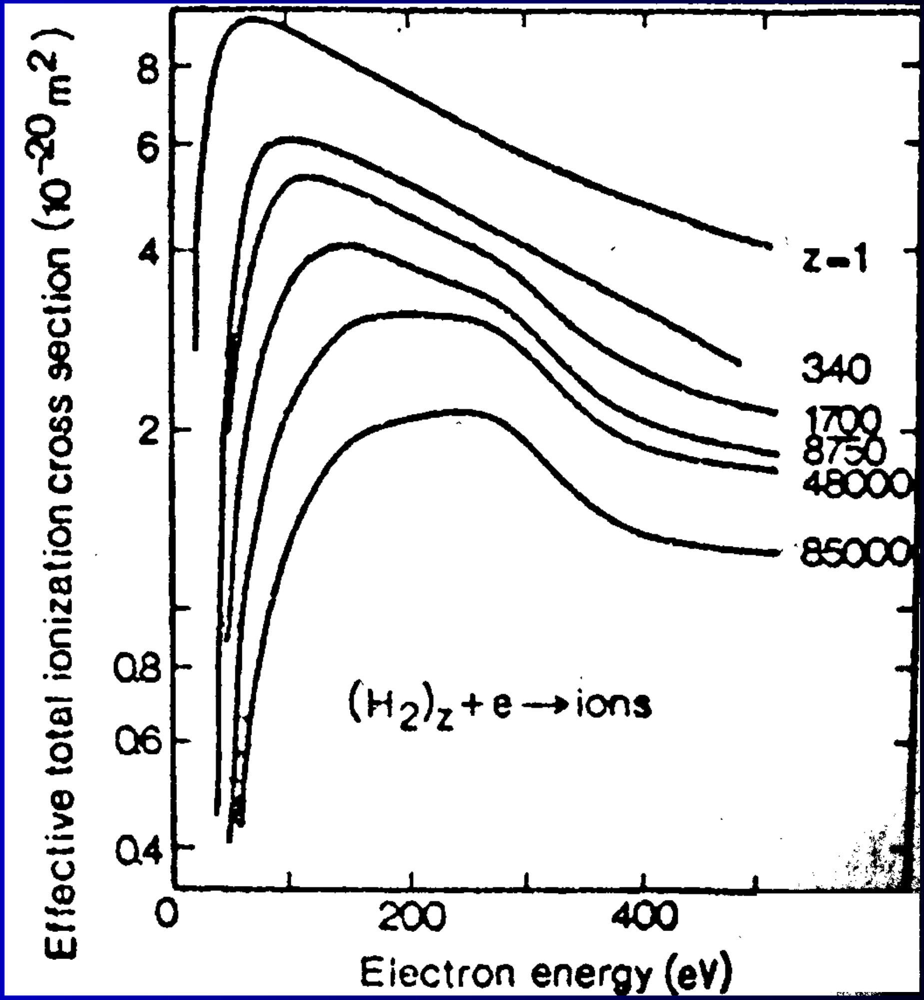

$(H_2)_Z + e \rightarrow$ ions

$\sigma_{\text{average total}} = Z.\ \sigma_{\text{effective}}$

Ionization of C60 Fulleren

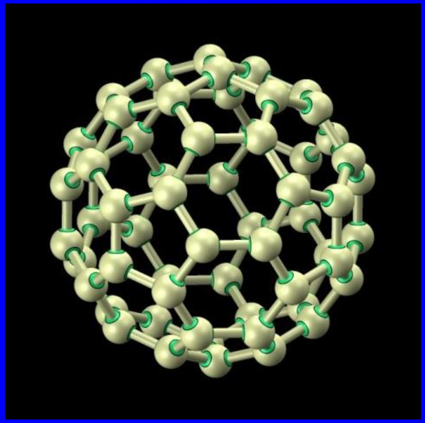

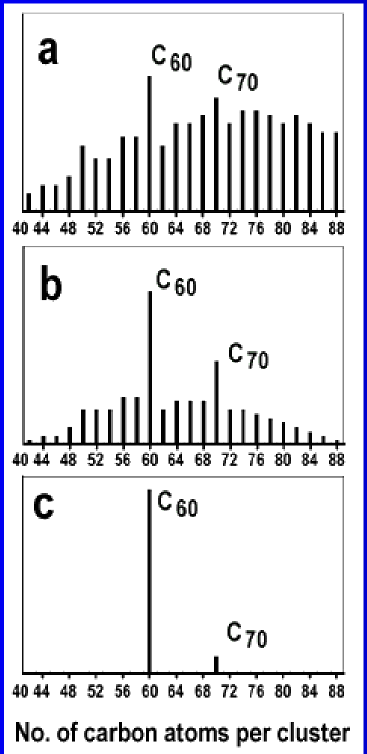

$$e^- + C_{60} \longrightarrow C_{60}^{+} + 2e^-$$

$$e^- + C_{60}^{+} \longrightarrow C_{60}^{2+} + 2e^-$$

$$e^- + C_{60}^{2+} \longrightarrow C_{60}^{3+} + 2e^-$$

$$e^- + C_{60}^{3+} \longrightarrow C_{60}^{4+} + 2e^-$$

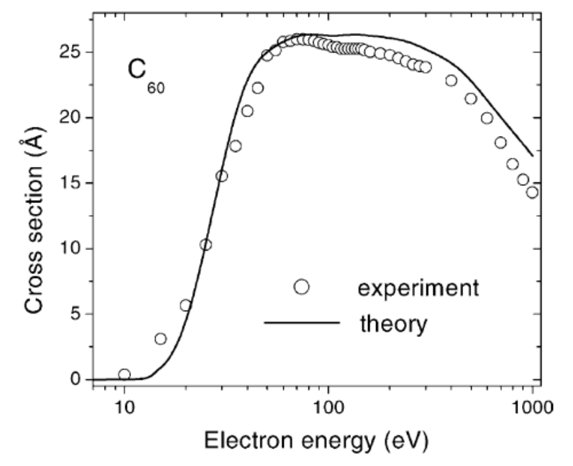

Fig. 6. Cross-section for the formation of C_{60}^{+} ions following electron-impact single ionization of C_{60}. The experimental data (○) are from Ref. [18], the solid line represents the present calculation.

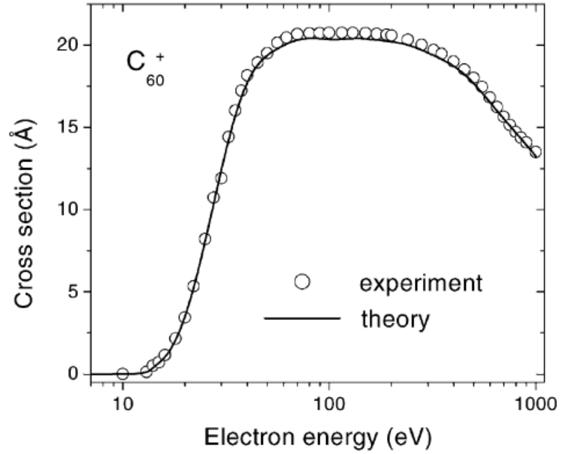

Fig. 3. Cross-section for the formation of C_{60}^{2+} ions following electron-impact single ionization of C_{60}^{+}. The experimental data (○) are from Ref. [23], the solid line represents the present calculation.

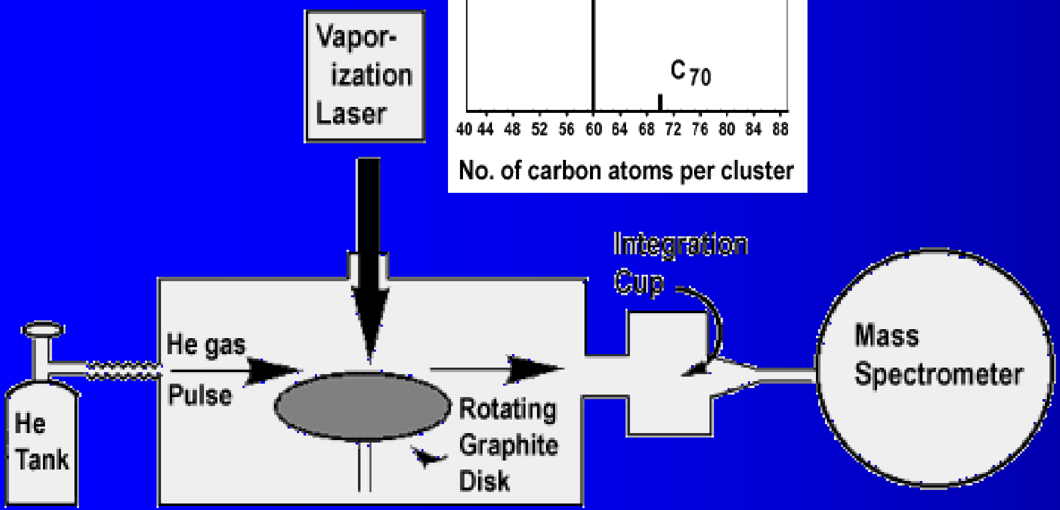

Distribution of carbon clusters produced under various experimental conditions.

a) Low helium density over graphite target at time of laser vaporization.

b) High helium density over graphite target at time of laser vaporization.

c) Same as b), but with addition of "integration cup" to increase time between vaporization and cluster analysis.

Electron-Impact Induced Fragmentation of Fullerene Ions

The measurements were performed employing the electron-ion crossed-beam setup. A commercially available powder of fullerenes was evaporated with an electrically heated oven. The neutral vapor was introduced into a 10 GHz Electron Cyclotron Resonance Ion Source (ECRIS). The extracted ion beam was collimated to 2x2 mm^2 after mass to charge analysis and crossed with an intense electron beam. The energy of the electrons can be varied between 10 and 1000 eV. After the electron-ion interaction the fragment ions $C_{58}{}^{q+}$ were separated from the incident ion beam of $C_{60}{}^{q+}$ by a 90^0 magnet and detected by a single-particle detector. The flight time between the interaction of the $C_{60}{}^{q+}$ ions and the analysis of the product ions is in the order of 10 μs. The current of the parent ion beam was measured simultaneously in a Faraday cup.

Binding energy value of about 11 eV

$$e^- + C_{60}{}^{+} \rightarrow C_{58}{}^{+} + C_2 + e^-$$

$$e^- + C_{60}{}^{2+} \rightarrow C_{58}{}^{2+} + C_2 + e^-$$

$$e^- + C_{60}{}^{3+} \rightarrow C_{58}{}^{3+} + C_2 + e^-$$

IONIZATION

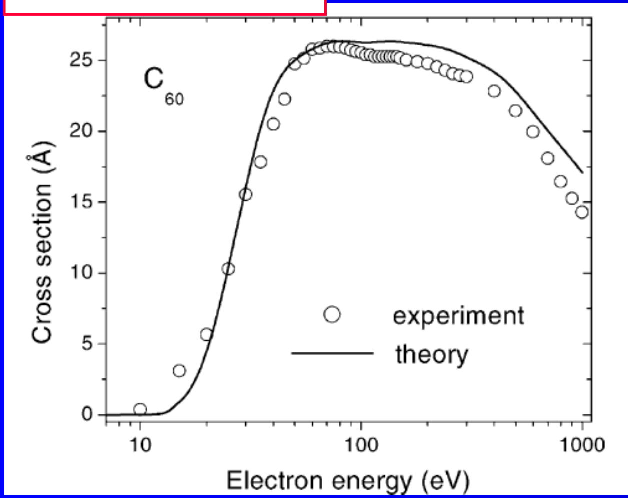

FRAGMENTATION

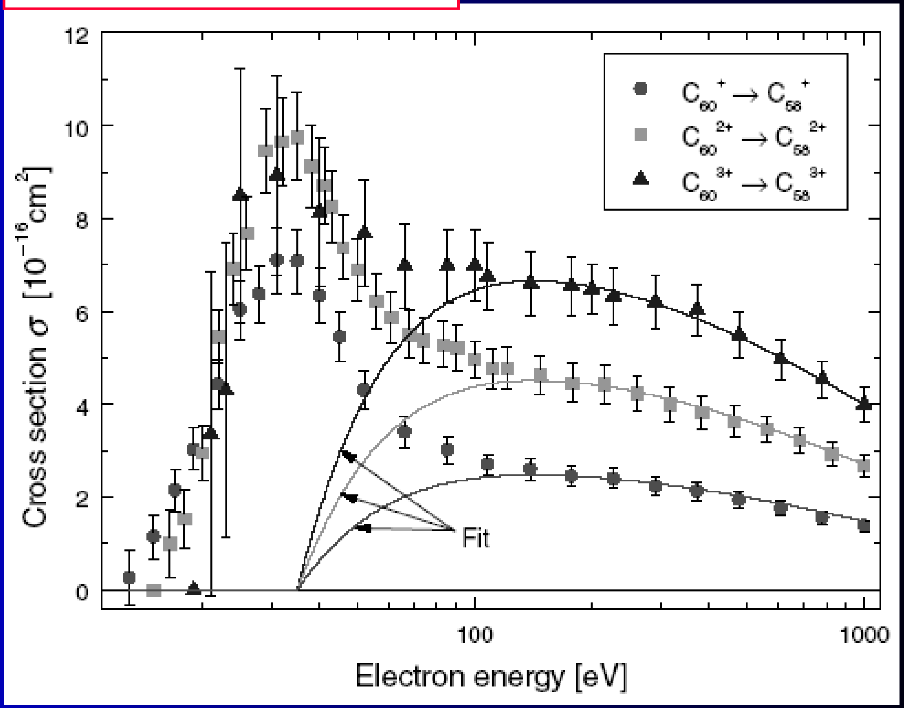

Absolute cross sections s for the electron-impact induced C_2 fragmentation of $C_{60}{}^{q+}$ ions.

Electron-Impact Induced Ionization of Fullerene Ions

IONIZATION

A semi-empirical concept for the calculation of electron-impac ionization cross-sections of neutral and ionized fullerenes

International Journal of Mass Spectrometry 223–224 (2003) 1–8

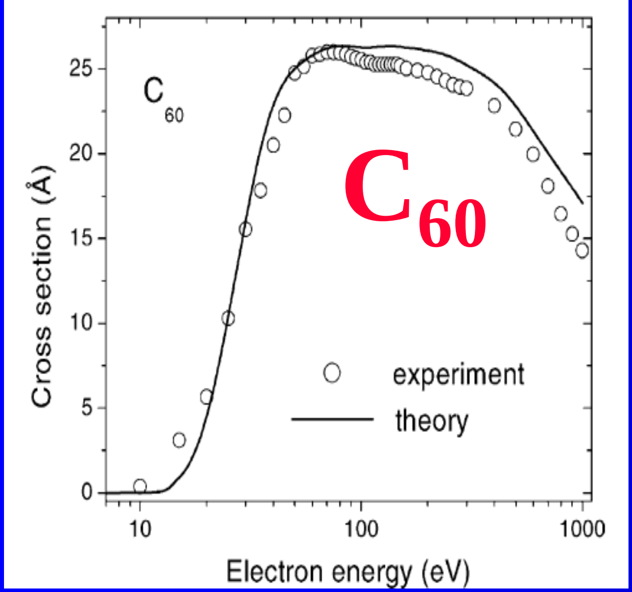

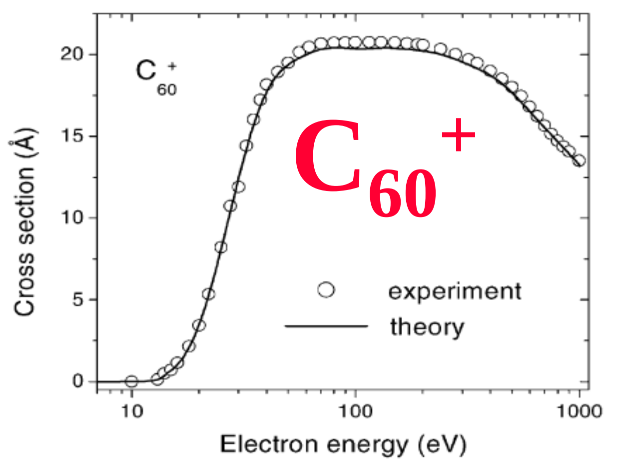

Fig. 3. Cross-section for the formation of C_{60}^{2+} ions following electron-impact single ionization of C_{60}^{+}. The experimental data (○) are from Ref. [23], the solid line represents the present calculation.

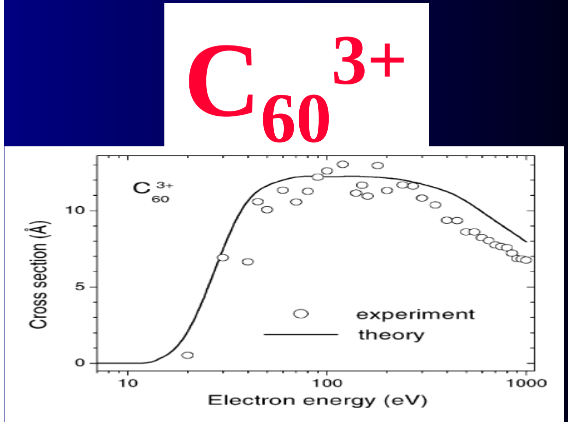

Fig. 4. Cross-section for the formation of C_{60}^{4+} ions following electron-impact single ionization of C_{60}^{3+}. The experimental data (○) are from Ref. [23], the solid line represents the present calculation.

Cross sections for vibrational excitation, dissociation, ionization…H_2

$H_2 + e$	→	$H_2(v) + e$ …….	Vibrational excitation
	→	$H + H + e$…….	Dissociation
	→	$H_2^* + h\nu + e$ …	Photon excitation
	→	$H_2^+ + e + e$…..	Ionization
	→	$H^+ + H + e + e$	Dissociative Ionization

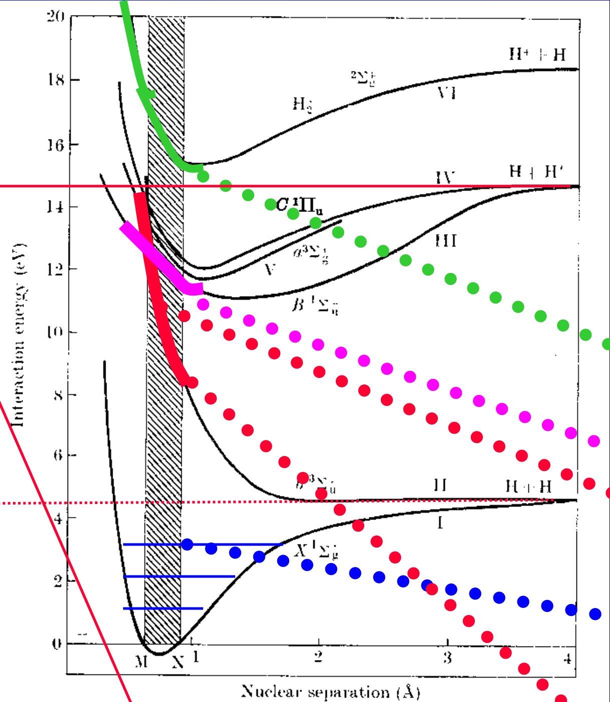

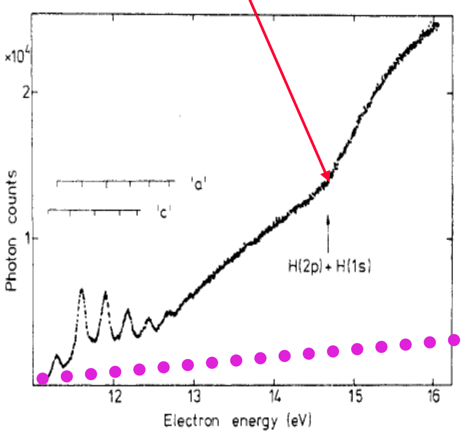

Figure 3. Optical excitation function for VUV photons measured with channeltron and MgF_2 window (1120–1300 Å); pressure 4×10^{-7} bar; collection time 7 h; 4·9 meV/channel. Energy positions of known resonances are indicated. The dissociation energy for H(2p) + H(1s) is marked by an arrow.

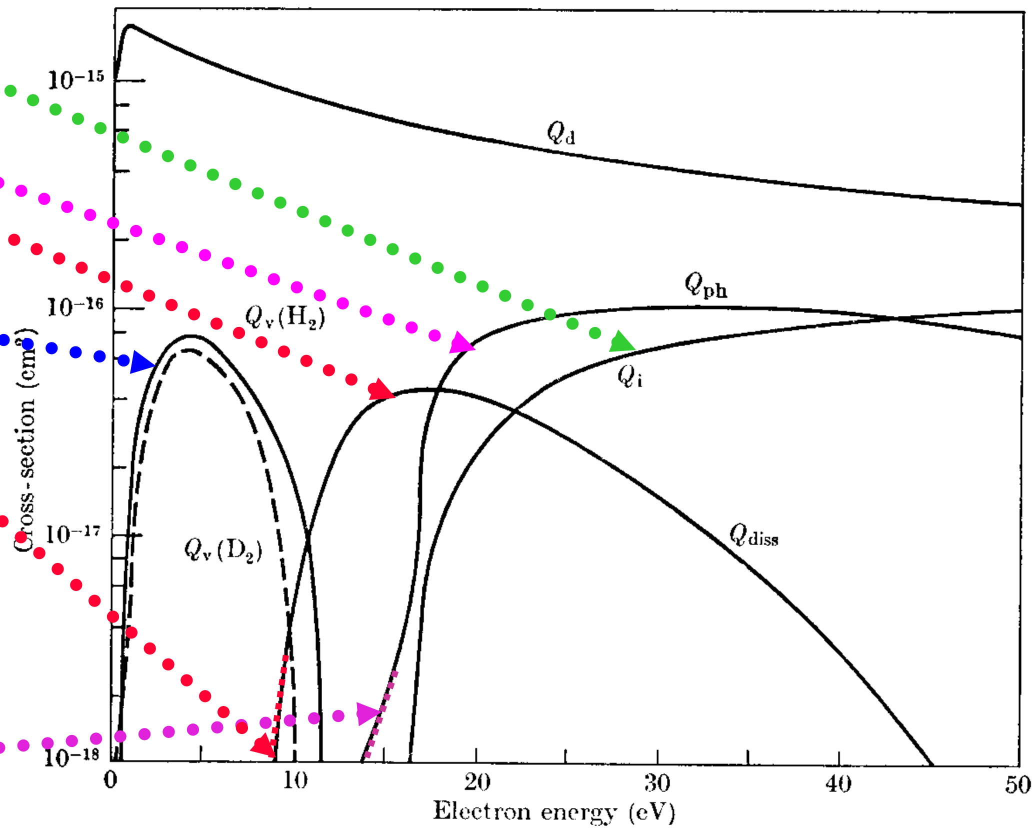

FIG. 13.37. Cross-sections assumed by Engelhardt and Phelps in their analysis of swarm data in H_2 and D_2 for electrons of characteristic energy greater than 1 eV. Q_d momentum-transfer cross-section, Q_i, ionization cross-section, Q_{diss} dissociation cross-section, Q_{ph} photon excitation cross-section, Q_v vibrational excitation cross-section (—— H_2, – – – D_2).

Cross sections for ionization…H_2

$H_2 + e$	→ $H_2(v) + e$ …….	Vibrational excitation
	→ $H + H + e$…….	Dissociation
	→ $H_2^* + h\nu + e$ …	Photon excitation
	→ $H_2^+ + e + e$…..	Ionization
	→ $H^+ + H + e + e$	

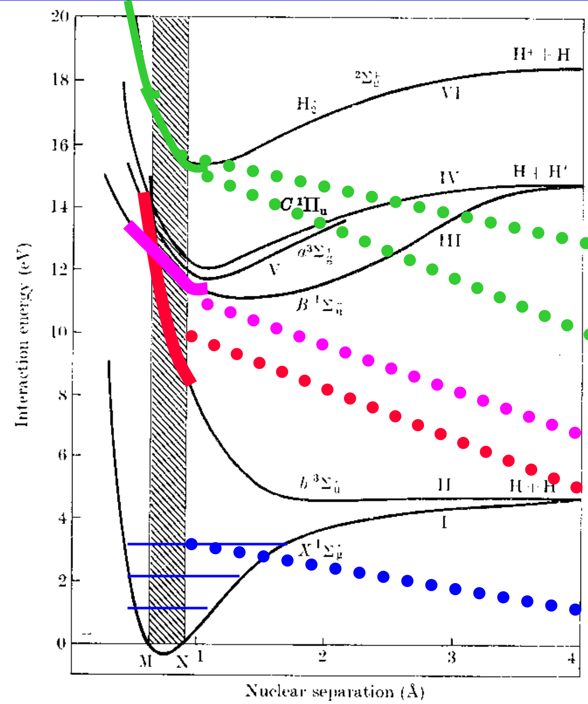

FIG. 13.1. Potential energy curves for electronic states of H_2 and H_2^+ lying within 20 eV of the …

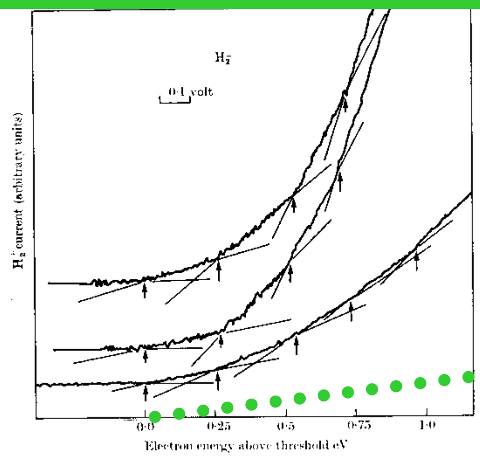

FIG. 13.19. Variation of the ionization cross-section of H_2 near the threshold as observed by Marmet and Kerwin.

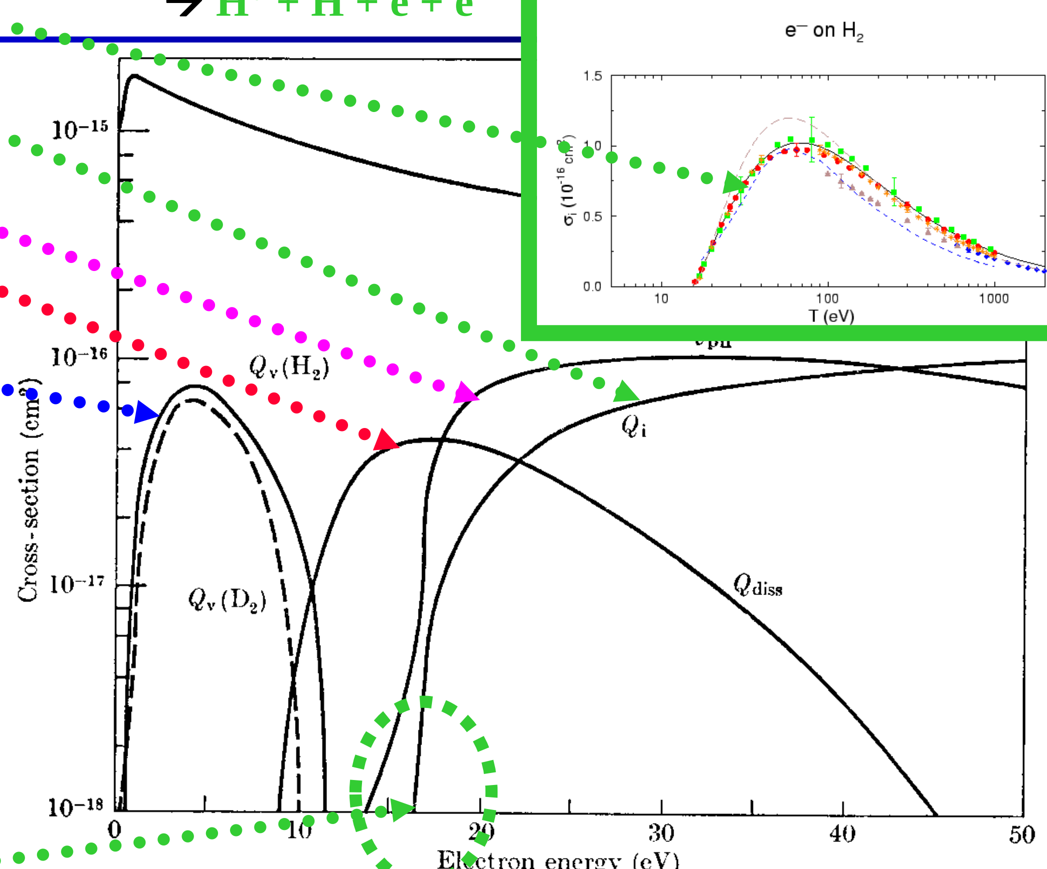

FIG. 13.37. Cross-sections assumed by Engelhardt and Phelps in their analysis of swarm data in H_2 and D_2 for electrons of characteristic energy greater than 1 eV. Q_d momentum-transfer cross-section, Q_i, ionization cross-section, Q_{diss} dissociation cross-section, Q_{ph} photon excitation cross-section, Q_v vibrational excitation cross-section (—— H_2, – – – D_2).

Koniec rospravky

Ionization, excitation …..

Complicated

$N_2(\nu,j) + e^-(\varepsilon_0) \rightarrow N_2^+(\nu,j) + e_1^-(\varepsilon_1) + e_2^-(\varepsilon_2)$
$\rightarrow N^+(\varepsilon_{KIN}) + N(\varepsilon_{KIN}) + e_1^-(\varepsilon_3) + e_2^-(\varepsilon_4)$

$NH_3 + e^-(\varepsilon_0) \rightarrow$ **…..to several product - channels**

Neutral – Rydberg interaction

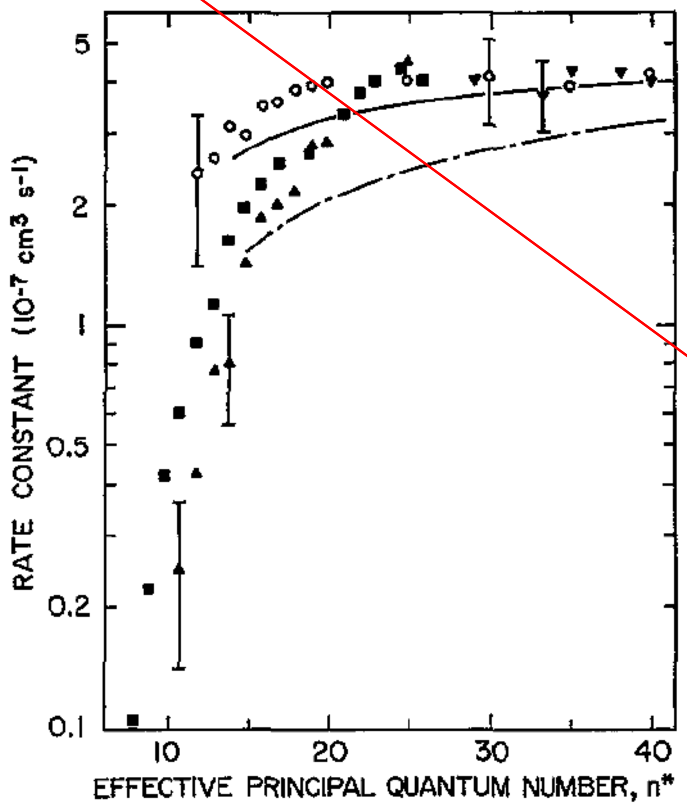

Figure 8. Rate constants for Rydberg destruction and free-ion production in Rydberg atom collisions with SF_6. The data are plotted as a function of $n^* = n - \delta$ when δ is the quantum defect. ○, K(*n*p) destruction (Zheng *et al* 1990); ▲, K(*n*d) free-ion production (Zollars *et al* 1986); ■, Ne(*n*s) free-ion production (Harth *et al* 1989); ——, — · —, calculated values $l=2$, $l=l_{max}=n-1$ (Klar *et al* 1994a).

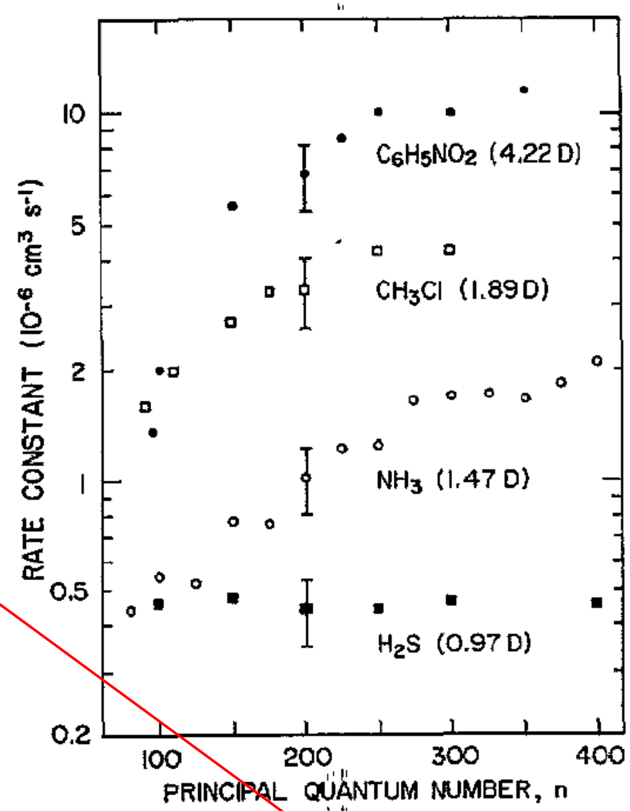

Figure 9. Rate constants for Rydberg atom destruction in collisions with polar targets. The data for H_2S are for destruction of parent K(*n*p) atoms; the data for NH_3, CH_3Cl and $C_6H_5NO_2$ are for an *l*-mixed population (Ling *et al* 1993a, Frey *et al* 1994a, b). The numbers in parentheses give the dipole moment of each target.

$$K(np) + H_2S(J, \tau) \rightarrow K^+ + H_2S(J', \tau') + e^-.$$

Photoionization from Ar metastable

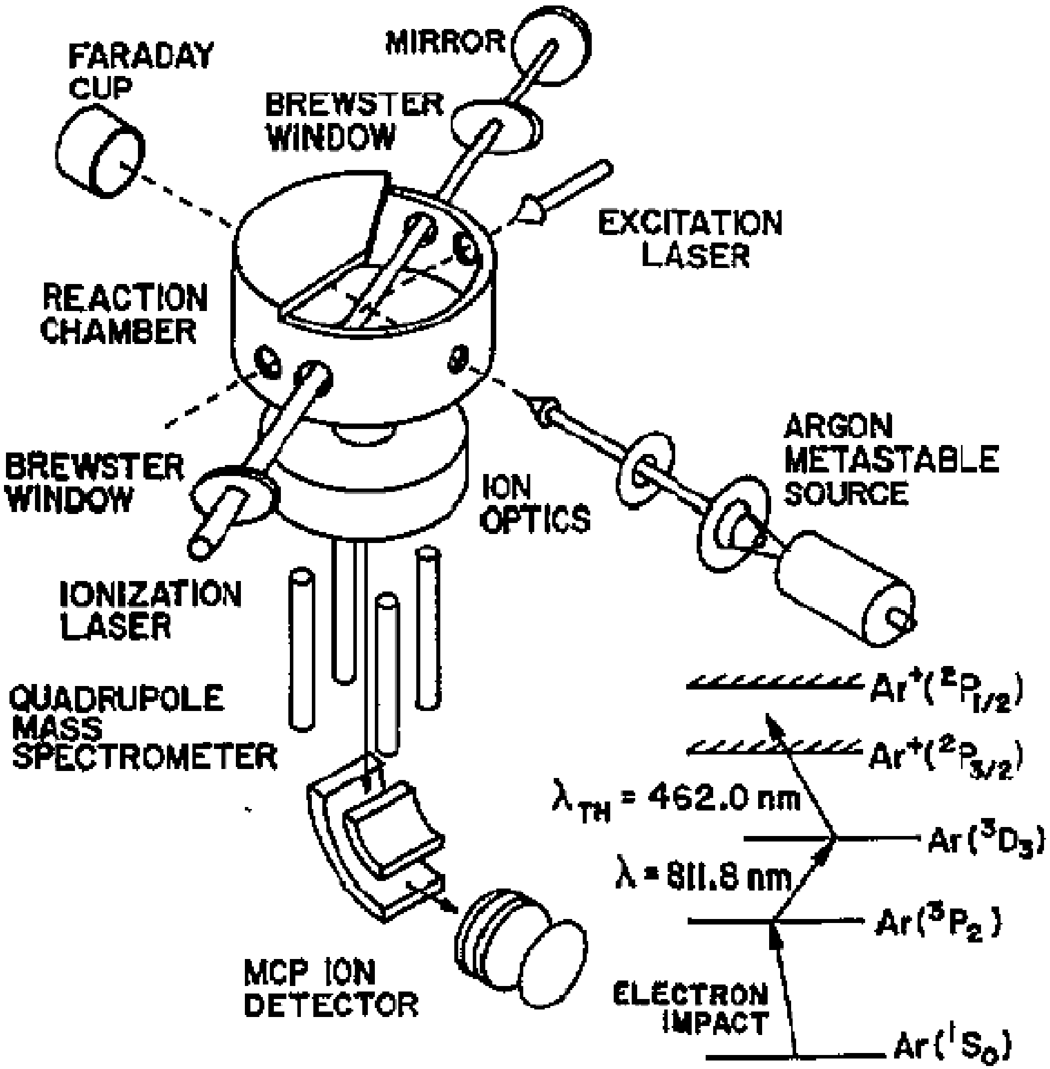

Figure 4. Schematic diagram of the laser-induced photoionization apparatus used fo
attachment studies (Klar *et al* 1994b).

Franck-Condon principle - FOTOIONIZATION

MO diagram for the three highest occupied MOs in CO accessible by HeI radiation. PES of CO obtained by HeI radiation and potential energy curves for the neutral molecule and the three ionized states.

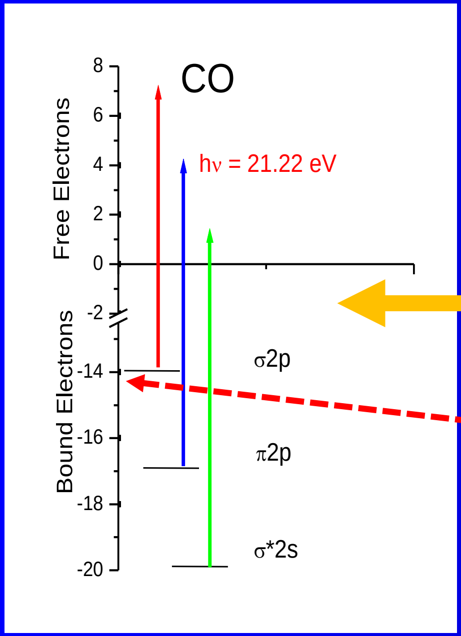

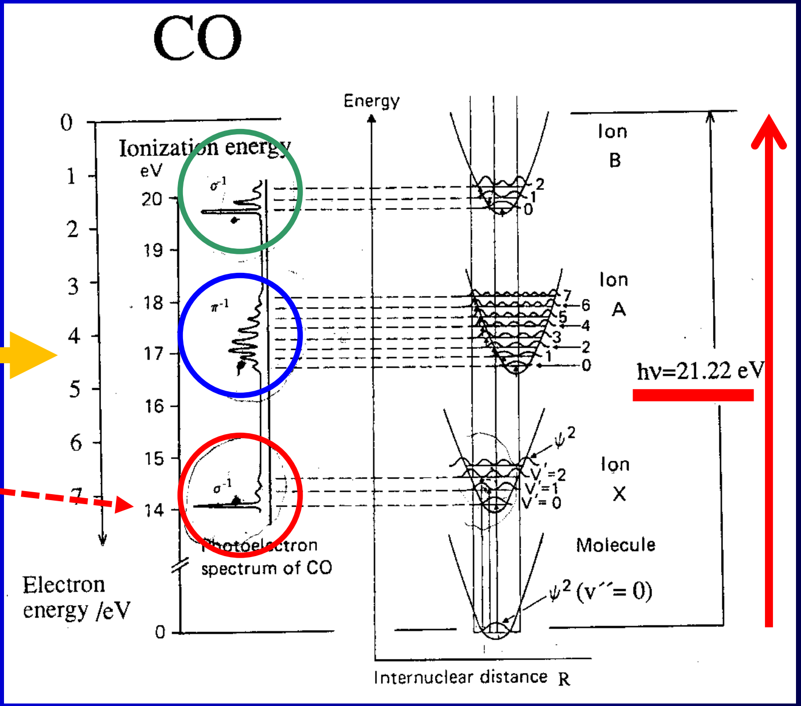

Total collision cross sections Na, K, Cs…

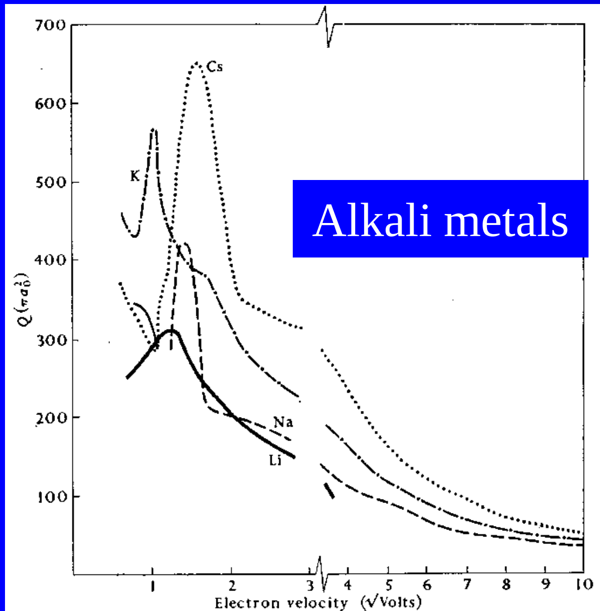

FIG. 1.16. Observed total collision cross-sections of Li, Na, K, and Cs.

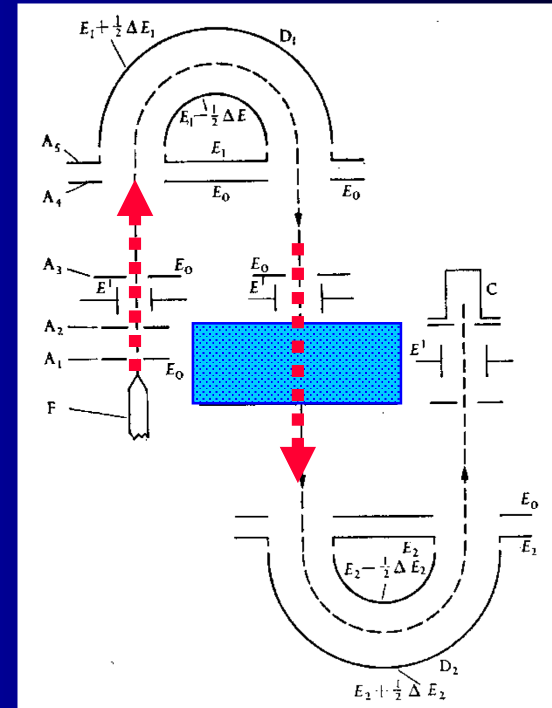

FIG. 1.6. Schematic diagram of the arrangement of apparatus developed by Simpson for observing fine structure in the variation with energy of the transmission of electrons through gases.

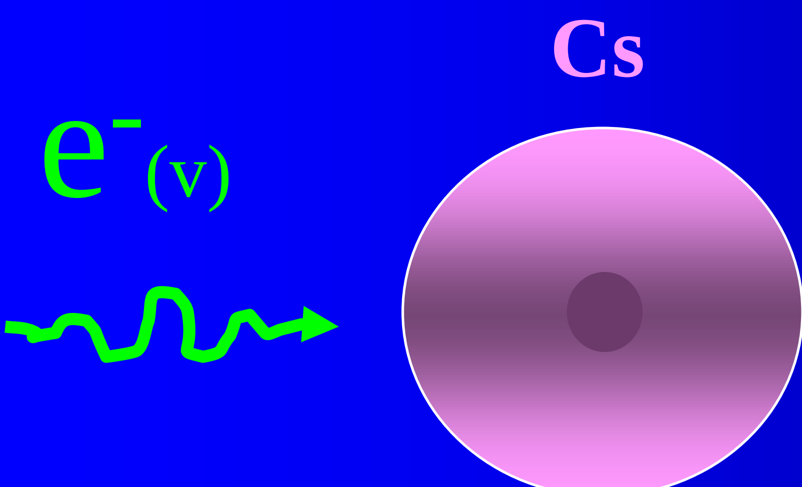

Very low collision energies

TOPICAL REVIEW

Electron–molecule collisions at very low electron energies

F B Dunning

Department of Physics and the Rice Quantum Institute, Rice University, PO Box 1892, Houston, TX 77251, USA

J. Phys. B: At. Mol. Opt. Phys. 28 (1995) 1645–1672. Printed in the UK

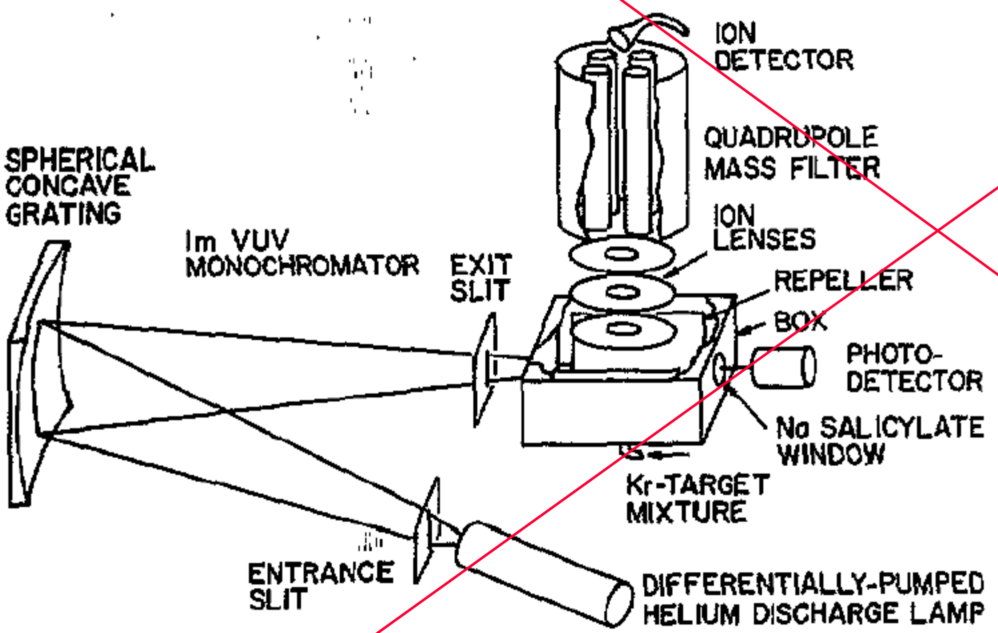

Figure 1. Schematic diagram of the vuv photoionization apparatus used for attachment studies (Chutjian and Alajajian 1985a, b).

$$Kr(^1S_0) + \hbar\omega \rightarrow Kr^+(^2P_{1/2}) + e^-(\varepsilon)$$

$$e^- + SF_6 \rightarrow SF_6^{-*}$$

$$e^- + CCl_4 \rightarrow CCl_4^{-*} \rightarrow CCl_3 + Cl^-$$

Electron attachment at very low electron energies

10^5 Å

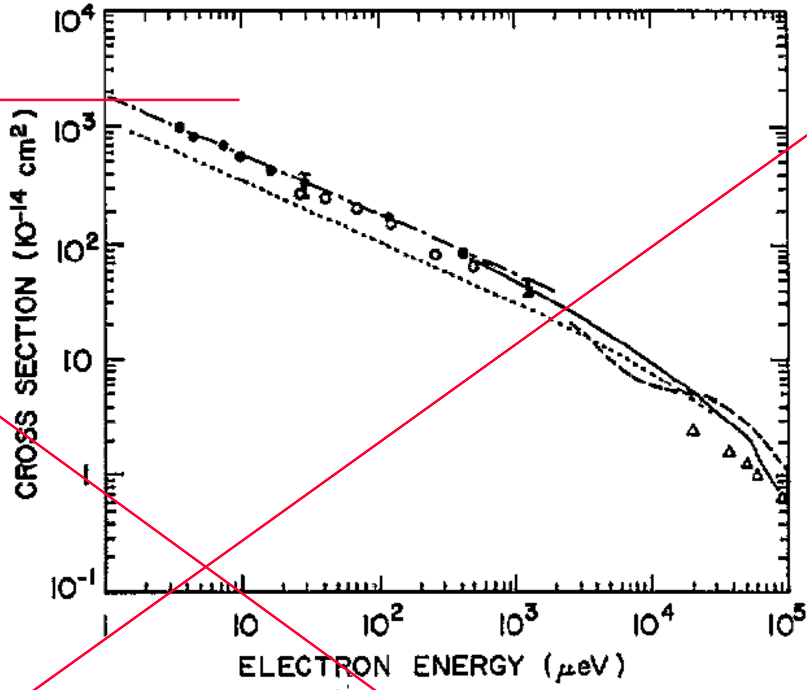

Figure 3. Cross sections for electron attachment to CCl_4. ●, $\bar{\sigma}_e$-K(np); — · —, $\sigma_e(\nu)$-K(np) (Frey *et al* 1994b); ○, $\bar{\sigma}_e$-K(np) (Ling *et al* 1992); ——, free electrons (Hotop 1994); – – –, free electrons (Orient *et al* 1989); Δ, free electrons (Christodoulides and Christophorou (1971); -----, theory (Klots 1976).

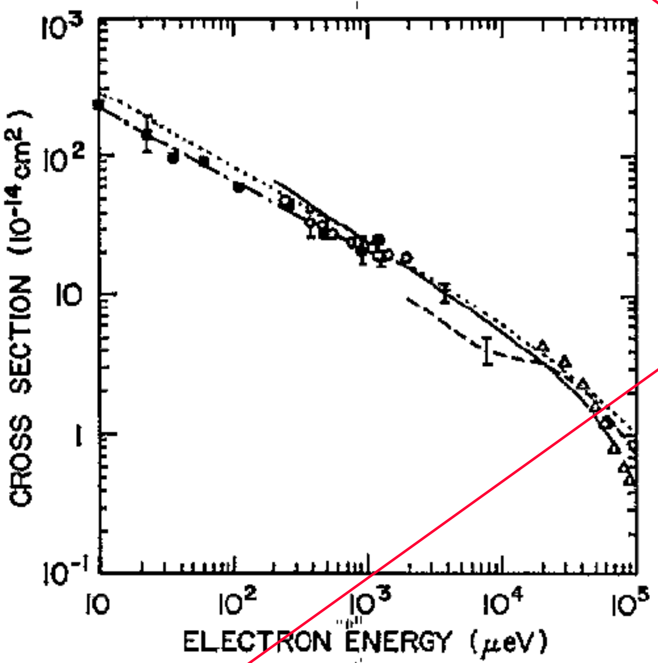

Figure 2. Cross section for electron attachment to SF_6. ■, $\bar{\sigma}_e$-K(np); — · —, $\sigma_e(\nu)$-K(np) (Ling *et al* 1992). ○, $\bar{\sigma}_e$-Rb(ns) (Zollars *et al* 1985); ——, free electrons (Klar *et al* 1992a, b); – – –, free electrons (Chutjian and Alajajian 1985); Δ, free electrons (Pai *et al* 1979, Chutjian and Alajajian 1985a); -----, theory (Klots 1976).

Partial cross section for excitation

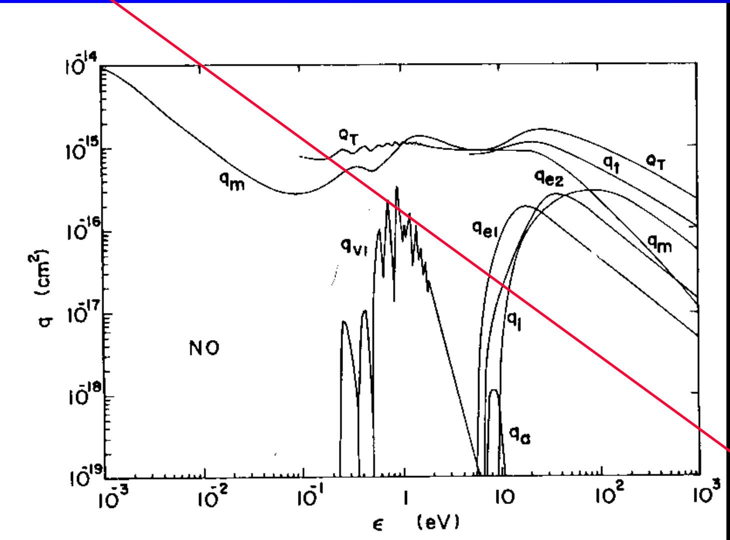

Fig. 4. Cross-section set for NO (1986).

NO + e

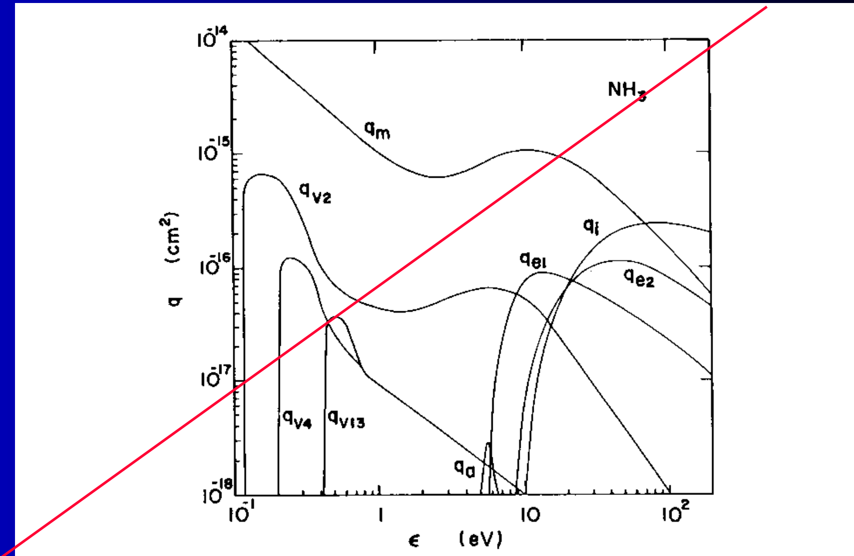

Fig. 6. Electron collision cross-section set for NH_3 (1986).

NH_3 + e

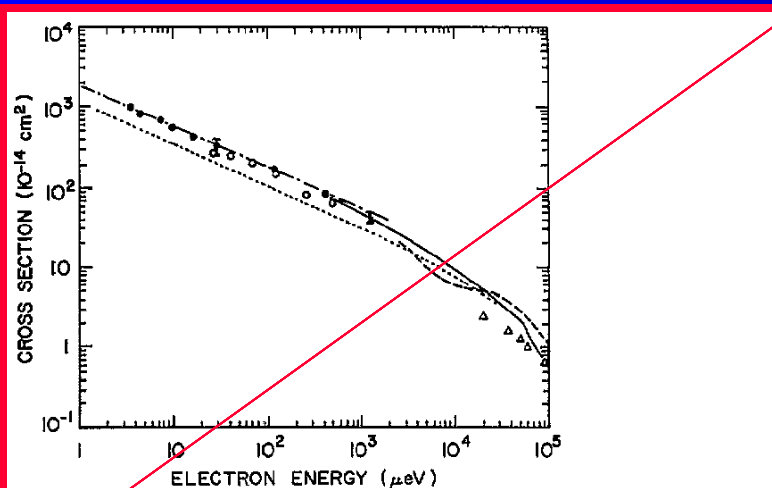

Figure 3. Cross sections for electron attachment to CCl_4. ●, $\bar{\sigma}_e$-K(*n*p); — · —, $\sigma_e(\nu)$-K(*n*p) (Frey *et al* 1994b); ○, $\bar{\sigma}_e$-K(*n*p) (Ling *et al* 1992); ——, free electrons (Hotop 1994); - - -, free electrons (Orient *et al* 1989); △, free electrons (Christodoulides and Christophorou (1971); -----, theory (Klots 1976).

$$e^- + SF_6 \rightarrow SF_6^{-*}$$

$$e^- + CCl_4 \rightarrow CCl_4^{-*} \rightarrow CCl_3 + Cl^-$$

Rate coefficients of elementary processes

$$A + B \xrightarrow{k} C + D$$

$$A + B \xrightarrow{k} products$$

$$\frac{d[A]}{dt} = -k[A][B]$$

~300 K

	reactants	products	rate coefficient
Electron atomic ion rec.	$Ar^+ + e^-$	$Ar + h\nu$	$\sim 10^{-11} cm^3 s^{-1}$
Electron - ion recomb.	$O_2^+ + e^-$	$O + O$	$2x10^{-7} cm^3 s^{-1}$
Ion – ion recombination	$Ar^+ + Cl^-$	$Ar + Cl$	$2x10^{-8} cm^3 s^{-1}$
Ion – molecule reactions	**$H_2^+ + H_2$->**	**$H_3^+ + H$**	**$2x10^{-9} cm^3 s^{-1}$**
Attachment	$CCl_4 + e^-$	$Cl^- + CCl_3$	$\sim 10^{-7} cm^3 s^{-1}$
Penning ionization	$He^* + Ar$	$Ar^+ + e^- + He$	$7x10^{-11} cm^3 s^{-1}$
.			

Kinetics of elementary process

$$H_2^+ + Ar \Rightarrow ArH^+ + H$$

$$d(n_{H2^+})/dt = -k\, n_{H2^+} \cdot n_{Ar}$$

$$n_{H2^+} \ll n_{Ar}$$

$$n_{H2^+} = (n_{H2^+})_0 \exp(-k n_{Ar} t)$$

Multiple collision @ T

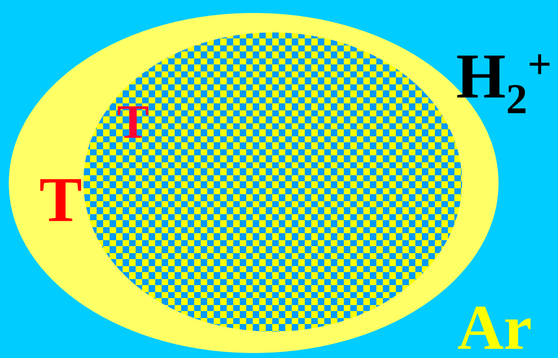

reaction rate coefficient

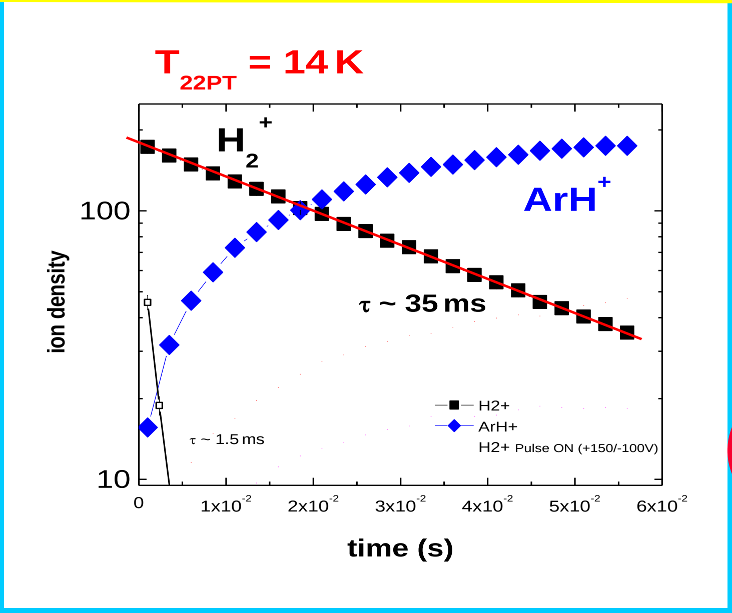

k(T)

Electron attachment at very low electron energies

10^5 Å

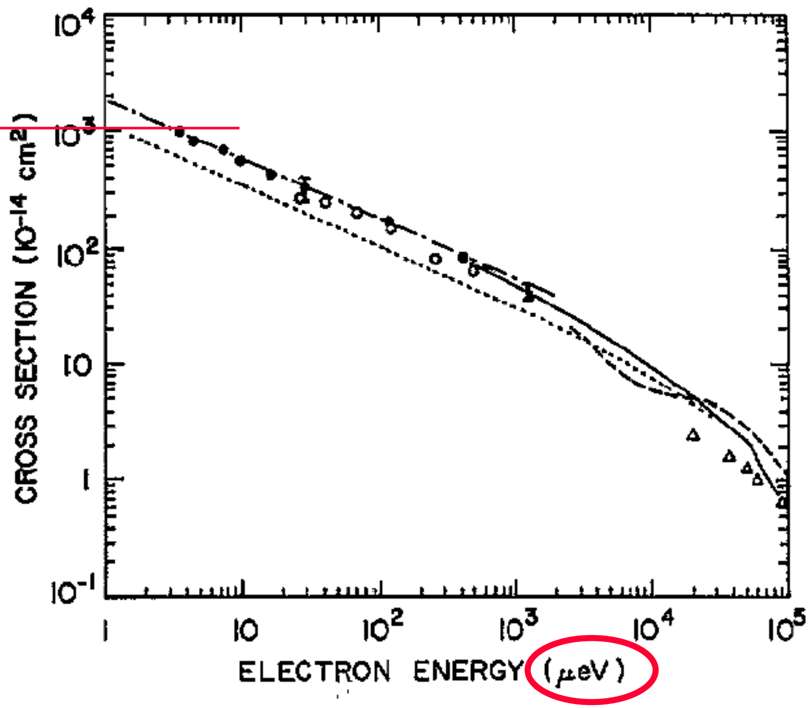

Figure 3. Cross sections for electron attachment to CCl_4. ●, $\bar{\sigma}_e$–K(np); — · —, $\sigma_e(\nu)$–K(np) (Frey *et al* 1994b); ○, $\bar{\sigma}_e$–K(np) (Ling *et al* 1992); ——, free electrons (Hotop 1994); – – –, free electrons (Orient *et al* 1989); Δ, free electrons (Christodoulides and Christophorou (1971); -----, theory (Klots 1976).

10^5 Å

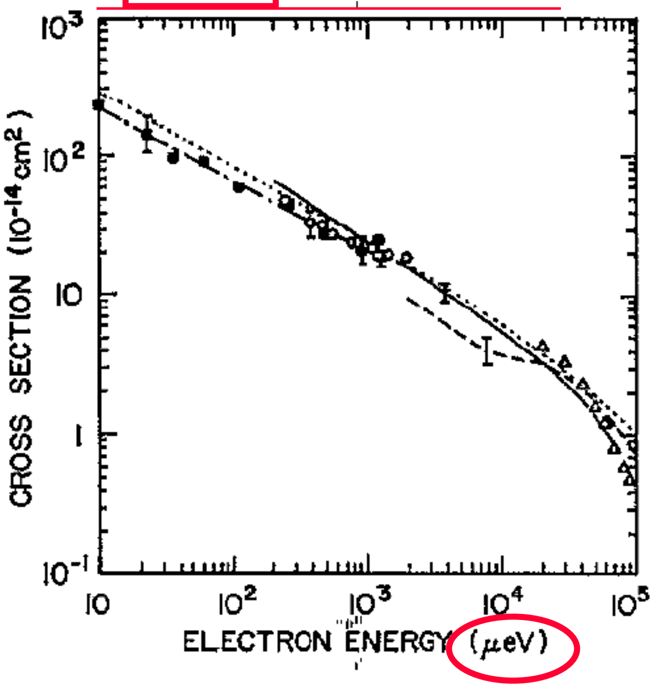

Figure 2. Cross section for electron attachment to SF_6. ■, $\bar{\sigma}_e$–K(np); — · —, $\sigma_e(\nu)$–K(np) (Ling *et al* 1992). ○, $\bar{\sigma}_e$–Rb(ns) (Zollars *et al* 1985); ——, free electrons (Klar *et al* 1992a, b); – – –, free electrons (Chutjian and Alajajian 1985); Δ, free electrons (Pai *et al* 1979, Chutjian and Alajajian 1985a); -----, theory (Klots 1976).

Collisions of electrons with atoms – Ramsauer's method

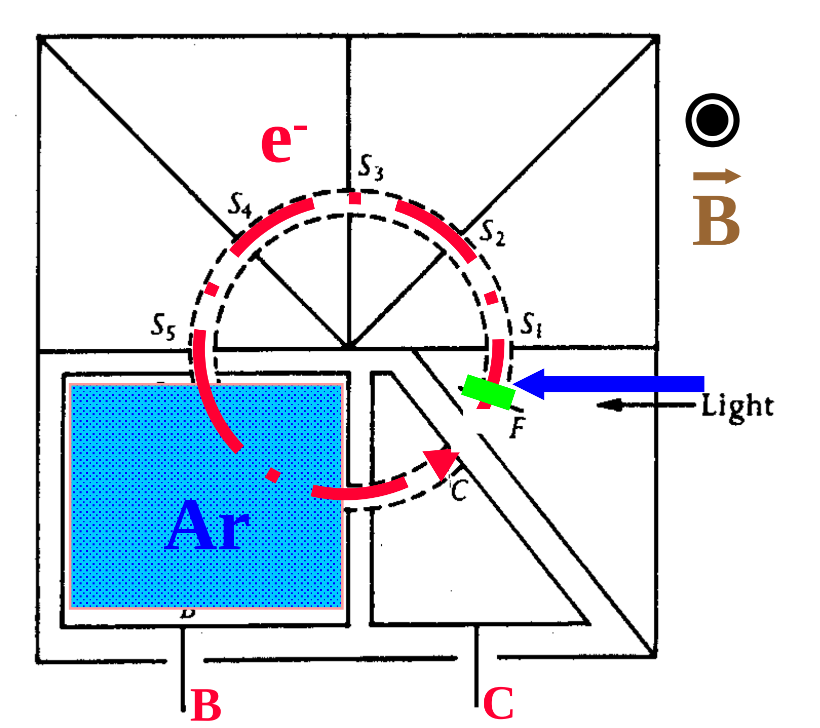

FIG. 1.1. Ramsauer's apparatus for measurement of collision cross-sections.

Lenard 1903
Akesson 1916
Ramsauer 1921

ATENUATION METHOD

$$\delta I \sim -N I\, \delta x$$

$$\delta I = -N \sigma I\, \delta x$$

$$I = I_0 \exp(-\sigma N x)$$

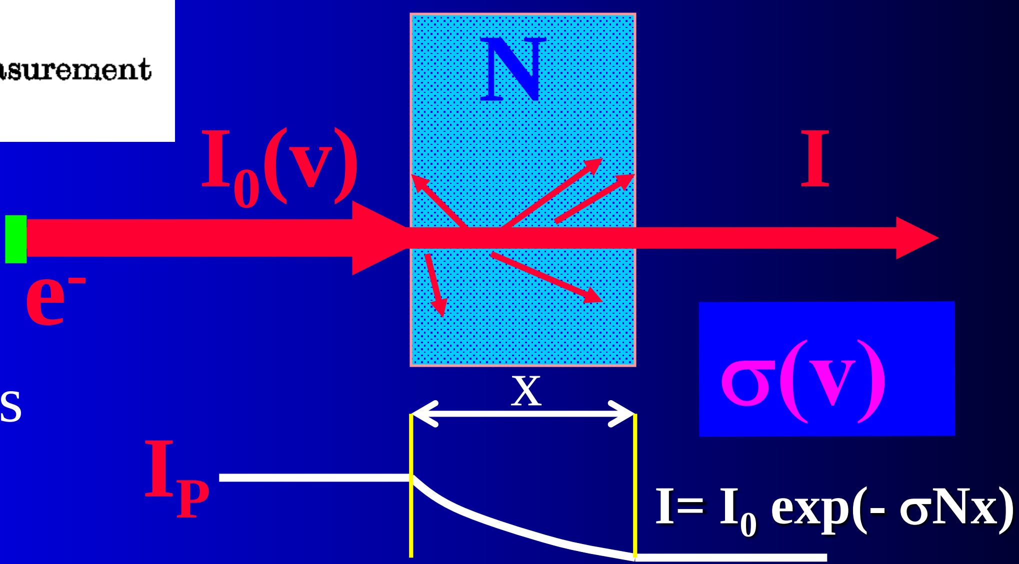

Mono energetic electrons

Collisions of electrons with atoms – Ramsauer's method

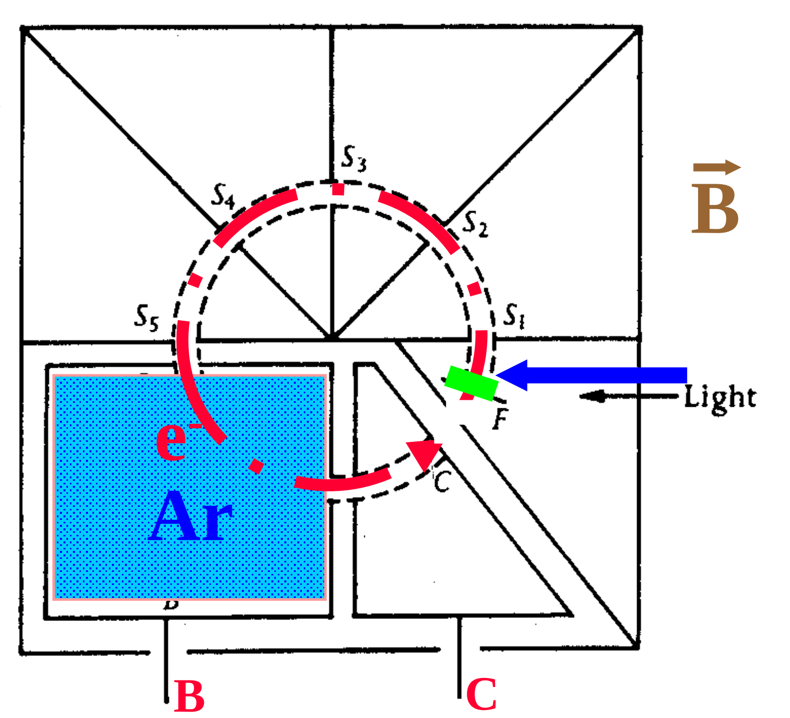

FIG. 1.1. Ramsauer's apparatus for measurement of collision cross-sections.

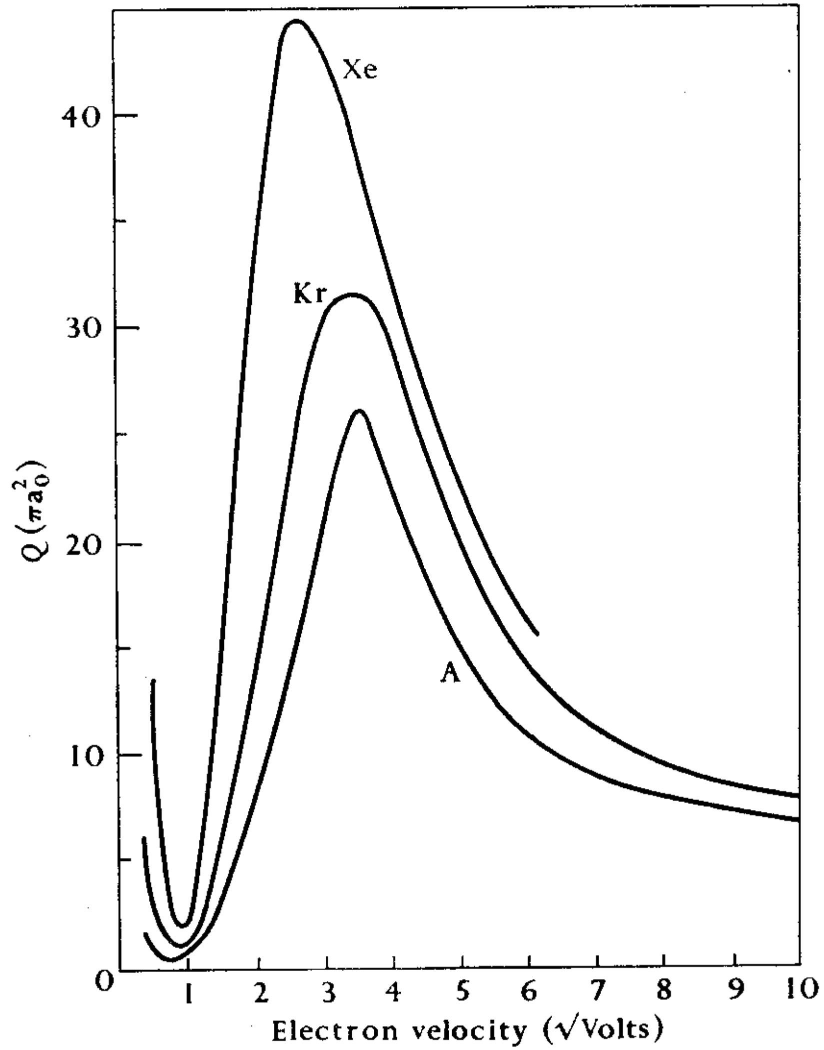

FIG. 1.9. Observed total collision cross-sections of A, Kr, and Xe.

Lenard 1903
Akesson 1916
Ramsauer 1921

Collisions of electrons with atoms – Rams

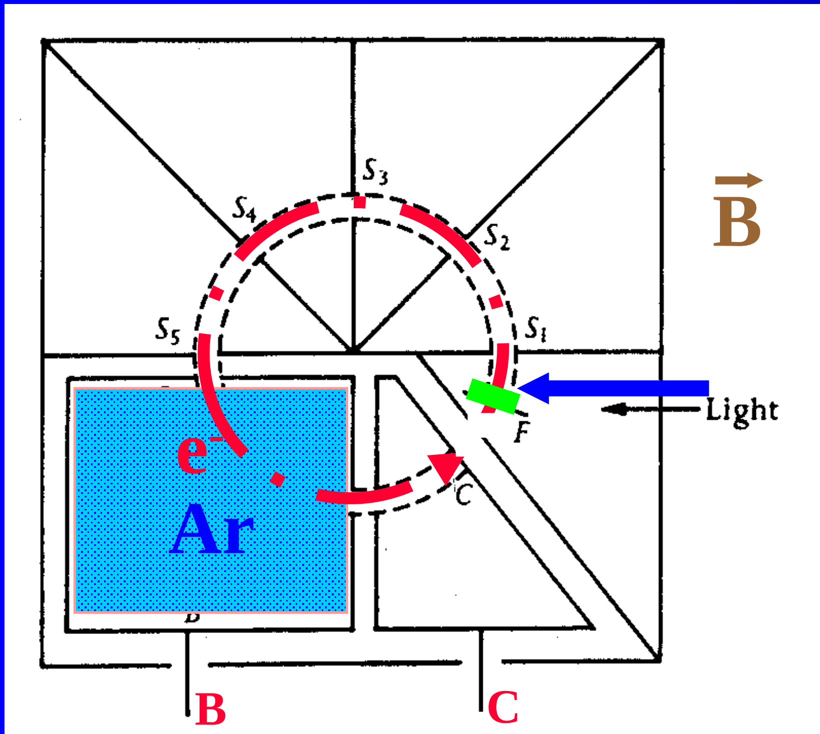

FIG. 1.1. Ramsauer's apparatus for measurement of collision cross-sections.

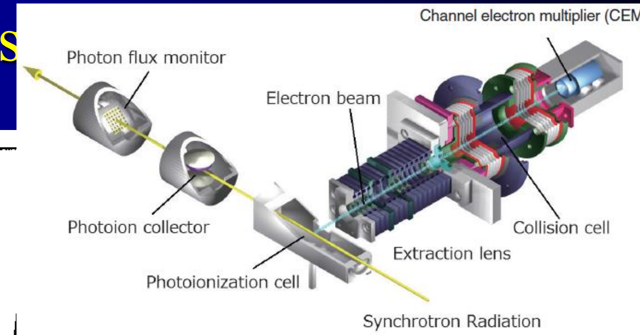

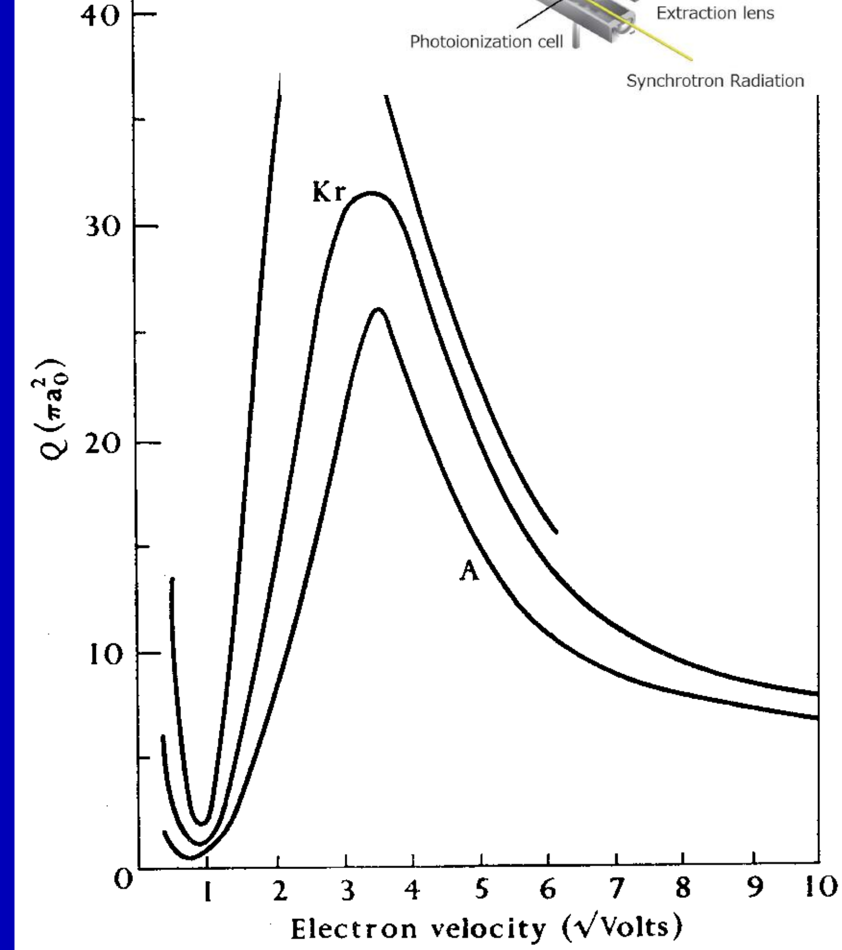

FIG. 1.9. Observed total collision cross-sections of A, Kr, and Xe.

Lenard 1903
Akesson 1916
Ramsauer 1921

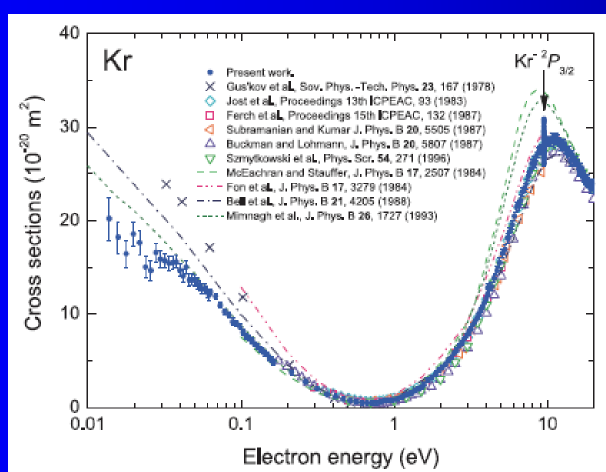

Total collision cross section – e/atoms

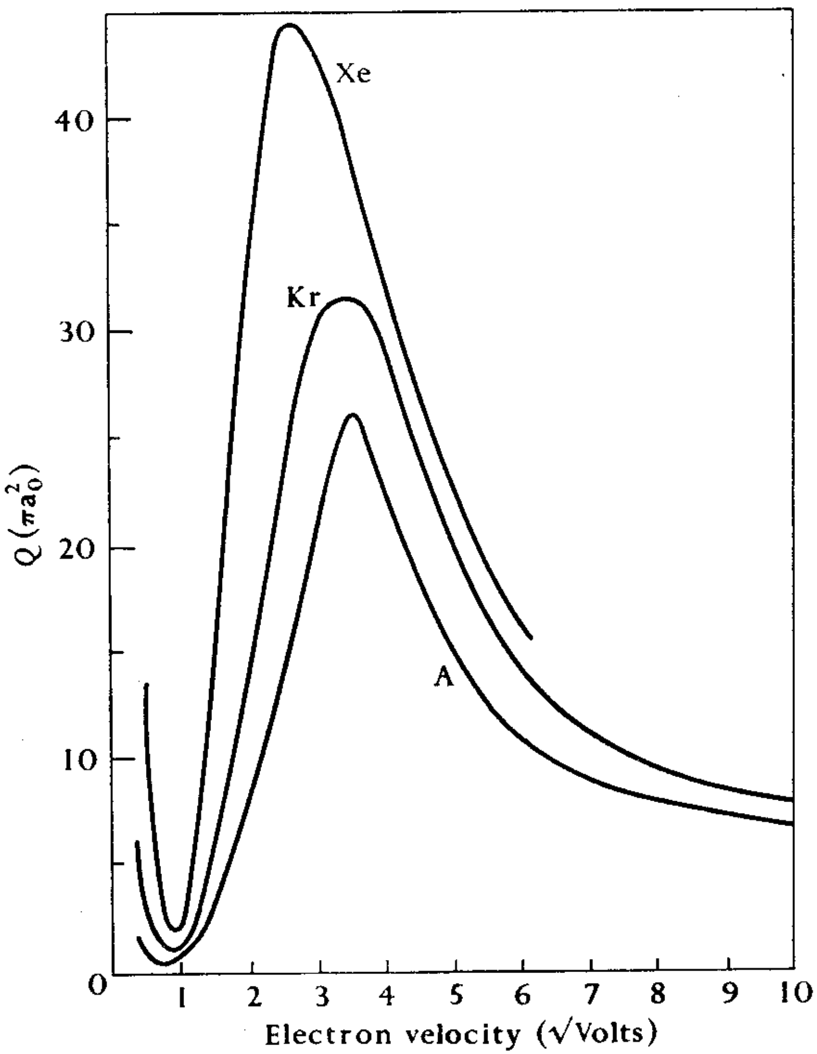

FIG. 1.9. Observed total collision cross-sections of A, Kr, and Xe.

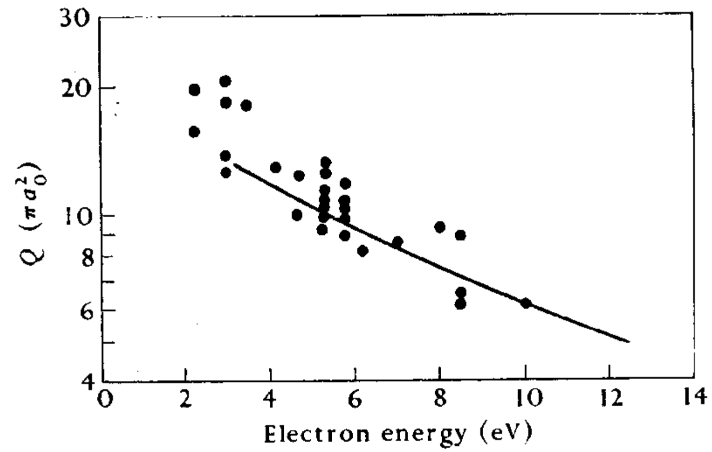

FIG. 1.11. Total collision cross-sections of atomic hydrogen. ● observed by Brackmann, Fite, and Neynaber; —— observed by Neynaber, Marino, Rothe, and Trujillo.

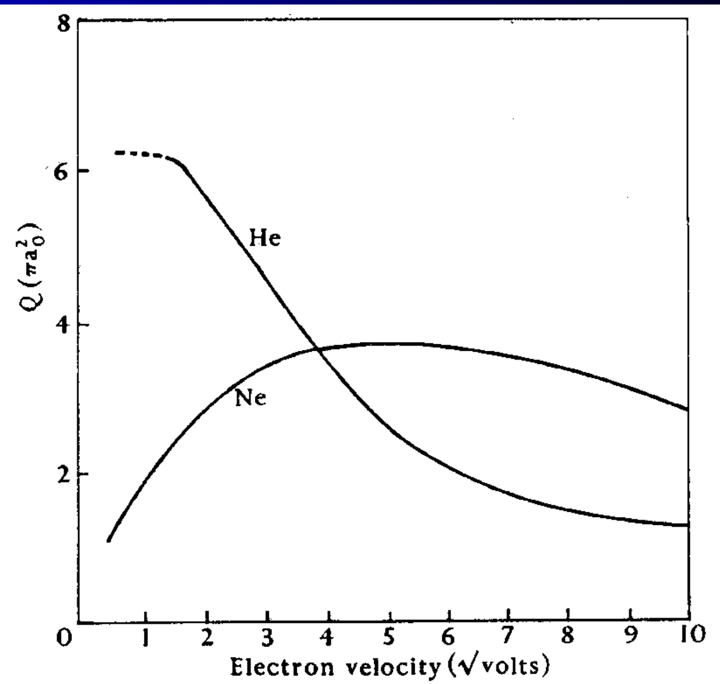

FIG. 1.10. Observed total collision cross-sections of He and Ne.

a_0=0.53x10^{-8}cm~0.5A

Radius of the first Bohr orbit of H atom

Understanding plasma

Collisions

Classification of collisions → elastic
→ inelastic

The concept of collision cross-section

$$\delta I = -NQI_p \, \delta x$$

$$I_P = I_0 \exp(-QNx)$$

Hypothetical gas of rigid spheres of cross section Q

Slow decrease of interaction potential - Small deviation ….
→ problem with concept of integral cross section

Electronic and ionic impact phenomena
Volume 1 – Collisions of electrons with atoms
H.S.W. Massey and E.H.S.Burhop, Oxford, Clarendon Press, 1969

Kinetics of elementary process

$$e + Ar \Rightarrow Ar^{+} + 2e$$

Multiple collision – plasma

@ T

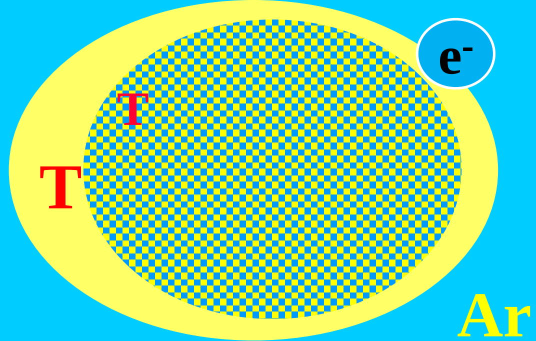

Ionization rate coefficient

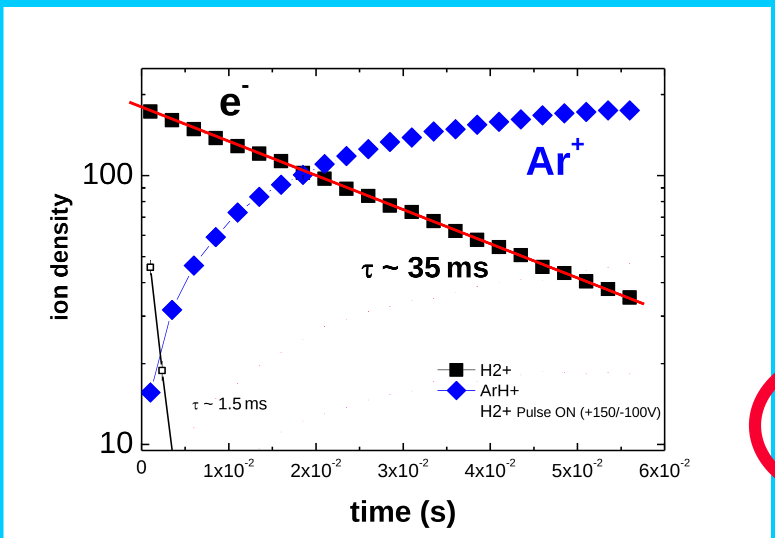

k(T)

Collisions of electrons with atoms (atomic beams)

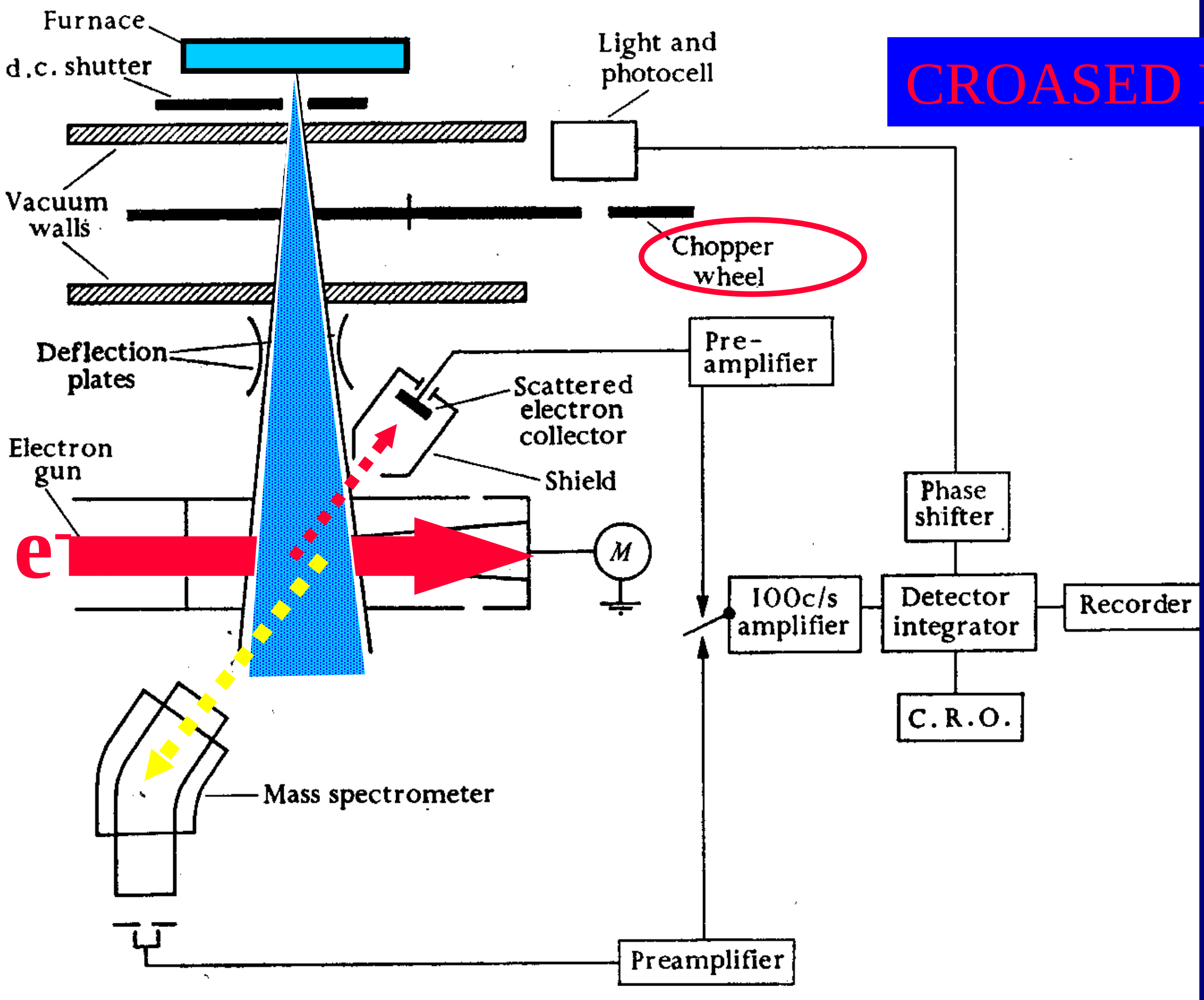

FIG. 1.2. Schematic diagram of the arrangement of apparatus used by Fite, Brackmann, and Neynaber for observation of elastic scattering of electrons by atomic hydrogen.

CROASED BEAM METHOD

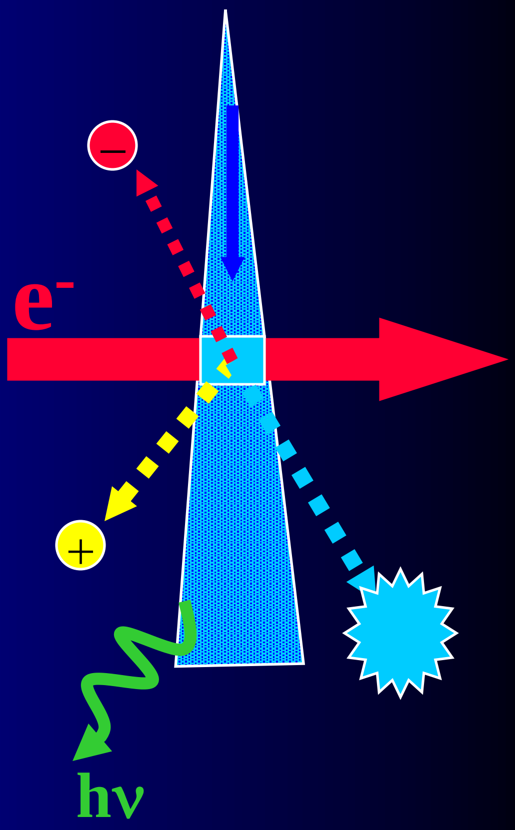

Position (angle), mass and energy sensitive detectors

low energies - 2010

Threshold Photoelectron Source for Ultra-Low-Energy Electron Collision Experiments

We have developed a new experimental technique for measuring the total cross section of ultra-low energy electron collisions with atoms and molecules utilizing synchrotron radiation. The present technique employs a combination of the penetrating field technique and the threshold photoionization of rare gas atoms using synchrotron radiation as an electron source in order to produce a high resolution electron beam at very low energy. The total cross sections for electron scattering from Kr in the energy range from 14 meV to 20 eV are obtained with the new technique. In addition, resonant structures in the total cross sections due to Kr^- $(4p^5 5s^2\ ^2P_{3/2})$ and Kr^- $(4p^5 5s^2\ ^2P_{1/2})$ Feshbach resonances are also observed for the first time.

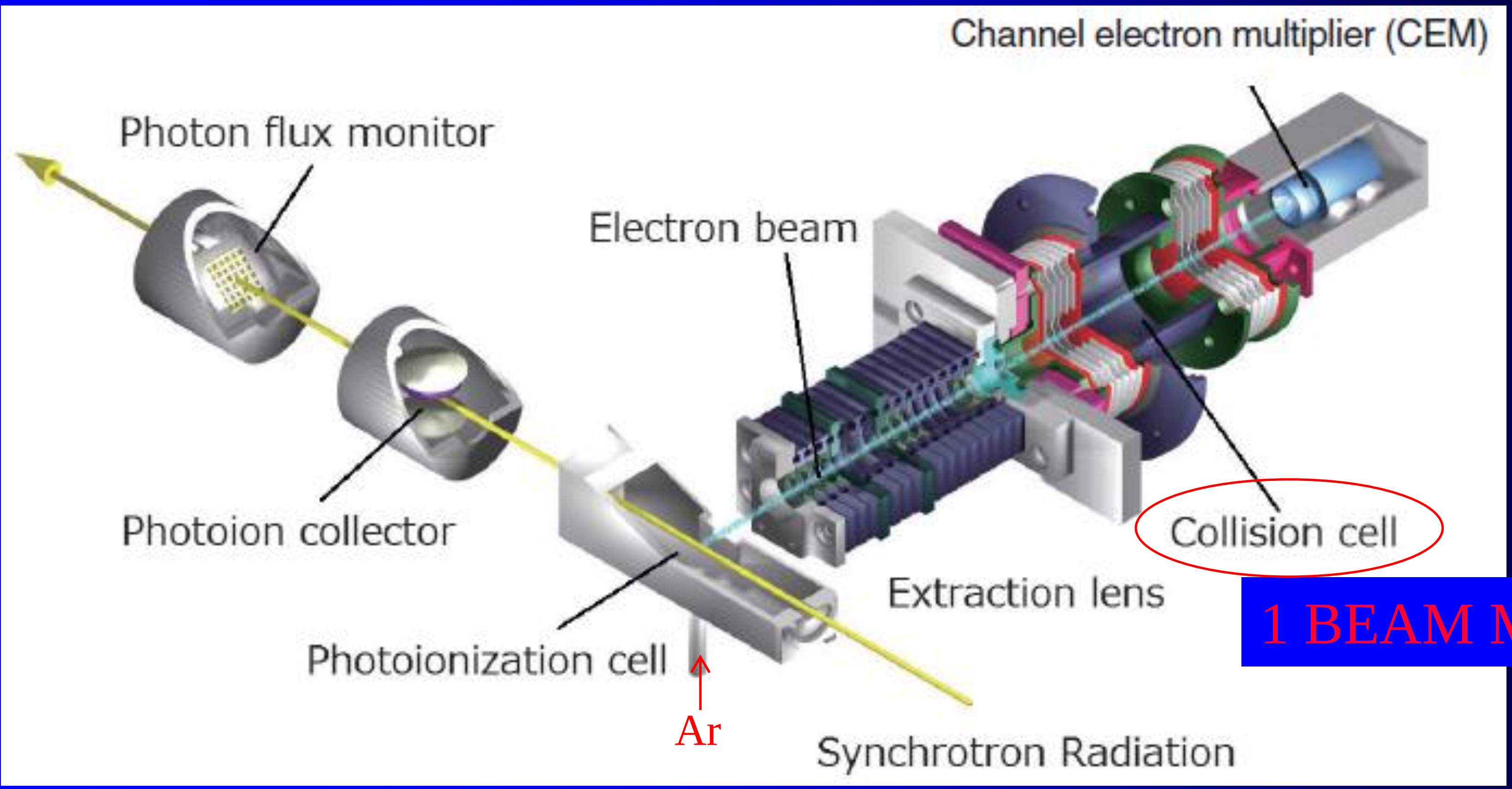

1 BEAM METHOD

Figure 1
Schematic view of the experimental set-up. The system consists of an electron scattering apparatus with a photoionization cell, a photoion collector, and photon flux monitor of the monochromatized SR.